

This electronic thesis or dissertation has been downloaded from the King's Research Portal at <https://kclpure.kcl.ac.uk/portal/>



Modulation of the murine lymphatic system to decipher its role in the allo-immune response

Meader, Lucy

Awarding institution:
King's College London

The copyright of this thesis rests with the author and no quotation from it or information derived from it may be published without proper acknowledgement.

END USER LICENCE AGREEMENT



Unless another licence is stated on the immediately following page this work is licensed

under a Creative Commons Attribution-NonCommercial-NoDerivatives 4.0 International

licence. <https://creativecommons.org/licenses/by-nc-nd/4.0/>

You are free to copy, distribute and transmit the work

Under the following conditions:

- Attribution: You must attribute the work in the manner specified by the author (but not in any way that suggests that they endorse you or your use of the work).
- Non Commercial: You may not use this work for commercial purposes.
- No Derivative Works - You may not alter, transform, or build upon this work.

Any of these conditions can be waived if you receive permission from the author. Your fair dealings and other rights are in no way affected by the above.

Take down policy

If you believe that this document breaches copyright please contact librarypure@kcl.ac.uk providing details, and we will remove access to the work immediately and investigate your claim.

**MODULATION OF THE MURINE LYMPHATIC SYSTEM
TO DECIPHER ITS ROLE IN THE ALLO-RESPONSE**

A thesis submitted to
King's College London

By

Lucy Jane Meader

For the degree of
Doctor of Philosophy

Abstract

The adaptive immune response to an allograft is initiated when donor-derived foreign antigens are recognised by the host immune system. This process relies on efficient trafficking of immune cells out of the graft to secondary lymphoid organs which provide a suitable niche for interactions between antigen presenting cells and allo-reactive T cells. The role of the lymphatic system in the allo-response is poorly understood, and there is evidence that lymphatics can have either a negative or a positive impact on graft survival, depending on a variety of complex factors.

The contribution of lymphatics to the allo-response has been studied using mouse models of skin, heart and kidney transplantation, in conjunction with pharmacological or genetic modulation of lymphatic function. Allogeneic kidney graft survival was significantly prolonged following treatment of recipients with anti-ICAM-1, an effect which correlated with reduced density of donor passenger leukocytes within recipients' draining lymph nodes in the immediate post-transplantation period. In addition, skin, heart and kidney grafts with lymphatic deletion of ephrin B2 benefitted from prolonged survival compared with wild-type grafts. This could not be attributed to reduced trafficking of donor cells to the draining lymph nodes and was likely a result of a local protective effect of ephrin B2 deficiency in the graft. The draining lymph node lymphatic response to heart transplantation was assessed; however, no significant changes were detected.

Varied models and organ types have been used to provide evidence for the role of donor and recipient lymphatics in allogeneic transplantation. Disruption of lymphatics resulted in delayed rejection or even permanent graft survival in some models. The mechanisms involved are complex, and may be independent of leukocyte trafficking. Future research focus should concentrate on elucidating the mechanisms involved so that they can be harnessed and translated into clinically applicable protocols to prolong allograft survival in the clinic.

Table of Contents

ABSTRACT	2
TABLE OF CONTENTS.....	3
TABLE OF FIGURES	7
TABLE OF TABLES.....	10
ACKNOWLEDGEMENTS	11
DECLARATION	12
ABBREVIATIONS.....	13
CHAPTER 1 INTRODUCTION	14
1.1 TRANSPLANTATION	15
1.1.1 Clinical situation	15
1.1.2 The immune response to an allograft- mechanisms of rejection	17
1.1.3 The immune response to an allograft- allo-recognition	21
1.1.4 Tolerance.....	27
1.1.5 T-cell co-stimulation.....	28
1.1.6 The importance of cell trafficking in transplantation	29
1.2 LYMPHATICS	30
1.2.1 Introduction to the lymphatic system.....	30
1.2.2 Historical perspective.....	31
1.2.3 Development of the lymphatic system	31
1.2.4 Physiological role of the lymphatic system.....	33
1.2.5 Disorders of the lymphatic system.....	34
1.2.6 Structure of the lymphatic system	35
1.2.7 Lymphatics and immunity	38
1.2.8 Lymphangiogenesis.....	42
1.3 THE LYMPH NODES.....	50

1.3.1 Structure.....	50
1.3.2 Development.....	52
1.3.3 Response to inflammation	52
1.3.4 Lymphatic endothelial cells.....	53
1.4 OUTLINE OF THESIS	56
CHAPTER 2 MATERIALS AND METHODS	57
2.1 REAGENTS	58
2.2 ANIMALS	59
2.2.1 Breeding	60
2.3 GENOTYPING	61
2.3.1 Primers	61
2.3.2 DNA products	62
2.4 ANIMAL MODELS OF TRANSPLANTATION	63
2.4.1 Technical success	63
2.4.2 Splenectomy.....	63
2.4.3 Skin transplantation	64
2.4.4 Heart transplantation.....	65
2.4.5 Kidney transplantation.....	66
2.5 BLOOD UREA NITROGEN MEASUREMENT (BUN)	67
2.6 MONOCLONAL ANTIBODY THERAPY.....	67
2.7 TAMOXIFEN TREATMENT	68
2.8 TISSUE HARVESTING	68
2.8.1 Mediastinal lymph nodes	68
2.8.2 Immunohistochemistry	69
2.8.3 Histology.....	70
2.9 REAL-TIME PCR.....	71
2.9.1 Genomic DNA extraction.....	71

2.9.2 <i>zfy1</i> PCR.....	71
2.9.3 <i>cre</i> PCR.....	72
2.9.4 Calculation of cell number	72
2.10 TISSUE DIGESTION FOR FLOW CYTOMETRY	73
2.10.1 Heart.....	73
2.10.2 Kidney.....	74
2.10.3 Lymph nodes	74
2.11 FLOW CYTOMETRY	76
2.11.1 Lymphatic endothelial cells.....	77
2.11.2 Kidney and heart leukocytes.....	77
2.11.3 Splenocytes	78
2.11.4 Analysis of flow cytometry data.....	78
2.12 STATISTICS.....	78
 CHAPTER 3 USING ANTI-ICAM-1 ANTIBODY THERAPY TO BLOCK POST- TRANSPLANTATION LYMPHATIC TRAFFICKING OF DPL.....	 79
3.1 BACKGROUND.....	80
3.2 QUANTIFICATION OF DPL TRAFFICKING USING REAL-TIME PCR.....	82
3.3 SURVIVAL OF ALLOGENEIC KIDNEY GRAFT IN ANTI-ICAM-1 ANTIBODY-TREATED RECIPIENTS	85
3.4 QUANTIFICATION OF T CELL INFILTRATE IN ANTI-ICAM-1 ANTIBODY-TREATED ALLOGENEIC KIDNEY GRAFTS	89
3.5 SUMMARY	95
3.6 DISCUSSION	96
 CHAPTER 4 EFFECTS OF DISRUPTION TO DONOR LYMPHATICS ON THE ALLO- RESPONSE.....	 100
4.1 BACKGROUND.....	101
4.2 DELETION OF EPHRIN B2 FOLLOWING TAMOXIFEN TREATMENT.....	102

4.3 EFFECT OF EPHRIN B2 DEFICIENCY ON LYMPHATIC MORPHOLOGY WITHIN ORGANS.....	103
4.4 PHENOTYPE OF GRAFT ANTIGEN PRESENTING CELLS AFTER TAMOXIFEN TREATMENT	106
4.5 SURVIVAL OF EPHRIN B2 ^{-/-} GRAFTS IN ALLOGENEIC RECIPIENTS.....	111
4.6 QUANTIFICATION OF DPL TRAFFICKING USING REAL-TIME PCR.....	117
4.7 FURTHER EVALUATION OF EPHRIN B2 DEFICIENCY ON DPL TRAFFICKING	120
4.8 SUMMARY	124
4.9 DISCUSSION	125
 CHAPTER 5 DRAINING LYMPH NODE LEC RESPONSE TO TRANSPLANTATION	 129
5.1 BACKGROUND.....	130
5.2 ASSESSING CHANGES IN DRAINING LYMPH NODE LEC PHENOTYPE FOLLOWING HEART TRANSPLANTATION	132
5.3 ASSESSING DLN LYMPHANGIOGENESIS FOLLOWING TRANSPLANTATION	135
5.4 SUMMARY	136
5.5 DISCUSSION	137
 CHAPTER 6 DISCUSSION	 140
6.1 USING ANTI-ICAM-1 ANTIBODY THERAPY TO BLOCK POST-TRANSPLANTATION LYMPHATIC TRAFFICKING OF DPL 141	
6.1.1 Summary of findings	141
6.1.2 Implications and limitations.....	142
6.2 EFFECTS OF DISRUPTION TO DONOR LYMPHATICS ON THE ALLO-RESPONSE.....	146
6.2.1 Summary of findings	146
6.2.2 Implications and limitations.....	147
6.3 DRAINING LYMPH NODE LEC RESPONSE TO TRANSPLANTATION	150
6.3.1 Summary of findings	150
6.3.2 Implications and limitations.....	151
6.4 CONCLUDING REMARKS	152

Table of Figures

Figure 1.1- The hierarchical structure of the lymphatic system.....	36
Figure 1.2- Active transmigration of leukocytes across lymphatic endothelium during inflammation.	41
Figure 1.3- Proposed mechanism of lymphatic vessel activation following transplantation.	42
Figure 1.4- Structure of the lymph node.....	51
Figure 2.1- Photograph showing dilated lymphatic vessel in the abdomen of an ephrin B2 ^{-/-} mouse eight days after tamoxifen treatment. Original magnification 20x.	60
Figure 2.2- Schematic of floxed <i>ephrin B2</i> showing location of primer sequence (a,b,c) binding.....	62
Figure 2.3- Location of the mediastinal lymph nodes in the mouse.	68
Figure 2.4- Location of mediastinal lymph nodes.	69
Figure 3.1- Experimental design of quantification of DPL trafficking after anti-ICAM-1 antibody therapy.....	82
Figure 3.2- Real-time PCR standard curve for <i>zfy1</i> using male BALB/c genomic DNA.	83
Figure 3.3- Quantification of donor DNA within recipient DLN 24 hours post-transplantation.	84
Figure 3.4- Quantification of donor cells within recipient DLN 24 hours post-transplantation.	85
Figure 3.5- Experimental design of assessment of survival of kidney allografts in anti-ICAM-1 antibody-treated recipients.....	86
Figure 3.6- Survival of kidney allografts in recipients treated with anti-ICAM-1 antibody.	87
Figure 3.7- Blood urea nitrogen (BUN) measurements from kidney allograft recipients.	88
Figure 3.8- Histology of long-term surviving kidney grafts.	89

Figure 3.9- Experimental design of assessment of T cell infiltration of kidney allografts in anti-ICAM-1 antibody-treated recipients.....	90
Figure 3.10- Gating strategy for T cells.....	91
Figure 3.11- Size of T cell populations within kidney grafts at day 5 post-transplantation (proportion).....	92
Figure 3.12- Size of T cell populations within kidney grafts at day 5 post-transplantation (absolute number).....	93
Figure 3.13- Activation status of T cells infiltrating kidney grafts at day 5 post-transplantation.....	94
Figure 3.14- Foxp3 expression within kidney grafts at day 5 post-transplantation.....	95
Figure 4.1- PCR to demonstrate successful deletion of <i>ephrin B2</i>	103
Figure 4.2- Quantification of lymphatic vessel density in skin, heart and kidney.....	104
Figure 4.3- Quantification of lymphatic vessel size in skin, heart and kidney.....	105
Figure 4.4- LYVE-1 staining of skin, heart and kidney tissue from tamoxifen-treated wild-type (WT) and <i>ephrin B2</i> ^{-/-} mice.....	105
Figure 4.5- Experimental design for assessment of antigen presenting cell numbers and phenotype in <i>ephrin B2</i> ^{-/-} and wild-type mice.....	106
Figure 4.6- Gating strategy for heart antigen presenting cells.....	107
Figure 4.7- Proportions of antigen presenting cells in heart tissue from <i>ephrin B2</i> ^{-/-} and wild-type (WT) mice after tamoxifen treatment.	108
Figure 4.8- Absolute numbers of antigen presenting cells in heart tissue from <i>ephrin B2</i> ^{-/-} and wild-type (WT) mice after tamoxifen treatment.	109
Figure 4.9- Phenotype of heart resident CD11c ⁺ cells wild-type (WT) and <i>ephrin B2</i> ^{-/-} hearts following tamoxifen treatment.....	110
Figure 4.10- Phenotype of heart resident CD11b ⁺ cells wild-type (WT) and <i>ephrin B2</i> ^{-/-} hearts following tamoxifen treatment.	111
Figure 4.11- Experimental design for assessment of survival of <i>ephrin B2</i> ^{-/-} grafts in allogeneic recipients.	112
Figure 4.12- Survival of <i>ephrin B2</i> ^{-/-} skin on allogeneic recipients.....	113

Figure 4.13- Survival of ephrin B2 ^{-/-} hearts in allogeneic recipients.....	114
Figure 4.14- Survival of ephrin B2 ^{-/-} kidneys in allogeneic recipients.	115
Figure 4.15- Histology of long-term surviving ephrin B2 ^{-/-} kidney grafts.....	116
Figure 4.16- LYVE-1 staining of long-term surviving ephrin B2 ^{-/-} kidney grafts.	117
Figure 4.17- Experimental design for quantification of DPL trafficking form ephrin B2 ^{-/-} and wild-type heart grafts.....	118
Figure 4.18- Quantification of donor DNA within recipient DLN 24 hours post-transplantation.	119
Figure 4.19- Quantification of donor cells within recipient DLN 24 hours post-transplantation.	120
Figure 4.20- Experimental design for double skin transplantation.	121
Figure 4.21- Survival of double ephrin B2 ^{-/-} skin grafts compared with double wild-type skin grafts in allogeneic BALB/c recipients.....	122
Figure 4.22- Survival of double ephrin B2 ^{-/-} skin grafts compared with double wild-type skin grafts on allogeneic BALB/c recipients.....	123
Figure 5.1- Experimental design for assessment of phenotypic changes in lymph node LECs after transplantation.	132
Figure 5.2- Gating strategy for lymph node LECs.	133
Figure 5.3- Phenotype of DLN LECs following transplantation.....	134
Figure 5.4- Quantification of DLN LECs after transplantation (proportion).....	135
Figure 5.5- Quantification of DLN LECs after transplantation (absolute number).	136

Table of Tables

Table 1- Clinical transplantation figures for 2016	15
Table 2- Table showing antibodies used for flow cytometry. All antibodies were supplied by Biolegend.....	76

Acknowledgements

Many people have helped me during the course of this project and the writing of this thesis. Firstly, I would like to thank my supervisor Dr Wilson Wong, for his constant support, guidance and enthusiasm. And thanks to my second supervisors Prof. Giovanna Lombardi and Dr Lindsey Edwards for their scientific input. I particularly acknowledge Lindsey's input in the beginning with setting up the ephrin B2^{-/-} colony, and her co-ordination of the initial survival experiments. And thank you to Dr Taija Makinen for kindly providing the initial ephrin B2^{-/-} mice for the colony. I would like to thank Dr Kathryn Hillman, not only for her hard work in proof-reading this thesis, but also for her friendship and guidance in the lab. And thank you to Simon, Julia and Anna for making the lab a fun place to work. In addition, I would like to thank all of the staff at the FWB and Rayne BSUs for being friendly and helpful.

A very special thank you to my parents for their never-ending love and support; for giving me a beautiful place to live and always being great company. And thank you to my in-laws for providing a relaxing environment in which to escape from London. Thank you to my brother and sister-in-law, my extended family and friends for their understanding, support and encouragement. Last but not least, I thank David, my angel, for his patience, encouragement, and love. I couldn't have done this without him.

Declaration

All of the work presented in this thesis was carried out by Lucy Meader, except the following:

- Skin transplantation for the survival experiment presented in section 4.4 was carried out by Dr Lindsey Edwards
- Approximately 50% of the heart and kidney transplants for the survival experiment presented in section 4.4 were carried out by Dr Wilson Wong and Dr Kathryn Hillman.
- Approximately 50% of the kidney transplants in the PCR experiment presented in section 3.2 were carried out by Dr Wong

Abbreviations

Abbreviation	Meaning
APC	Antigen presenting cell
BEC	Blood endothelial cell
BUN	Blood urea nitrogen
CCL21	Chemokine (c-c motif) ligand 21
CCR7	c-c chemokine receptor type 7
CTLs	Cytotoxic T lymphocytes
DAMPs	Damage associated molecular patterns
DC	Dendritic cell
DLN	Draining lymph node(s)
DPL	Donor passenger leukocytes
FRC	Fibroblastic reticular cell
HA	Hyaluronan
HEV	High endothelial venule
ICAM-1	Intercellular adhesion molecule 1
LEC	Lymphatic endothelial cell
LFA-1	Leukocyte function-associated antigen 1
LT	Lymphotoxin
LYVE-1	Lymphatic vessel endothelial hyaluronan receptor 1
MHC	Major histocompatibility complex
NK cell	Natural killer cell
PAS	Periodic acid Schiff's
PBS	Phosphate buffered saline
PD1	Programmed cell death receptor 1
PDL1	Programmed cell death ligand 1
S1P	Sphingosine-1-phosphate
SLO	Secondary lymphoid organs(s)
SPECT/CT	Single-photon emission computed tomography/ computed tomography
TCR	T cell receptor
TLRs	Toll-like receptors
VEGF-C	Vascular endothelial growth factor C
VEGFR3	Vascular endothelial growth factor receptor 3

Chapter 1 Introduction

1.1 Transplantation

1.1.1 Clinical situation

For patients suffering end-stage organ failure, transplantation is a life-saving operation. Although significant improvements in the short-term survival of allografts have been realised in recent years, consistent long-term graft survival remains a clinical challenge. One year survival rates for kidney transplants in the UK are currently 94-97%; however, this declines to 86-92% after 5 years. For other solid organs such as the heart this figure is as low as 71% (1); (Table 1).

Table 1- Clinical transplantation figures for 2016
(adapted from data available from NHS blood and transplant) (1), (Deceased brain death, DBD; deceased circulatory death, DCD)

Organ	# registered	# performed	5-year survival
Heart	248	194	71%
Kidney	5275	DBD= 1134	87%
		DCD= 851	86%
		Living donor= 957	92%
Lung	316	DBD= 151	59%
		DCD= 35	60% (3 years)
Liver	584	DBD= 672	82%
		DCD= 206	73%

Currently, rejection of allografts is prevented by the life-long administration of potent immunosuppressive drugs. Immunosuppressive therapy for transplant recipients comprises two main categories: induction reagents, which aim to reduce the occurrence of acute rejection early after transplantation; and maintenance reagents, for preventing the development of chronic graft rejection and for treating acute rejection episodes throughout the life of the graft. Induction therapy consists of various antibodies that target different aspects of the immune response.

Basiliximab is an Interleukin (IL) 2 receptor antagonist that has shown safety and efficacy in multiple clinical trials in renal transplantation patients (2-5). Another induction reagent, rabbit anti-thymocyte globulin (ATG), has been associated with the risk of cytokine release syndrome and increased infections (6), and is therefore being replaced by other agents. Alemtuzumab is an anti-CD52 antibody which targets mature T and B lymphocytes and has demonstrated efficacy in pre-sensitized patients (7), although it was associated with increased infections. For maintenance therapy, the most effective drugs are the calcineurin inhibitors, which target the activation of T cells. Tacrolimus and ciclosporin have shown great efficacy in prolonging the survival of renal grafts (8, 9). However, the side effects of these drugs which include nephrotoxicity, post-transplantation diabetes and hypertension, can be severe and thus dosing is carefully monitored (10). Another class of immunosuppressive drugs, the mammalian target of rapamycin (mTOR) inhibitors, have been introduced in the hope of sparing the use of calcineurin inhibitors (11). Sirolimus and everolimus work by inhibiting the regulatory kinase, mTOR, which blocks the responsiveness of lymphocytes to IL-2. Although less effective at reducing graft rejection (11), these agents are not as nephrotoxic as the calcineurin inhibitors. Certain patients may be switched to mTOR inhibitors to avoid the long-term use of calcineurin inhibitors (12). However, the mTOR inhibitors can lead to development of lymphoedema in transplant patients (13) because they impair the signalling pathways involved in VEGF-C production and responsiveness (14), which has a negative effect on restorative lymphangiogenesis. In addition, Fingolimod (FTY720), which is a modulator of the sphingosine-1-phosphate (S1P) receptor, initially showed efficacy in pre-clinical models of transplantation. It results in immunosuppression caused by inhibition of lymphocyte re-circulation with sequestration of activated lymphocytes within lymph nodes, and is efficacious at preventing graft rejection (15). However, its use in renal transplant patients was halted because of adverse ocular effects (16). The third class of maintenance immunosuppressive drugs are the anti-proliferative agents, which provide an additive effect in combination with calcineurin inhibitors (17). Azathioprine is a purine analogue which disrupts RNA and DNA synthesis and thus suppresses B-cell

and T-cell proliferation. Mycophenolic acid, a newer anti-proliferative drug, is a reversible inhibitor of inosine monophosphate dehydrogenase, the enzyme used in purine synthesis by proliferating T and B cells. Its efficacy has been demonstrated by multiple clinical trials (18, 19); however, it is associated with gastrointestinal disturbances and leukopenia (17). In addition to the specific immunosuppressive agents mentioned above, the majority of transplant recipients receive steroid therapy, typically in the form of Prednisolone, which is a synthetic corticosteroid. This provides broad spectrum immunosuppression, which is very effective for the prevention of graft rejection. However, the use of steroids must be carefully monitored because of adverse side effects, including increased blood sugar levels, mood disturbances and weight gain (reviewed in (20)).

In our unit, kidney transplant recipients currently receive steroids, tacrolimus and mycophenolic acid as standard. Low-risk and standard-risk recipients receive Basiliximab as induction therapy and high-risk recipients, such as those with human leukocyte antigen (HLA) antibody incompatibility, receive Alemtuzumab.

There is a pressing need for the development of new therapies for the prevention and treatment of transplant rejection. With a greater understanding of the biological processes involved, scientists and clinicians can develop novel approaches to improve the survival of allografts.

1.1.2 The immune response to an allograft- mechanisms of rejection

1.1.2.1 Innate response

All vascularised transplants are subject to ischemia-reperfusion injury due to the transplant procedure. As a result, the innate immune system of the host is stimulated by the release of danger associated molecular patterns (DAMPs) from damaged cells, which activate Toll-like receptors (TLRs) on cells within the graft. TLR engagement on

dendritic cells (DCs) causes them to up-regulate molecules crucial to T-cell stimulation, such as CD80 and CD86, and also increases their migratory capacity (21).

Ischemic injury can also activate the complement system. Local production of the complement component C3 within the graft has been shown to be essential for graft rejection to occur (22), and this is achieved through various mechanisms. There is strong evidence that the small peptide fragments, C3a and C5a, mediate dendritic cell activation (23), and provide co-stimulatory and survival signals to T cells (24).

1.1.2.2 Innate cellular response

Neutrophils infiltrate allogeneic graft tissue within the first few hours following reperfusion; producing cytokines, such as IL-1 β , and chemokines, such as CCL1, 2 and 5, which contribute to the inflammatory environment (25). Blocking neutrophil infiltration or function shows an initial beneficial effect and when combined with co-stimulation blockade can improve graft survival in animal models (26).

Monocytes are the circulating precursors of dendritic cells and macrophages, and rapidly infiltrate inflamed sites. Once within the graft they differentiate into mature DCs or macrophages; within days following transplantation the majority of graft DCs are host monocyte-derived (27), and these cells can interact with cognate T cells within the graft (28). It is also now clear that host-derived monocytes can initiate adaptive immune responses via a process termed 'innate allo-recognition'. Transplantation studies using RAG^{-/-} γ ^{-/-} mice that lack T, B and natural killer (NK) cells showed that grafts in these mice are infiltrated with host monocytes, which adopt a mature DC phenotype with high levels of major histocompatibility complex (MHC) class II and co-stimulatory molecules. These cells were more potent and long-lasting in allogeneic grafts compared with syngeneic grafts, indicating that this was a specific allogeneic response (29). By contrast, host

myeloid-derived suppressor cells have been described as mediators of tolerance in transplant models (reviewed in (30)).

NK cells are known to play a negative role in transplantation in that they promote rejection of grafts via the 'missing self' theory. This refers to the fact that NK cells recognise a lack of MHC class I on the surface of allogeneic cells and become activated leading to release of cytokines such as IFN- γ and TNF- α , and cytotoxicity (31).

However, NK cells have also been demonstrated to dampen the allo-immune response (31), and this is attributed to the fact that they rapidly kill donor passenger leukocytes within recipient secondary lymphoid organs (32).

It has recently become clear that there is a distinct interplay between the innate and adaptive immune systems following transplantation, and there is evidence suggesting that adaptive immune responses, in particular T cell responses, are limited or lacking in the absence of innate immune activation (33, 34). The innate immune system plays a critical role in graft rejection not only by providing initial danger signals to immune cells in the graft (23), but also by providing crucial co-stimulatory signals to T cells (24).

1.1.2.3 Antibody-mediated rejection

Antibody-mediated rejection can cause acute or chronic injury to the graft and in some cases leads to complete graft loss. The antibodies which cause this type of injury can be targeted towards donor HLA molecules, endothelial cell antigens, or ABO blood group antigens present on red blood cells and endothelial cells.

Acute antibody-mediated rejection can occur within days after transplantation and can be triggered by either preformed or *de novo* generated donor-specific antibodies. It is characterised by deposition of the complement component C4d in the graft, and occurs in up to 7% of kidney transplant recipients (35).

Chronic antibody-mediated rejection is often the result of donor-specific antibodies that collect in the graft and are deposited on capillary endothelium. In the case of kidney grafts this injury is observed histopathologically as glomerulopathy characterised by endothelial hypertrophy and fibrillary deposition.

1.1.2.4 T cell-mediated rejection

Allo-reactive T cells can be activated by various mechanisms, all of which involve the recognition of non-self antigens; therefore the T cell response is referred to as allo-specific. Allo-reactive CD4⁺ T cells differentiate upon stimulation into various subtypes each of which has a different set of effector functions (reviewed in (36)), and is capable of causing graft rejection in isolation (37, 38).

T helper (Th) 1 cells produce the cytokines interferon gamma (IFN- γ) and IL-2, which help in the; priming of cytotoxic T cells (CTL), and the production of IgG2a by B cells leading to complement activation, both of which are implicated in graft rejection. Although the Th1 response is traditionally considered pro-inflammatory, recent evidence has suggested that IFN- γ plays a regulatory role in the allo-response, supporting Treg development and dampening Th17 responses (39).

Th17 cells produce IL-17, IL-21 and IL-22 which act to recruit neutrophils and macrophages to the graft (40). Th17 cells are mainly implicated in the early post-transplantation period and many studies have found increased levels of IL-17 in acutely rejecting grafts (41). In addition, neutralization of IL-17 has also shown beneficial effects in animal models of transplantation (42).

Th2 cells produce the cytokines IL-4, IL-5, IL-9, IL-10 and IL-13, which aid B cell activation and recruitment of eosinophils, promoting rejection. There is experimental

evidence linking expression of Th2 cytokines and eosinophil infiltration of grafts (43). Additionally, *in vitro* Th2 polarized cells adoptively transferred into immunodeficient mice can cause acute allograft rejection (44).

Allo-reactive CD8⁺ T cells function as CTLs and kill graft cells via perforin and granzyme B, or Fas and Fas ligand-dependant pathways. Cytotoxic CD8⁺ T cells with a memory phenotype have proven to be a barrier to tolerance induction in experimental models (45).

Memory T cells produce a fast and effective allo-response. This is because they respond to lower concentrations of antigen, and have a smaller need for co-stimulation in order to produce effector functions. The reason for this may be because memory cells do not require multiple rounds of cell division before producing cytokines (46). Additionally, there is evidence that memory cells can circumvent the conventional trafficking pathways of naïve T cells and become activated regardless of lymph node occupancy (47). These properties of allo-reactive memory cells make them resistant to tolerance induction protocols (48). Many studies have found a correlation between the presence of allo-reactive memory T cells before transplantation and the occurrence of rejection episodes in human transplant recipients (reviewed in (49)).

1.1.3 The immune response to an allograft- allo-recognition

Recipient T cells need to be primed with allo-antigen before acquiring graft destructive capabilities, and this can occur via three pathways of allo-recognition: the direct, indirect and semi-direct. In the direct pathway, which predominates in the early acute phase of the allo-response, foreign MHC-expressing cells are directly recognised by recipient T cells. Contrary to this, the indirect pathway involves the presentation of donor peptides to cognate T cells by self MHC-expressing antigen presenting cells (APC). Cross-talk

between the two pathways can also occur when MHC-peptide complexes are transferred between donor and recipient APC in the semi-direct pathway.

1.1.3.1 The direct pathway

The direct pathway of allo-recognition was first demonstrated in the mixed leukocyte reaction (MLR), where leukocytes from two genetically different individuals were co-cultured, resulting in a significant increase in cell activation compared with co-cultures from genetically identical individuals (50). These results were further validated *in vivo* in rodent models of allogeneic transplantation, and the strength of the response was attributed to the presence of donor passenger leukocytes (DPL). DPL are leukocytes present within the graft tissue which are transferred to the recipient at the time of transplantation, and recognised by T cells via the direct pathway. The contribution of DPL to the rejection process was determined in studies by Lechler *et al.*, where grafts were 'parked' in temporary hosts to deplete DPL, prior to transplantation. These grafts survived longer than non-depleted grafts, and the survival could be reversed by the addition of donor strain DCs (51).

DPL leave the graft rapidly after transplantation and traffic to the secondary lymphoid organs (SLO) of the recipient, namely the spleen and local draining lymph nodes (52). Here they come into contact with T cells that directly recognise the MHC on their surface as foreign. The potency of the direct pathway lies in the fact that a large proportion of the T cell repertoire can react to foreign MHC-peptide complexes; and there are two proposed models to explain this phenomenon. Firstly, the 'peptide-centric' model states that it is the diversity of the allo-peptides presented in the context of donor MHC that drives the intense direct allo-response, rather than the MHC molecule itself. As donor APC will be presenting a plethora of different peptides, multiple T cell clones can be activated. This has been proved to some extent by the co-culture of T cells with allogeneic APC lacking peptide, which led to limited T cell responses (53, 54).

By contrast, the 'MHC-centric model' proposes that the observed alloreactivity of DPL is due to structural differences between self and allo-MHC molecules; single amino acid polymorphisms found in the allo-MHC may drive recognition by the T cell receptor (TCR). These interactions may also be higher affinity than self MHC-TCR interactions. In addition, it is likely that the high density of MHC molecules expressed by DPL enhances the response (55). Evidence for this model comes from studies where alterations in the TCR binding site of allo-MHC molecules led to perturbations in binding and subsequent effector functions (56).

The direct pathway produces an intense T cell response directed at the graft that is short-lived and levels off a short time after transplantation. It is known that DPL are rapidly killed within recipient SLO by NK cells which recognise them as foreign due to their lack of self-MHC (32), and are only identifiable in SLO for a short time following transplantation (57, 58). Immunosuppressive therapy inhibits directly-activated T cells and prevents acute rejection in transplant recipients (59).

1.1.3.2 Donor passenger leukocytes

Since the description of the passenger leukocyte theory of direct allo-reactivity, attempts have been made to deplete donor organs of passenger leukocytes either before or after transplantation, in order to prolong survival in allogeneic recipients. Irradiation of donors prior to transplantation is one method of removing passenger leukocytes and has proved successful in prolonging survival of grafts in animal models of transplantation (60, 61); however, this is not a feasible strategy for clinical transplantation. Passenger leukocytes can also be removed by *ex vivo* perfusion of the organ before transplantation, and this has shown some efficacy in animal models (62). Pharmacological depletion of DPL has been studied, and efficacy has been shown in animal transplantation models with the use of anti-MHC class II antibodies (63, 64); however, there were issues with specificity

and whether or not the target cells were depleted. In addition, a study by Goldberg *et al.* reported the use of anti-CD45 antibodies in human renal transplantation, which were perfused into donor kidneys before transplantation, and showed efficacy in diminishing rejection episodes for patients (65). Recent work from our laboratory has demonstrated the effectiveness of a donor MHC class II-specific immunotoxin in a mouse kidney transplantation model, where donor cells were specifically killed and grafts survived indefinitely with normal function, reduced donor-specific antibody formation, and delayed rejection of third party skin grafts (66). This provides evidence for the efficacy of therapies aimed at the immune system of the donor rather than the recipient, and could be an approach to limit the use of systemic immunosuppression in the clinic.

1.1.3.3 The indirect pathway

The indirect pathway of allo-recognition refers to the concept that recipient APCs can uptake and process donor antigens for presentation to T cells within the context of self-MHC molecules. This was first evidenced *in vitro* for donor MHC class I peptides presented to CD8⁺ cytotoxic T cells in the context of self MHC class I on recipient APCs (67), followed by *in vivo* studies leading to direct evidence of presentation of donor MHC class II peptides in the context of recipient MHC class II, and activation of a donor-specific CD4⁺ T cell response (68-70).

The initial T cell response following indirect activation is oligoclonal in that it involves a limited number of T cell clones, recognizing 'dominant' peptides. However, this changes throughout the life of the allograft and previously uninvolved T cells can become activated by recognition of 'cryptic' donor-derived peptides. Benichou and colleagues have demonstrated this phenomenon in transplant recipients and found that new clones of T cells can become activated by recognition of allo- and also auto-peptides in response to inflammatory signals such as IFN γ (71). In this way, not only is the indirect pathway active for the life of the graft, but can also strengthen over time.

As mentioned previously, most human allografts are protected from acute rejection by immunosuppressive therapy; however, many still succumb to chronic rejection. The indirect pathway of allo-recognition is heavily implicated in the progression of chronic rejection, and has been shown to be sufficient to cause chronic rejection in various animal models. In particular, presentation of donor MHC-derived peptides by recipient B cells is key to the pathogenicity of chronic rejection, and key studies have shown that when this interaction is blocked, graft survival is prolonged due to diminished allo-antibody production and limited CD4⁺ T cell responses (72).

It is also now certain that regulatory T cell (Tregs) with indirect specificity are key to tolerance induction in a variety of animal transplantation models (73, 74), and that regulatory responses are enhanced when the indirect pathway is the dominant contributor to alloreactivity (75).

1.1.3.4 The semi-direct pathway, MHC transfer and exosomes

The semi-direct pathway of allo-recognition relies on the fact that leukocytes exchange cell surface molecules. This pathway describes recipient APCs presenting both donor allo-peptides in the context of self MHC (indirect presentation), and intact donor MHC molecules acquired from DPL or graft endothelial cells. The exchange of MHC molecules can occur via cell-cell contact, nanotubes, or the release of extracellular vesicles such as exosomes.

Although this pathway of allo-recognition has only recently been discovered, the evidence for its occurrence in transplantation is indisputable. The paper by Brown *et al.* showed extensive exchange of MHC class II molecules between donor and recipient APCs in mouse models of kidney and heart transplantation; these double positive cells

expressed co-stimulatory molecules and so were likely to influence the allo-response (76).

More recently a paper by Smyth *et al.* has described the semi-direct pathway as the major contributor to CD8⁺ cytotoxic T cell responses in a skin transplantation model. Transfer of donor MHC class I to recipient DCs occurred for at least one month following transplantation and T cells activated via the semi-direct pathway contributed to the allo-response *in vivo* (77). This paper highlighted the importance of targeting both indirectly and directly activated T cells to prolong graft survival and induce tolerance.

Work from Benichou and colleagues (58) and Morelli and colleagues (57) has recently provided the first evidence for the role of donor-derived exosomes in the allo-response. Their work using both skin and heart transplantation models provides evidence for the fact that DPL, and likely graft endothelial cells, release exosomes containing MHC molecules and co-stimulatory molecules, which are taken up by recipient APCs within draining lymphoid organs. These 'cross-dressed' APCs are then able to elicit an allo-immune response via the semi-direct pathway. Interruption of the exosome release pathway prolonged graft survival, and cross-dressed cells isolated from transplant recipients initiated proliferation of allo-reactive CD8⁺ T cells *ex vivo*. These papers support the idea that a relatively small number of DPL can elicit a potent immune response in transplant recipients, and this is at least in part due to the release of exosomes from DPL resulting in a larger pool of APCs presenting donor MHC for T-cell activation. Although interesting, these new findings fail to demonstrate how exosomes released from DPL and graft endothelial cells traffic to the spleen and lymph nodes where the T cell response is initiated. It is still unclear whether the exosomes are released by DPL within the graft and enter the lymphatic system for traffic to SLO, or whether they are released upon entry into lymphoid tissue. These are vital questions which need to be answered in order to target therapies towards donor-derived exosomes.

1.1.4 Tolerance

The key objective of much research in the area of transplantation is the induction of donor-specific tolerance in transplant recipients. This means that the foreign graft is tolerated by the recipient in the absence of long-term conventional immunosuppressive therapy, without graft function being compromised.

Immune tolerance is essential to prevent reaction of the immune system to self-antigens (auto-antigens). This is achieved by two distinct mechanisms. Central tolerance occurs in the thymus, the location of T cell development, where only cells that recognise auto-antigens with low avidity are selected for subsequent maturation and release from the thymus. However, this process is not entirely efficient and some auto-reactive cells will be released into the periphery. Therefore, there is a requirement for suppression of these cells to avoid the development of auto-immunity. Tregs, generated either in the thymus (natural), or in the periphery from CD4⁺ T cells (inducible), are able to suppress auto-immunity, and restrain responses against bacterial and viral antigens, as well as restricting transplant rejection and tumour immunity. DCs are also crucial for peripheral tolerance as they take up and process antigen from apoptotic cells, and present it to Tregs to induce their maturation.

Methods to induce tolerance to an allograft are therefore aimed at either central or peripheral tolerance mechanisms. Central tolerance to an allograft has been achieved in non-human primate models by the induction of mixed chimerism prior to transplantation. This refers to the presence of both donor and recipient bone marrow cells in the recipient. Mixed chimerism is achieved by hematopoietic bone marrow transplantation with pre-conditioning of the recipient to allow engraftment of donor cells. Although this method of transplantation tolerance induction has proved successful in pre-clinical models, its use in humans is limited by the ethics of myeloablative pre-conditioning; however, trials in humans have been conducted with some success (reviewed in (78)).

Induction of peripheral tolerance to an allograft is a much safer approach for transplant patients; however, unanswered questions remain. There is strong evidence from rodent models that tolerance to an allograft can be achieved by the adoptive transfer of Tregs (reviewed in (79)), and the use of this cell type has recently moved into the clinic with several trials underway (80). Transplantation tolerance can also be induced by immature DCs, which present donor antigen without sufficient co-stimulation, leading to T-cell tolerance. Research in this area is focused on optimising protocols to maintain DCs in an immature state to reduce allo-reactive T-cell stimulation and induce tolerance. In addition, regulatory macrophages, which produce the anti-inflammatory cytokine IL-10 and induce Th2 responses, have recently been identified in mice and humans and show promise for tolerance induction in the clinic (81).

Many transplantation tolerance induction protocols have the potential to decrease the use of immunosuppressive drugs in transplantation patients; however, much research remains needed to assess the effectiveness of adoptive cell therapy, and to improve the safety of mixed chimerism induction.

1.1.5 T-cell co-stimulation

It was initially believed that TCR engagement with MHC was sufficient to induce activation of naïve T cells; however, experiments with primary T cell cultures proved that for optimal activation a second signal is required. This second signal comes from co-stimulatory molecules expressed by T cells binding to ligands on APCs. CD28 is the putative co-stimulatory molecule expressed by all T cells, and in the absence of signalling through CD28 T cells undergo anergy whereby they become unresponsive to antigen (82). The ligands for CD28 are CD80 and CD86, which are upregulated on APCs during inflammation. CD152 expressed on T cells can also bind CD80 and CD86 although with very different functional outcomes. CD152 is known as a co-inhibitory molecule as its

engagement leads to down-regulation of CD80 and CD86 on APCs and thus a dampening of the immune response. Approaches for blocking co-stimulation in transplantation models have used CTLA-4Ig with success (83). This has now been developed into a clinical strategy with the development of Belatacept, a CTLA-4Ig drug available for human use that has been used as immunosuppressive therapy for renal transplantation patients (84).

CD40 and its ligand CD154 are essential co-stimulatory molecules for the effective generation of high affinity isotype-switched antibodies. CD40/CD154 interactions are also important for DC survival, proliferation of B cells and activation of some antigen-specific T cells. Efforts to translate anti-CD154 therapy into the clinic was unfortunately halted, despite promising results in pre-clinical models, due to the expression of CD154 on activated platelets which led to adverse thromboembolic effects in treated individuals (85).

The programmed death (PD) 1 receptor is expressed on many cells of the immune system including NK cells and some DCs, and binds the ligands PDL1 and PDL2. It is not constitutively expressed on T cells but is up-regulated following activation, and ligation leads to down-regulation of T cell effector cytokines such as IFN- γ , TNF- α , and IL-2. This pathway has also shown importance in transplantation with PD1 knock-out recipients overcoming co-stimulation blockade-induced tolerance (86). As yet there are no reagents available for the activation of PD1 in humans, although recent efforts to switch off this pathway for the treatment of cancer have demonstrated its importance in human immune responses (87).

1.1.6 The importance of cell trafficking in transplantation

All of the pathways mentioned above require the activation of recipient T cells by APCs, for the initiation of graft rejection. In this context the APCs are most likely DCs of myeloid

lineage; although plasmacytoid DCs have also been implicated (88). As both the number of APCs and cognate T cells are low, specialised niches are required for them to encounter each other for an effective allo-immune response. It was originally thought that, in the case of fully-vascularised solid organ transplants, allo-sensitisation only occurred in the graft itself. A pivotal paper by Larsen *et al.* (52) first described an alternative route involving trafficking of donor-derived DCs from the graft to the spleen for interaction with CD4⁺ T cells. Contrary to this, the rejection of allogeneic skin grafts is dependent on the presence of local draining lymph nodes (DLN) (89); until recently the role of DLN in the allo-response to fully vascularized solid organ grafts had not been investigated.

A paper from Lakkis and colleagues demonstrated that mice lacking SLO failed to reject fully allogeneic heart grafts, and it was concluded that the lymph nodes and spleen provided the correct niche for interactions between APCs presenting donor antigen and recipient T cells, and that when absent recipient T cells were 'ignorant' to the presence of allo-antigen (90). However, the evidence presented in this paper has been disputed. It has been suggested that the *aly/aly* mice used in the study have a fundamental defect in antibody isotype switching and T cell homing, and this may explain the observations rather than the lack of lymph node tissue (91). This implies that a greater understanding of the mechanisms of immune cell trafficking between the graft and lymphoid tissue of the recipient is required.

1.2 Lymphatics

1.2.1 Introduction to the lymphatic system

The lymphatic system is the second circulatory system of the body, and is responsible for drainage of interstitial fluid from peripheral tissue back to the blood vasculature. In addition to its role in fluid homeostasis, the lymphatic system forms a vital network of

conduits for efficient trafficking of the cells and molecules of the immune system. This section will outline the physiological function of the lymphatic system, its development, and its dysfunction in disease.

1.2.2 Historical perspective

Although it was Hippocrates ‘the father of medicine’ who first described the presence of lymph nodes and chyle in humans in the 5th century BC, it wasn’t until much later, in the 16th century, that the Swedish intellectual Olaus Rudbeck explained the proper structure of the lymphatic system. Helped by the discovery by William Harvey of the blood circulatory system, Rudbeck correctly observed that fluid in lymphatic vessels drained away from tissue and converged at the thoracic duct, where it re-entered circulation via the blood. He also described the presence of valves in the large lymphatic vessels. The most comprehensive study of the human lymphatic system was published in 1938 by the French anatomist Rouviere. This was a continuation of the work of Sappey, who had developed a technique to visualise the lymphatic vessels of human cadavers using mercury (92).

1.2.3 Development of the lymphatic system

For many years the embryonic origins of lymphatic vessels had been debated, and it wasn’t until the discovery of the transcription factor *Prox1* that mouse studies confirmed a vascular origin for the lymphatic system (93). When *Prox1* was knocked out in mice, embryos did not survive past day E15 and were found to lack lymphatic vessels (94). *Prox1*-positive cells were found to migrate from the embryonic veins and form sprouting lymphatic vessels (95). Work then moved to finding the signalling pathway for this sprouting mechanism, and it was discovered that vascular endothelial growth factor (VEGF) C signalling via VEGFR3 is crucial for lymphatic endothelial progenitor cell migration from the veins (96). After migration from the veins, sprouting lymphatic

endothelial progenitor cells form lymph sacs which develop further into mature lymphatic vessels (97). Later in development of the mouse embryo, clusters of *Prox1*-positive cells have been observed in tissue such as skin (98) and heart (99), and lineage tracing experiments using inducible knockout mice have demonstrated a non-venous origin for these cells, which can migrate and proliferate to form lymphatic vessel networks within tissues.

For the blood and lymphatic systems to function properly they need to be mostly separated, to avoid entry of blood into lymph but to allow passage of lymph into blood. This is achieved by specialised lymphatic valves which develop at the junction of the thoracic duct and the jugular vein, the point where lymph drains into the blood circulation. Again *Prox1* is key to this process, and *Prox1* heterozygous mice have defective valves (100). Lymphatic valve development and maintenance are highly co-ordinated processes which are tightly controlled through specific signalling pathways, which will be discussed in detail later.

The adult lymphatic system consists of a hierarchical network of vessels, starting with the initial lymphatics (sometimes termed lymphatic capillaries) within tissue parenchyma, leading onto pre-collector then collector vessels which converge at the thoracic duct. There are two main processes involved in development of the lymphatic vessel network beyond the lymph sac: recruitment of smooth muscle cells and pericytes, and lymphatic valve formation. Recruitment of smooth muscle cells seems to be dependent on the extracellular matrix protein Reelin which is released from lymphatic endothelial cells (LECs) upon contact with smooth muscle cells (101). Valve formation and vascular remodelling in pre-collector and collector vessels is controlled by the EphB4/ephrin B2 and angiopoietin/Tie axes (102).

The interaction between macrophages and lymphatic endothelial cells has been highlighted in lymphatic remodelling in disease settings, which will be discussed later,

but there is also evidence that macrophages interact with lymphatic endothelial cells during embryogenesis. It has been found that macrophages provide essential growth and patterning signals to developing lymphatic vessels in the form of VEGF-C (103).

1.2.4 Physiological role of the lymphatic system

The lymphatic system carries out the vital function of draining proteins and cells from the interstitium of tissues which are too large to be absorbed by the blood capillary network. The majority of peripheral organs and tissue contain lymphatic vessels through which fluid containing cells and proteins can drain and be transported back to the blood circulation in a uni-directional flow. Lymph from the lower half of the body and the left upper half drains directly into the thoracic duct which empties into the blood at the junction of the left jugular vein and left subclavian vein; whereas lymph from the right upper half of the body drains into the right lymph duct which enters the blood at the right jugular and right subclavian vein. As well as draining proteins and cells from peripheral tissues, the lymphatic system plays a role in nutrient absorption in the gut, particularly the absorption of dietary fats.

The rate of lymph flow from the periphery is controlled by the rate of leakage of proteins from the blood network into the interstitium. As the interstitial protein concentration increases, the osmotic force causes fluid to move from the blood into the tissue. This increase in fluid pressure causes the lymphatic capillaries to open at the junctions between lymphatic endothelial cells to allow fluid to enter the vessel. The pressure inside the capillary then increases causing the junctions to close and lymph to flow away from the tissue. Therefore, eventually the transport of fluid away from the tissue by the lymphatics balances out the effect of leakage from the blood vessels, and homeostasis of extracellular fluid concentration is achieved (104).

1.2.5 Disorders of the lymphatic system

The understanding of how defective lymphatic vessel function can cause or exacerbate human disease is improving. The most notorious lymphatic vessel disorder is lymphoedema; a common condition with multiple and complex aetiology. It can be the result of genetic abnormalities affecting lymphatic vessel function, or be secondary to lymphatic vessel insult. The disease is characterized by the disproportionate accumulation of interstitial fluid, and in chronic cases can be aggravated by fibrosis, adipose deposition and inflammation. There are currently no treatments aimed at curing the disease; and therapies aim to relieve pain and disability. However, new insights are being made into the genetic basis of primary lymphedema, and the importance of the VEGF-C/VEGFR3 signalling pathway has been highlighted, with many components being mutated in affected patients (105).

Also there is now known to be a definite link between cardiovascular disease and lymphatic vessel function. The heart has a high density of lymphatic vessels, which show a proliferative response to myocardial infarction, atherosclerosis, and infectious disease (106). However, data from mouse models have shown that the promotion of lymphatic vessel proliferation using pro-lymphangiogenic factors such as VEGF-C improves resolution of damage caused by myocardial infarction (99). So the proliferation of LECs in this case may be a protective response.

It is also interesting to note the emerging link between lymphoedema and obesity. In *Prox1* heterozygous mice, lymph containing pro-adipogenic factors leaks from dysfunctional lymphatic vessels and leads to the development of obesity (107). This coincides with long-standing clinical observations of lymphoedema patients suffering from obesity (108).

In conclusion, a greater understanding of how lymphatic vessels function, and the signalling pathways involved in the proliferation and maintenance of vessels, is leading

to the development of new therapies for patients suffering from diseases caused by lymphatic vessel dysfunction.

1.2.6 Structure of the lymphatic system

In contrast to the blood circulatory system, the lymphatic system is linear. This means that lymph containing interstitial fluid, large extracellular molecules and cells drains from tissue and organs into initial lymphatics, moves through to larger collecting vessels which are interconnected with lymph nodes, and is eventually returned to the blood system via the thoracic duct. The hierarchical structure of the lymphatic system is key to its function.

1.2.6.1 The initial lymphatics

The initial lymphatics, sometimes referred to as lymphatic capillaries, are blind-ended vessels found in nearly all vascularised tissue, and express high levels of the lymphatic vessel endothelial hyaluronan receptor 1 (LYVE-1). Typically they are 30-80µm in diameter and comprise a single layer of LECs with no basement membrane. Unlike the structure of blood capillaries, the LECs making up initial lymphatics are joined together by dis-continuous 'button like' junctions, which make the vessels extremely permeable to fluid and cells (109). The LECs are connected to the extracellular matrix of tissue by anchoring filaments that are in turn attached to collagen fibres (110). These fibres tighten in response to tissue swelling, which causes the lymphatic vessel to open and fluid to enter the lumen. From here lymph moves into pre-collector vessels, which are surrounded by a thin layer of smooth muscle cells.

1.2.6.2 The collecting lymphatics

The pre-collector vessels drain into collecting lymphatics which are vessels specialized for the transport of lymph rather than drainage from tissue. Collecting lymphatics are

characterized by the presence of a basement membrane, a defined layer of smooth muscle cells, and continuous 'zipper-like' junctions (109). The action of the associated smooth muscle cells and surrounding skeletal muscle propels the lymph in uni-directional flow towards re-circulation. The collecting lymphatic vessels from distinct segments, called lymphangions, separated by valves which open and close in a co-ordinated sequence to ensure the uni-directional flow of lymph (Figure 1.1).

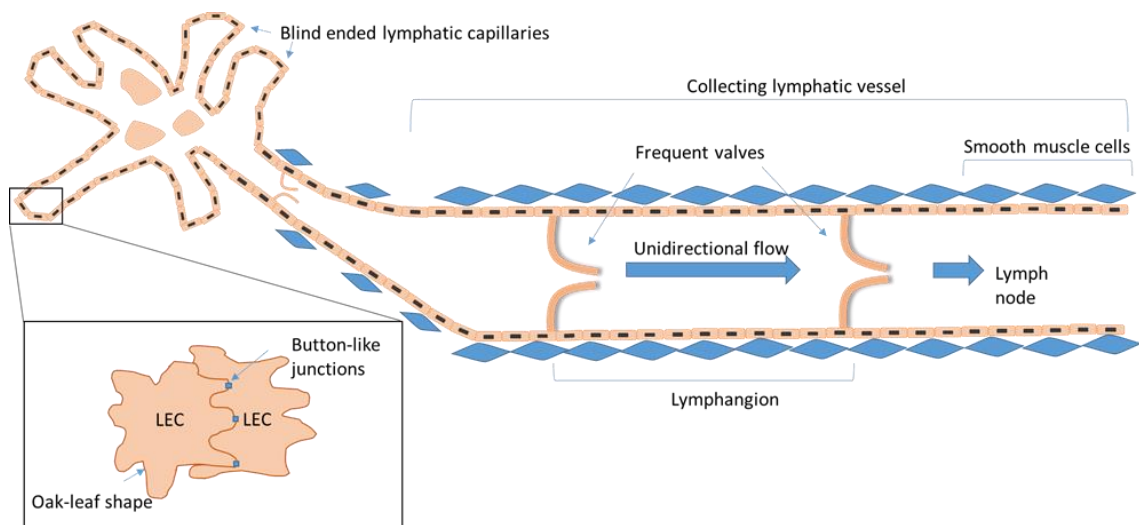


Figure 1.1- The hierarchical structure of the lymphatic system.

Blind-ended lymphatic capillaries in tissue are composed of oak leaf-shaped LECs with button-like junctions to allow for efficient drainage of fluid and cells. Collecting lymphatics are accompanied by a smooth muscle cell layer and contain frequently spaced valves to prevent backflow of lymph.

1.2.6.3 Lymphatic valves

Lymphatic valves are essential to prevent the retrograde flow of lymph back into tissue, and indeed patients with lymphedema have been found to have genetic abnormalities in key pathways of lymphatic valve development and maintenance (111).

Recent elegant studies in the mouse have elucidated the mechanism of how lymphatic valves form during embryogenesis and in early life (reviewed in (112)). Firstly, there is clustering of LECs at branch points of lymphatic capillaries, which coincides with up-

regulation of the transcription factors *Prox1* and *Foxc2*, as well as down-regulation of LYVE-1 expression. These cells then develop an elongated morphology and re-arrange their cell-cell junctions, and eventually form a protrusion into the vessel lumen. This process is dependent on expression of the adhesion molecule receptor, integrin- α 9, which allows for proper arrangement of the extracellular matrix at the edges of the LEC protrusions. Mice deficient in integrin- α 9 fail to develop fully elongated valve leaflets, and missense mutations in human foetuses causes a lethal phenotype (113). Maturation of the valve is then controlled by various signalling pathways including ephrin B2-eph4 (114), angiopoietin2-Tie2 (115) and phosphoinositide (PI) 3 kinase-protein kinase B (116). Mutations in the PDZ cytoplasmic domain of ephrin B2 result in embryonic lethality characterized by chylothorax due to inhibition of lymphatic drainage into the thoracic duct (102). EphrinB2-eph4 signalling has also been shown to play an essential role in lymphatic and blood vessel angiogenesis. A link between the ephrin B2-eph4 and VEGFR3-VEGF-C pathways was found by Wang *et al.* Stimulation of cultured LECs with recombinant ephrin B2 led to internalisation of VEGFR3, which is required for downstream signalling, and this process was compromised in ephrin B2 knock-out cells (117).

1.2.6.4 Additional roles of ephrins in immunity

In addition to the role that the eph/ephrin signalling pathway plays in lymphatic development and maintenance, it has more recently become implicated in other settings. The eph family of neuronal guidance molecules and their ligands, the ephrins, are the most abundant group of receptor tyrosine kinases in the mammalian genome. The role they play in embryogenesis and cancer pathology has been well established; however, they are now being implicated in inflammation and immunity. Expression of ephs and ephrins across cell types is varied, and signalling can occur either through the receptor (forward) or the ligand (reverse) (118).

Eph/ephrin signalling most commonly results in changes in cell motility; either repulsion or adhesion of cells to guide in the organisation of cells in developing tissue, or during *de novo* growth such as in lymphangiogenesis (102). In addition to patterning responses, signalling via the eph/ephrin pathway can affect cell differentiation, proliferation and gene expression (118), further indicating a potential role in chronic inflammation.

Enhanced expression of ephrin B2 has been found on the blood endothelium in areas of atherosclerotic plaque formation, where it was found to aid adhesion and transmigration of infiltrating monocytes which express the ephB4 receptor (119). Also, addition of immobilized ephrin B2 to monocytes in culture caused them to upregulate expression of chemokine (c-c motif) ligand (CCL) 21 (119). In fact, many leukocytes express ephrins, and have been found to modulate their expression in response to pro-inflammatory signals such as TNF- α (120). In particular, ephrin B2 has been demonstrated as a co-stimulatory molecule for T cells (121). In the study by Yu *at al.* ephrin B2 mRNA was found to be expressed in the white pulp of the spleen and the cortex of the thymus. At the protein level it was found to be expressed on the surface of T cells and monocytes, whereas its receptors were mainly found on T cells. T-cell stimulation could be induced using solid phase ephrin B2 and sub-optimal amounts of CD3. This led to the production of IFN- γ and enhanced cytotoxic activity of CD8⁺ T cells. Evidence was also provided for ephrin B2 localisation in the immunological synapse, linking it directly with T-cell co-stimulation (121).

1.2.7 Lymphatics and immunity

Recently, it has become more fully appreciated that the lymphatic system plays an essential role in immunity (122). The structure of the system, with drainage from the interstitium to the lymph nodes and back into blood circulation, means that antigens in the periphery are transported to the sites where they can be recognised effectively by cells of the adaptive immune system. The lymph nodes provide a perfect niche for interactions

between APCs and T and B lymphocytes, and once activated, lymphocytes are guided out of the lymph nodes, also via lymphatic vessels, back towards blood circulation where they can access the peripheral sites where the antigen is present. Lymphatic vessels are ideally suited to the function of transporting APCs to the draining lymph nodes under inflammatory conditions, reacting promptly to inflammatory stimuli to change surface expression of adhesion molecules and thus allowing co-ordinated migration of APCs to the site of T-cell activation.

Lymphatic vessels also show a proliferative response in immune reactions, and via a process called lymphangiogenesis, vessels expand in size and number in sites where there is an ongoing immune response. The exact function of this lymphatic response is unknown, and it seems to be dependent on whether the prevailing conditions are pro- or anti-inflammatory.

In this section, the mechanisms of immune cell trafficking through lymphatics, and the process of lymphangiogenesis, will be discussed in detail, with relation to their influence on the immune response following transplantation.

1.2.7.1 Leukocyte trafficking

DCs are known to be the most potent APCs of the immune system, and much of the work towards elucidating the mechanisms of lymphatic transmigration has therefore used DCs. In homeostasis, DCs continue to migrate from the periphery to the DLN in order to present self-antigens. This is crucial for the maintenance of tolerance to self, and indeed mice lacking lymphatic vessels develop severe autoimmunity due to a defect in the homeostatic transport of DCs (123). Under steady-state conditions, DCs move in an amoeboid fashion towards the lymphatic vessel in an integrin-independent process (124, 125), that requires a chemotactic chemokine gradient (126). The chemokine-receptor pair crucial for lymphatic migration of DCs is CCL21, which is produced by

LECs, and CCR7, which is expressed by DCs. DCs then enter the lymphatic vessel at portals, which are areas between LEC adherens junctions where basement membrane is least dense (127). From here they move inside the vessel in the direction of lymph flow towards the collecting vessel and ultimately enter the DLN.

Under inflammatory conditions, the extra-cellular matrix of the interstitium is not conducive to the amoeboid movement of DC due to loosening of the collagen fibres (128). Therefore, entry of DC into the lymphatic vessel lumen becomes an active process dependent on integrins, particularly intercellular adhesion molecule (ICAM) -1 (Figure 1.2). The seminal paper by Johnson *et al.* showed that DC transmigration across the lymphatic endothelium in inflammatory conditions was dependent on ICAM-1, and that this process could be blocked *in vitro* by administering anti-ICAM-1 antibodies (129). In inflammation, movement of DCs towards the vessel is still dependent on a CCL21 chemokine gradient, and in fact LECs increase secretion of CCL21 following an inflammatory stimulus (130). As interstitial flow increases toward the lymphatic vessel, more CCL21 is needed to maintain the gradient in favour of guiding DCs towards the vessel. CCL21 is also able to bind to heparan sulphates within the extra-cellular matrix in order to prevent it being washed away by the flow of fluid in the opposite direction (131). In addition, it has been found that migration of immune cells to DLN is unaffected when lymphatic vessels are sparse, even if flow is dramatically decreased, because the CCL21 gradient becomes more favourable (132). Again DCs then enter the lymphatic vessel lumen at portals where basement membrane is least dense. It is apparent that DC migration through lymphatics under inflammatory conditions is an active process involving co-ordinated up-regulation of various molecules by LEC and DC, which is crucial for recruitment of DC from the interstitium towards the vessel and also for transmigration across the endothelium.

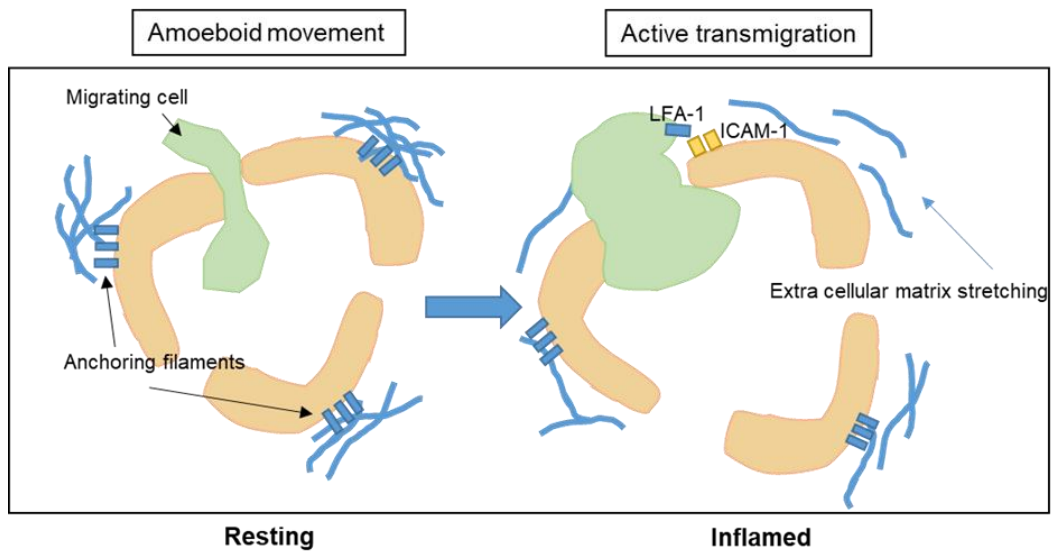


Figure 1.2- Active transmigration of leukocytes across lymphatic endothelium during inflammation.

Under normal conditions DCs move in amoeboid fashion and enter lymphatic vessels at portals, and traffic to draining lymph nodes. During inflammation, collagen fibres loosen and DCs require integrin binding (namely ICAM-1 to its receptor LFA-1) to enter lymphatic vessels.

LECs express a crucial immune regulatory molecule called D6 that scavenges excess inflammatory chemokines, preventing lymphatic congestion and facilitating resolution of inflammation. Inflammation is exacerbated when this molecule is absent (133).

As mentioned previously, initial lymphatics express high levels of LYVE-1, and indeed this molecule is often used exclusively as a marker for lymphatics (134). LYVE-1 is a receptor for hyaluronic acid (HA) and is crucial for lymphatic uptake of HA from the interstitium and transport to the lymph node for degradation (135). The presence of HA fragments has been implicated in transplant rejection, and in a model of lung transplantation increased lymphatic vessel density was correlated with greater clearance of HA from the graft and improved survival (136). It is also true that LYVE-1 is involved in adhesion of DCs and macrophages to the lymphatic endothelium (137); however, more research is needed to fully elucidate the role of LYVE-1 in lymphatic transport.

The fact that under inflammatory conditions LECs actively recruit DCs from within tissue interstitium for mobilization to lymph nodes means that the lymphatic vessels of the donor

and the recipient could potentially play a role in the immune response following transplantation (Figure 1.3). Indeed, LECs express TLR4 which as mentioned previously is a receptor for DAMPs and has been heavily implicated in ischemia-reperfusion injury following transplantation (138). Activation of TLR4 on LECs leads to activation of the transcription factor NF- κ B (139), which leads to up-regulation of inflammation-associated molecules including ICAM-1 (140). In this way, inflammation-induced activation of the lymphatic endothelium within graft tissue could promote migration of donor-derived DCs to the DLN where they would activate recipient T cells via the direct pathway of allo-recognition, ultimately exacerbating the immune response.

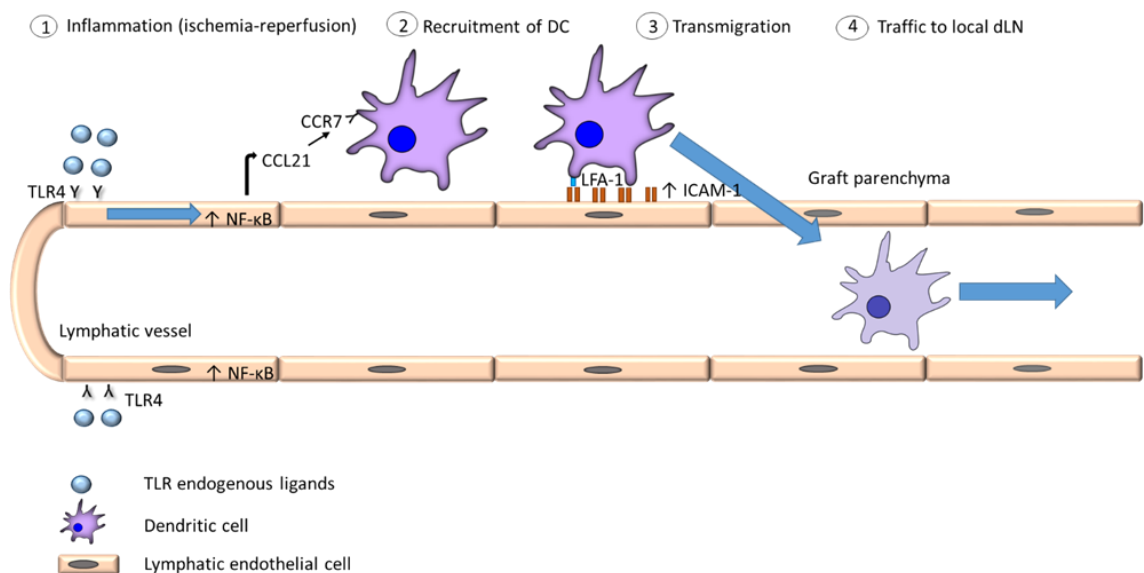


Figure 1.3- Proposed mechanism of lymphatic vessel activation following transplantation. (1) Inflammation caused by ischemia reperfusion releases TLR ligands such as DAMPs, which bind TLR4 on LECs within the graft parenchyma. (2) This leads to activation of NF- κ B, and subsequent upregulation of expression of CCL21 and ICAM-1. (3) DCs migrate towards CCL21, transmigrate across the endothelium in an ICAM-1-dependent manner and (4) traffic towards the local DLN.

1.2.8 Lymphangiogenesis

The term lymphangiogenesis refers to the process of growth and expansion of lymphatic vessels from pre-existing vessels. This process is essential in development, as outlined above; however, in adults it is usually associated with pathological conditions.

Lymphangiogenesis has been implicated in cancer (141), chronic inflammation (142) and transplant rejection (143). Although it has been clear for many years that lymphatic networks expand within tissues of patients suffering these diseases, the mechanisms involved in the initiation and progression of lymphangiogenesis are only now starting to be deciphered, and targeted therapies towards them developed. This section will discuss these mechanisms, specifically how they relate to the role of lymphangiogenesis in transplantation.

1.2.8.1 Mechanisms of lymphangiogenesis

The VEGF-C/D and VEGFR3 pathway is the central pathway in lymphangiogenesis (144). As mentioned previously, VEGFC/VEGFR3 signalling is essential for lymphatic sprouting from the cardinal vein in embryogenesis (145). Activation of VEGFR3 leads to phosphorylation of the serine kinases AKT and extracellular signal-related kinase (ERK), which promotes proliferation, migration and survival of LECs (146). PI3K, which is upstream of AKT, interacts directly with VEGFR3 and promotes tube formation (147). Interestingly, defects in the PI3K pathway affect lymphatic vasculature only and have no effect on blood vessels; suggesting that AKT functions distinctively in LECs. The congenital primary lymphedema condition Milroy's disease is caused by missense mutations in the tyrosine kinase domain of VEGFR3 (105).

The VEGF and VEGFR2 pathway plays less of a role in lymphangiogenesis than the VEGFC/VEGFR3 pathway. Specific activation of this pathway causes vessel enlargement but does not initiate sprouting (148), and deletion of the VEGFR2 gene in LECs does not affect lymphatic vessel function in embryogenesis and adult mice (149). There are also data to show that the Notch pathway plays a role in VEGF/VEGFR2-induced lymphangiogenesis. It was found that lymphangiogenesis occurring via this pathway was enhanced when the Notch pathway was inhibited; and this was not seen in VEGFC/VEGFR3-induced lymphangiogenesis (150).

The collagen and calcium-binding EGF domain-containing protein 1 (CCBE1) is a highly conserved lymphangiogenic factor, and the result of deletion of this protein is similar to VEGFC deletion, with embryos not forming lymphatic vessels (151). Mutations in the CCBE1 gene in humans cause primary lymphedema in Henneken's syndrome (152). Exogenous CCBE1 has little effect on inducing lymphangiogenesis, but seems to interact with the VEGFC pathway (153).

Semaphorins and neuropilins have traditionally been described for their pivotal role in the central nervous system; however, they are now becoming recognised in the field of lymphangiogenesis. Neuropilin (NRP) 2 is a co-receptor for VEGFC and binding causes co-internalization of the two receptors which enhances VEGFC signalling (154). NRP2-deficient mice have normal blood vasculature but decreased density of lymphatic capillaries in tissue (155). The NRP1 ligand semaphorin (SEMA) 3A is highly expressed in LECs and is particularly involved in lymphatic valve formation, where it has been shown to facilitate the migration of valve leaflet cells (156).

Angiopoietin (ANG) 1 causes phosphorylation of the endothelial cell-specific tyrosine kinase receptor (TIE) 2 receptor in LECs which promotes sprouting (157), as does ANG2; however, the latter acts in an autocrine fashion (158). ANG2-deficient mice survive embryogenesis but after birth develop disease due to lymphatic hypoplasia (159). In pathological lymphangiogenesis, up-regulation of ANG2 promotes lymphangiogenesis associated with wound healing (160).

Sphingosine 1-phosphate (S1P) is a bioactive phospholipid that has an essential role in vascular development and response to inflammation. It has been shown to induce LEC migration and tube formation *in vitro* (161). This molecule also stimulates ANG2 production by LECs (162). When it is specifically deleted in LECs, the result is disruptive lymphatic patterning due to defects in cell-cell junctions (163).

Many of the signalling pathways mentioned thus far function in a paracrine fashion with specific ligands being secreted by cells other than the LECs which make up the vessels, binding to receptors on the LEC and inducing signalling within the LEC. LECs themselves also communicate with each other via the Notch and ephrin B2 pathways. It is now becoming clear that Notch 1 is a regulator of lymphangiogenesis (150). As mentioned previously, inhibition of Notch 1 *in vitro* enhances lymphatic sprouting. Ephrin B2 mutant mice have miss-patterned lymphatic vasculature and lack lymphatic valves. In addition to its role in lymphatic development, ephrin B2 also functions in pathological lymphangiogenesis. It enhances VEGFR3 internalization following VEGFC stimulation, and blocking with specific antibodies has been shown to inhibit lymphangiogenesis in tumours (164).

In terms of inhibiting lymphangiogenesis, there are two main endogenous inhibitors of the process. Firstly, transforming growth factor (TGF) β has been shown to inhibit lymphangiogenesis and the migration of LEC *in vitro* (165), and dampen lymphangiogenesis in *in vivo* wound repair models (166). Secondly, IFN γ produced by T cells inhibits lymphangiogenesis in models of lymph node lymphatic expansion (167).

Pro-lymphangiogenic signalling is active during embryogenesis to ensure correct development of the lymphatic system; it then reduces significantly but can be re-activated during disease. In cancer, expansion of lymphatics in the tumour environment enhances lymph node metastasis, and in chronic inflammation increased lymphatic density exacerbates the immune response. Because of this there has been a drive to develop anti-lymphangiogenic therapies, with some success in pre-clinical animal models (168). Most therapies have focused on inhibition of VEGFR3 signalling as the central lymphangiogenic pathway. This can be achieved by blocking the ligands from binding to the receptor or blocking dimerization and internalization of the receptor after ligand binding.

The lymphangiogenic response in cancer and inflammation can also be inhibited indirectly by reducing the amount of VEGF-C in the diseased tissue. This is achieved mainly by reducing the influx of inflammatory cells into the tissue. Reducing pro-inflammatory cytokine production can halt recruitment of VEGF-C-producing macrophages. Indeed, in a model of airway infection, anti-TNF- α antibodies were used successfully to decrease leukocyte infiltration and ensuing lymphatic remodelling (169). Systemic depletion of macrophages has also been shown to be successful in treating injury-induced lymphangiogenesis of the cornea (170).

On the other hand pro-lymphangiogenic therapies are being developed for the treatment of lymphedema. VEGFC gene therapy has been used to restore lymphatic function in mouse models of lymphedema, and this has also been combined with lymph node transplantation to improve efficacy (171).

There are many questions remaining in the field of pathological lymphangiogenesis, for instance: how are newly-formed lymphatic vessels maintained in diseased tissue and how long do they persist, and do anti- and pro-lymphangiogenic therapies have differential effects on lymphatic capillaries compared with collecting vessels? This is an emerging field with much promise but more pre-clinical research is required.

1.2.8.2 Lymphangiogenesis in transplantation

Despite the relative importance of the lymphatic vasculature in leukocyte trafficking and the allo-response, its pathophysiology in this setting has received little attention. It is now clear that extensive lymphatic remodelling, of which there are two types, occurs following solid organ transplantation (172). The first involves reconnection of donor lymphatics to those of the recipient, which has been demonstrated to occur within three weeks in an early model of renal transplantation (173). The dynamics of this process, however, have

yet to be investigated. The second mode of lymphatic remodelling in the allo-response which has received more attention (143, 172, 174), is the phenomenon of *de novo* lymphangiogenesis, whereby new lymphatic vessels are generated in response to the inflammatory milieu of the transplanted organ. Increased lymphatic density within the graft could lead to enhanced clearance of inflammatory infiltrate or increased trafficking of APCs to the local DLN to perpetuate the allo-response. Expansion of lymphatic networks in lymph nodes draining inflamed tissue has also been observed (175), and would suggest increased likelihood of interactions between APCs and T cells. It is also unclear whether *de novo* lymphangiogenesis in transplantation is a function of the disease process, or the system's attempt to resolve it. The contribution of lymphangiogenesis and the lymphatic vasculature to the allo-response, and whether or not they impact positively or negatively on graft outcome, will be discussed in more detail later.

Donor DC can traffic to the spleen via reverse transmigration into the bloodstream, as shown for plasmacytoid DC after heart transplantation (88). Alternatively, DC may leave the donor organ via the open severed ends of the lymphatic vessels into the immediate surrounding area. They will then be taken up by the lymphatic capillaries in the local vicinity and traffic to the local DLN. This latter process has been investigated in our laboratory, where single photo emission computed tomography/CT (SPECT/CT) imaging technology has been used to visualise and quantify post-transplant lymphatic flow in murine models of heterotopic heart transplantation (176, 177). In these models, lymph flows from the graft to the mediastinal lymph nodes, the DLN of the peritoneum, and this was further confirmed by the presence of donor-specific T cells in the lymph nodes highlighted by SPECT/CT.

Lymphangiogenesis is frequently associated with transplant rejection (174, 178, 179), and the order of events leading to the appearance of new lymphatic vessels has been well characterised (174). The chief cellular constituent involved in the process of post-

transplant lymphangiogenesis is the macrophage. LECs that make up the lymphatic vessels proliferate in response to pro-lymphangiogenic VEGF-C, produced by macrophages, binding to VEGFR-3 (146). CD11b⁺ macrophages were found to be critical for the development of inflammation-induced lymphangiogenesis in the cornea, and expressed the LEC markers LYVE-1 and Prox-1, and could form tube-like structures *in vitro* (180). Activation of the NF-κB pathway in LECs via the binding of endogenous ligands produced in reaction to tissue stress to TLRs, upregulates Prox-1 and VEGFR3 expression which makes them more vulnerable to VEGF-C stimulation (181).

As previously mentioned, during the transplant procedure the lymphatics vessels of the donor are not reconnected to those of the recipient, therefore it is likely that the efficiency of the lymphatic traffic of leukocytes in the initial post-transplant period, in terms of speed and number of cells transported, would be affected compared with intact lymphatic vessels. Expansion of the lymphatic networks within the graft and local DLN in response to inflammation is also likely to have an effect on graft outcome, either positively by promoting clearance of inflammatory infiltrate, or negatively by increasing DC migration to DLN and priming of recipient T cells. Research in this area is limited to a few studies, providing circumstantial evidence only and with conflicting results; some suggest a beneficial role for lymphatics while others suggest the opposite, which will now be discussed.

It has been shown that rejected human cardiac allografts have a lower density of VEGFR3⁺ lymphatics compared with patients with only moderate rejection (182). In an experimental model of canine lung transplantation, lack of lymphatic drainage was associated with rejected organs (183). Additionally, in rat cardiac allografts, a decrease in lymphatic density was observed in the inner myocardium post-transplantation (184). It is thought that the decrease in lymphatic density contributes to rejection through the retention of graft-destructive cells, and the accumulation of cytokines that perpetuate the local immune response. In support of this theory, it was shown that mechanical

interruption of lymphatic drainage induced the expression of multiple genes involved in acute inflammation, complement activation and B-cell humoral immunity (185). Lymphatic vessels in human kidney transplants are associated with lymphocytic infiltrates (172). Although the density of lymphatic vessels was not associated with acute or chronic rejection, grafts with lymphatic vessels within infiltrates had better graft function one year after transplantation compared to those without such vessels. Put together, these data provide circumstantial evidence that increased lymphatic vessel density within transplanted vascularised organs is associated with better graft outcome. This suggests that pharmacological modulation of lymphangiogenesis may be a possible strategy to improve graft outcome.

Despite the evidence for a positive role for lymphatics in transplantation, it has been suggested that lymphatics may play the opposite role and impact graft survival negatively. Increased lymphatic drainage from donor organs may facilitate trafficking of APCs to SLO, promoting allo-immunity. In our laboratory, using a mouse kidney model of transplant tolerance, the density of lymphatic vessels increased with time; however, their presence within the tertiary lymphoid organs that formed within the allografts was associated with reduced graft function (186). In a study of human renal transplant biopsy material, transplant rejection was observed to be caused by a lymphocyte-rich inflammatory infiltrate that attacked cortical tubules and endothelial cells. This corresponded with a >50-fold increase of lymphatic vessel density. Numerous CCR7⁺ cells within the infiltrates seemed to be attracted by CCL21 produced and released by LECs. The authors of this paper speculated that lymphatic neo-angiogenesis not only contributes to the export of the infiltrate, but is also involved in the maintenance of the allo-reactive immune response in renal allografts (143). It has also been demonstrated in islet allografts that interfering with lymphatic function leads to inhibition of lymphangiogenesis and prolonged or indefinite allograft survival (178). It is not known whether an enhanced and more physiological connection between donor and recipient lymphatic vessels, through which DC can traffic, may result in a stronger or weaker

immune response. Evidence to date for and against lymphatics being beneficial in transplantation is sparse and mainly observational. Whether observed changes in lymphatic density are the cause or effect of the immune process is unknown. The effects of transplant rejection itself on the structure and function of lymphatic vessels also remains unclear.

1.3 The lymph nodes

Presentation of antigens to T cells is central to the function of the adaptive immune system. This is mostly carried out by migratory DCs which transport antigen from the periphery to the SLO where naïve T cells reside. The SLO including spleen, lymph nodes, Peyer's patches and tonsils are unique structures which provide the perfect conditions for immune surveillance of the periphery, ensuring close contact of the cells required to mount an effective immune response. Antigen arrives at these structures either passively through lymph draining from tissue, or actively through transport by migratory APCs.

In this section the specific role of the lymph nodes in adaptive immunity will be explored; including a detailed description of the emerging field of LEC biology.

1.3.1 Structure

Lymph nodes are highly organised structures that develop at junctions of collecting lymphatics draining interstitial fluid and cells from tissues. Afferent lymphatics draining lymph from the periphery converge into the sub-capsular sinus of the lymph node. This is a sinus system lined with LECs interspersed with CD169⁺ macrophages, which functions to guide antigen and leukocytes towards the paracortex. The paracortex contains follicles rich in B cells and follicular DCs, ensuring capture and presentation of

soluble antigens. Deeper within the lymph node structure are the paracortical T cell zones, supported by reticular fibres and stromal networks for guidance of T cells and DCs. Lymph eventually enters the medullary sinuses, which converge to the efferent lymphatic vessel and leaves the lymph node (this process is reviewed in (187)). Leukocytes can also enter the lymph node from the blood system via blood vessels called high endothelial venules (HEVs); these are specialized for the delivery of naïve lymphocytes into the lymph node paracortex (188); (Figure 1.4).

Dendritic cells which migrate to the lymph nodes from the periphery to present antigen to T cells eventually incorporate into the network of resident DCs, a process likely to be dependent on reduced signalling through CCR7 (189). By contrast, T cells that do not encounter cognate antigen in the lymph rapidly leave through the efferent lymphatics via cortical sinuses. Egress is dependent on S1P/S1PR1 signalling which over-rides the retention signals of CCR7 and CCL21 (190).

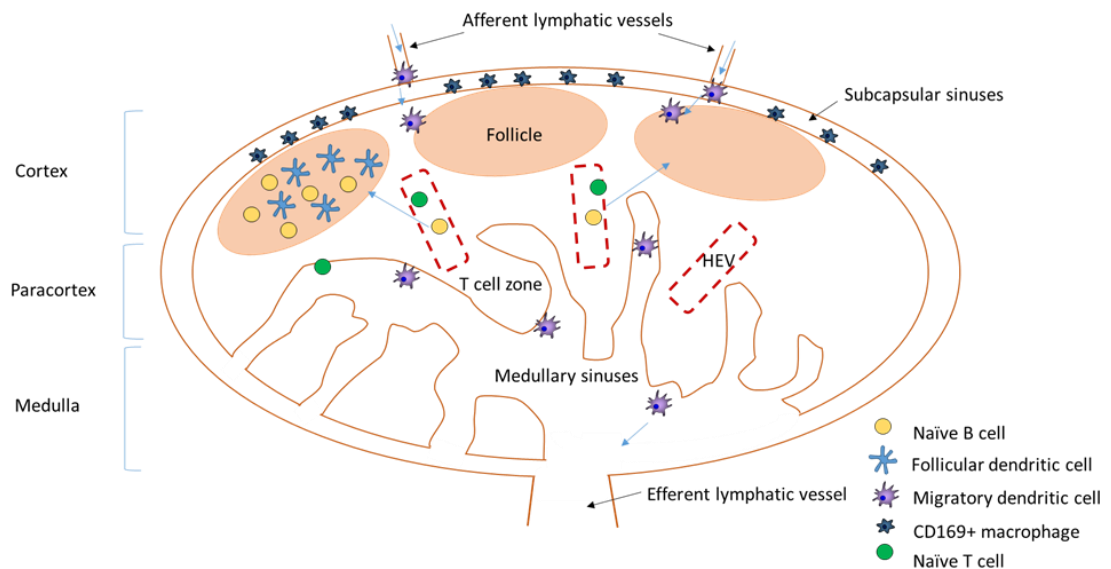


Figure 1.4- Structure of the lymph node. Leukocytes enter via the afferent lymphatic vessels and are guided towards the follicles which contain specialized DCs ensuring efficient delivery of antigen to naïve lymphocytes. They then enter the T cell zones within the paracortex. They leave via the medullary sinus which converges into the efferent lymphatic vessel. Leukocytes can also enter via HEVs.

1.3.2 Development

Development of the lymph nodes occurs during embryogenesis and is orchestrated by a subset of haematopoietic cells known as lymphoid tissue inducer cells (LTi). These cells interact with chemokine (c-x-c motif) ligand (CXCL) 13-producing mesenchymal cells, which give rise to lymph node stromal cells. It is thought that they are stimulated to produce CXCL13 by local production of retinoic acid by nerve fibres, although this is yet to be confirmed. CXCL13 attracts CXCR5-expressing LTi cells, and signalling via receptor activator of nuclear factor κ B (RANK)-RANKL in these cells leads to upregulation of lymphotoxin (LT) α 1 β 2. LT α 1 β 2 causes mesenchymal cells to differentiate into lymphoid organiser cells (LTo) which leads to further recruitment of LTi cells resulting in a positive feedback loop for continued recruitment of lymph node progenitor cells. LTo cells then secrete CCL19 and CCL21, and express adhesion molecules to attract lymphocytes. These LTo cells eventually become the different stromal cell populations of the lymph node, i.e. fibroblastic reticular cells and follicular DCs (reviewed in (191)).

1.3.3 Response to inflammation

Lymph nodes draining inflamed tissue expand in size and cellularity through lymphangiogenesis. Remodelling of the lymph node expands the conduit systems delivering antigen and APCs from the inflamed tissue. This results in an increase in lymph flow towards the lymph node cortex. Increases in expression of leukocyte attracting chemokines such as CCL21 by HEVs and LECs attracts mature DCs from the inflamed tissue, and increases the likelihood of interactions with cognate T cells. The process of lymph node lymphangiogenesis in response to inflammation has been found to be dependent on B cells (192). Downregulation of S1P1, the receptor for sphingosine 1 phosphate, on lymphocytes halts egress from the lymph node, again increasing cell-cell interactions.

1.3.4 Lymphatic endothelial cells

With the relatively recent discovery of specific markers for LECs in humans and mice such as LYVE-1 (134), podoplanin (193), and VEGFR3 (194); research in this field has grown. Pure populations of LEC can be isolated from a variety of tissue types and pathologies, allowing elucidation of their functionality, in particular their ability to regulate the adaptive immune response (reviewed in (122)).

LECs express MHC class I and can present self-antigen to CD8⁺ T cells for tolerance induction in non-transplant models (195, 196). Lymph node LEC (LN-LEC) express high levels of the co-inhibitory molecule PDL1, and low levels of the classic co-stimulatory molecules CD80 and CD86. The absence of sufficient co-stimulatory signals leads to upregulation of PD1 on CD8⁺ T cells and subsequent engagement with PDL1 on LEC in the lymph node leading to CD8⁺ T cell deletion (196). Therefore, LECs contribute to peripheral tolerance by inducing CD8⁺ T cell deletion via PDL1. Lymph nodes have been found to be an important site for self-tolerance induction, with many lymph node stromal cell types (including LEC) having the ability to directly present self-antigen and induce CD8⁺ T cell deletion (197). In a melanoma model, tumour expression of VEGF-C was found to promote immune tolerance of tumours by the host. Local tumour-specific CD8⁺ T cells were deleted, and LN-LECs were able to cross-present tumour antigen, and drive CD8⁺ T cell proliferation and apoptosis *ex vivo* (198).

LEC-mediated induction of CD4⁺ T cell tolerance is less well characterised, although some progress has been made. It appears that CD4⁺ T cell self-tolerance induction is mediated by interaction with DCs. MHC class II expression by LECs is under the control of the IFN- γ inducible promoter IV, therefore its expression is minimal in steady-state conditions. Dubrot *et al.* found that LECs acquire antigenic peptide-MHC class II complexes from DCs as a result of cell-cell contact and exosomes (199). These acquired complexes are presented to cognate CD4⁺ T cells, resulting in CD4⁺ T cell dysfunction

and resistance to further stimulation. Others have found that LEC can act as antigen reservoirs for DCs (200). Although LECs do express MHC class II (albeit minimally), they cannot load endogenous peptides onto MHC II molecules due to the lack of H2-M. Therefore, they transfer endogenous peptides to DCs, which are then loaded onto MHC class II and presented to CD4⁺ T cells for tolerance induction. It appears that endogenous MHC class II expression by LECs functions to provide inhibitory signals to CD8⁺ T cells via interaction with the lymphocyte activation gene (LAG)-3 ligand (200). When human LN-LECs were stimulated with IFN- γ they were shown to take up and process antigen, but failed to stimulate proliferation of allogeneic CD4⁺ T cells (201). Indoleamine 2,3 dioxygenase (IDO) was identified as a potential mediator of this inhibitory process, and the authors suggested a role for LEC in regulation of CD4⁺ responses *in vivo*.

As well as effects on antigen presentation and T cell activation, LECs in the LN and periphery regulate T cell survival via production of IL-7. The role of IL-7 in the survival of naïve T cells is well documented (202, 203). Many cell types present within the LN produce IL-7, but LECs were found to be the dominant source (204); and IL-7-producing LECs have also been found in peripheral organs like the lungs and gut (205). Interestingly, IL-7 production by LECs might function in a negative feedback loop with T cells, with T cells having a negative impact on lymphangiogenesis (206), and LECs providing an essential cytokine (IL-7) for T cell survival.

In addition to their impact on T-cell survival, LECs regulate trafficking of T cells within LN via S1P. LN-LECs were found to be the source of extracellular S1P which was essential for egress of activated T cells from lymph nodes (207). S1P acts via interaction with S1PR1 which is upregulated on T cells following activation (163).

The information presented here provides evidence for the role of LECs in regulating the adaptive immune response. It is clear that LECs play a pivotal role in maintaining tolerance to self through providing inhibitory signals to activated CD8⁺ T cells. VEGF-C-

activated LECs can also reverse anti-tumour immunity. Although LECs do not have a direct effect on CD4⁺ T cell immunity, as they are unable to present endogenous peptides in the context of MHC class II, they can regulate CD4⁺ T cell responses via interactions with DCs and the release of anti-inflammatory molecules such as IDO.

1.4 Outline of thesis

The role that the lymphatic system plays in the immune response to a transplanted organ is complex and dependent on many different factors, including the type of organ graft and the degree of damage to the graft as a result of ischemic injury and immunological rejection. As outlined above, the lymphatic system acts not only as a passive conduit system for cell and molecular trafficking, but reacts to stimuli by modulating expression of cell surface and secreted molecules to ensure optimal interactions between immune cells in order to mount an effective immune response. The lymphatic system also displays a proliferative response under certain conditions.

The aim of this thesis was to decipher the role of the lymphatic system in transplantation using mouse models of skin, heart and kidney transplantation. It was hypothesised that modulation of the lymphatic system of the donor and/or the recipient would prolong survival of allogeneic grafts as a result of reduced trafficking of donor passenger leukocytes between the graft and the recipient's lymph nodes in the immediate post-transplantation period. In addition to this it was hypothesised that the lymphatic endothelial cells of the lymph nodes draining a transplanted organ would undergo phenotypic changes as a result of the immune response.

In chapter 3, anti-ICAM 1 antibody is used to block donor passenger leukocytes leaving donor grafts, in order to see if this promotes survival of allogeneic kidney grafts. In chapter 4 using a mouse with a conditional knockout of ephrin B2, lymphatics in donor organs are disrupted, to observe effects on graft survival. In chapter 5 the response of DLN LECs to transplantation has been studied, to determine whether they have the potential to influence the allo-immune response.

Chapter 2 Materials and methods

2.1 Reagents

Phosphate-buffered saline (PBS)

PBS tablets (Oxoid, Ltd., Basingstoke, UK) were dissolved in distilled water (1 tablet per 100ml water).

Periodate Lysine Phosphate (PLP)

A lysine stock solution was made by adding 100ml of 0.2M lysine monohydrochloride (Sigma-Aldrich; Merck KGaA, Darmstadt, Germany) to an equal volume of disodium hydrogen orthophosphate (Sigma-Aldrich; Merck KGaA). The pH was adjusted to 7.4 and the solution stored at 4°C. Immediately before use 1 volume of 4% paraformaldehyde was added to 3 volumes of lysine stock, and 214mg sodium metaperiodate (Sigma-Aldrich; Merck KGaA) was added per 100ml.

Cell lysis buffer

1g sodium hydroxide (NaOH); (Sigma-Aldrich; Merck KGaA) and 74.4mg ethylenediamine-tetra-acetic acid (EDTA); (Sigma-Aldrich; Merck KGaA) were dissolved in 1000ml distilled water.

Neutralization buffer

6.5g TrisHCl (Sigma-Aldrich; Merck KGaA) was dissolved in 1000ml distilled water.

Fluorescence activated cell sorting (FACS) buffer

Consists of 2% fetal calf serum (FCS); (Sigma-Aldrich; Merck KGaA) in PBS.

Red blood cell lysis buffer

4.17g NH₄Cl, 0.0185g EDTA and 0.5g NaHCO₃ (all Sigma-Aldrich; Merck KGaA) were dissolved in 500ml de-ionised water.

The solution was autoclaved, kept sterile and stored at 4°C

Lymphatic endothelial cell media

Dulbecco's modified eagle media (DMEM); (Thermo Fisher Scientific, Inc., Waltham, MA, USA) was supplemented with 2% FCS and 1.2mM CaCl₂ (Sigma-Aldrich; Merck KGaA), and the required volume was filtered using a 0.45µm syringe filter.

Heart digestion media

Roswell Park Memorial Institute medium (RPMI 1640) plus L-glutamine (Corning Inc, Corning, NY, USA) was supplemented with 10% FCS, 0.1mM β -mercaptoethanol (Thermo Fisher Scientific, Inc.) and 25mM HEPES (Thermo Fisher Scientific, Inc).

2.2 Animals

BALB/c (H-2^d) mice, purchased from Harlan UK Ltd. (Oxon, UK), were used as organ donors for kidney and heart transplantation, and recipients for skin, cardiac and renal transplantation. C57BL/6 (H-2^b) mice, also purchased from Harlan, were used as recipients for cardiac transplantation.

C57BL/6 mice expressing the enhanced yellow fluorescent protein targeted to the ROSA-26 locus (abbreviated to EYFP) in which EYFP is expressed ubiquitously (208) were bred in house and were used as recipients for renal transplantation.

C57BL/6 mice with a spatially and temporally conditional knock-out for ephrin B2 (abbreviated as ephrin B2^{-/-}) were used as organ donors for skin, cardiac and renal transplantation. In these mice the CreER^{T2} recombinase is under the control of the *Prox1* promoter meaning that recombination of the floxed ephrin B2 gene only occurs in LECs. In addition, CreER^{T2} is an inducible Cre recombinase, and entry of the enzyme into the nucleus is dependent on the presence of tamoxifen. Adult ephrin B2^{-/-} mice treated with tamoxifen lose expression of ephrin B2 in LECs within one week. Because ephrin B2 plays an essential role in lymphatic valve maintenance, lymphatic vessels in these mice dilate and eventually disintegrate, causing death within two weeks (102). All ephrin B2^{-/-} mice were used as organ donors eight days after tamoxifen treatment, before showing any obvious detrimental effects of the knock-out externally. However, upon dissection the effect of the knock-out is visible, as lymphatic vessels are dilated (Figure 2.1). Ephrin B2^{-/-} mice were a kind gift from Dr Taija Makinen (Uppsala University, Sweden).

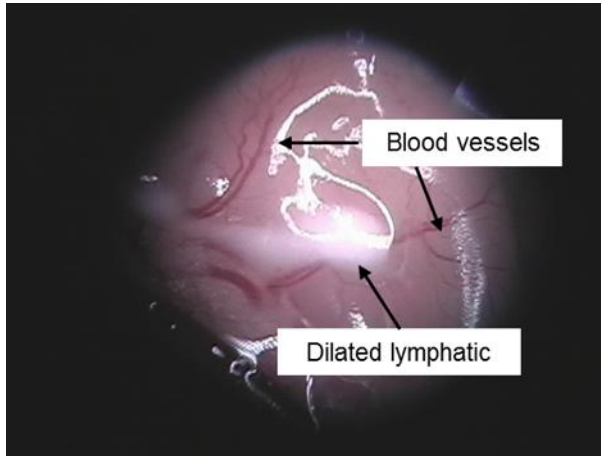


Figure 2.1- Photograph showing dilated lymphatic vessel in the abdomen of an ephrin B2^{-/-} mouse eight days after tamoxifen treatment. Original magnification 20x.

2.2.1 Breeding

Different combinations of genotype from the ephrin B2^{-/-} colony were used for experiments: fully floxed (i.e. both ephrin B2 alleles floxed) and cre positive were used as experimental mice and are referred to as ephrin B2^{-/-}, wild-type (i.e. neither ephrin B2 alleles floxed) and cre positive were used as controls for some experiments, and fully floxed and cre negative were used as controls for other experiments. For maintenance of the ephrin B2^{-/-} colony to ensure that all genotypes were available for experiments, two breeding pair combinations were used. Firstly for experimental ephrin B2^{-/-} mice and wild-type controls, a heterozygous ephrin B2 (i.e. only one ephrin B2 allele floxed) cre positive male was bred with a heterozygous cre negative female. This combination gives six possible outcomes for offspring: homozygous cre positive, homozygous cre negative, heterozygous cre positive, heterozygous cre negative, wild-type cre positive or wild-type cre negative. And for maintenance of a line with no cre expression, a heterozygous cre negative male was bred with a heterozygous cre negative female.

All animals were kept in specific pathogen-free animal facilities, and used in accordance with the Animals (Scientific Procedures) Act 1986. Male mice between 8 and 12 weeks of age were used in all experiments, unless otherwise specified.

2.3 Genotyping

Ear samples were taken from ephrin B2^{-/-} mice at weaning and genotyping performed to establish their cre and floxed ephrin B2 status. In addition, ear samples were taken from wild-type and ephrin B2^{-/-} mice after tamoxifen treatment to confirm successful deletion of *ephrin B2*.

DNA was extracted using the 'hotshot' method described by Truett *et al.* (209). Cell lysis buffer (75µl) was added to tubes containing ear sample, and heated to 95°C for 30 minutes with vortexing for 1 minute half way through incubation. Neutralization buffer (75µl) was then added to the tubes and they were stored at -20°C.

For PCR reactions, 2µl DNA was added into PCR tubes with: 12.5µl *Taq* PCR master-mix (Qiagen, Inc., Valencia, CA, US), 2.5µl Coral load 10x (Qiagen, Inc.), 9.5µl DNase free water (Qiagen, Inc.), and 0.5µl primer. The PCR conditions consisted of: an initial hold-step at 95°C for 5 mins, followed by 35 cycles of; 95°C for 30 seconds, 63°C (50°C for knockout genotyping) for 30 seconds and 72°C for 30 seconds. PCR products were run on a 3% agarose gel.

2.3.1 Primers

Primer sequences were obtained from the original publication using these mice (102). Primers (Sigma-Aldrich; Merck KGaA) were initially diluted to 100µM in AE buffer (Qiagen, Inc.), and then a 10µM working solution was made and stored at -20°C.

Floxed ephrin B2:

Forward (a): CTTCAGCAATATACACAGGATG

Reverse (b): TGCTTGATTGAAACGAAGCCCGA

Reverse (c): AATACTGTTACTACAGGGTCC

Cre:

Forward: GCCTGCATTACCGGTTCGATGCAACGA

Reverse: GTGGCAGATGGCGCGGCAACACCATT

2.3.2 DNA products

Primers (a) and (b) yield a DNA product sized 380 base pairs (bp) when the sample is homozygous for the floxed *ephrin B2* allele. If the sample is wild-type for the floxed allele (i.e. the gene is not floxed) the product is 262 bp. If the sample is heterozygous (i.e. one allele is floxed and one is not) the PCR yields two products, one 380 bp and one 262 bp.

Primers (a) and (c) yield a DNA product sized 320 bp when the sample is homozygous floxed and tamoxifen-treated (i.e. when a homozygous *cre* positive mouse has been treated with tamoxifen).

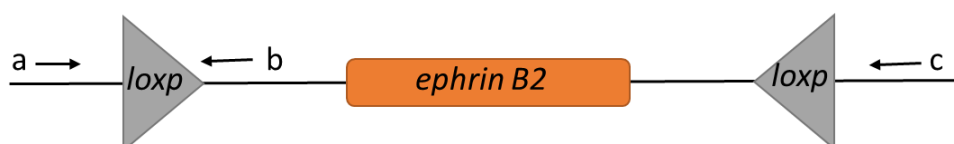


Figure 2.2- Schematic of floxed *ephrin B2* showing location of primer sequence (a,b,c) binding. The *ephrin B2* gene is flanked by two *loxP* sites which direct recombination by *cre* recombinase. When genotyping PCR is performed with primers **a** and **b** a DNA product of 380 bp is made. When genotyping PCR is performed with primers **a** and **c** on homozygous floxed mice after tamoxifen treatment a 320 bp product is made.

2.4 Animal models of transplantation

For all transplantation procedures, donor and recipient mice were anaesthetised with isoflurane (Merial animal health, Ltd., Essex, UK), and recipient mice received 0.1mg/kg buprenorphine hydrochloride as analgesic (Vetergesic) (Alstoed, Ltd., Melton Mowbray, UK) subcutaneously prior to surgery.

2.4.1 Technical success

Due to the technical challenges involved in mouse heart and kidney transplantation models it is important to note that not all procedures are successful. In the hands of both operators ~95% of heart transplant procedures are successful, and this can be demonstrated by perfusion of the heart after removal of clamps and initiation of heart beat in the transplanted organ. Similarly, success in kidney transplantation is also dependant on perfusion of the donor organ after removal of the clamps. This is easily determined by a change in colour of the kidney from pale to dark pink/red. In the hands of both operators ~70% of kidney transplant procedures are successful.

For results presented in this thesis, more than one person was involved in the transplantation procedures. In order to limit variability in data as a result of inter-operational variation in technical success, for experiments involving two operators such as that presented in section 3.2, both operators were responsible for transplanting a similar number of mice in both the experimental and control group. In all other experiments where more than one operator was to carry out procedures they were responsible for all transplants of a particular organ in that experiment.

2.4.2 Splenectomy

A splenectomy was performed before transplantation in some recipients in order for the impact of DPL trafficking via lymphatics on graft outcome to be studied in isolation. In

addition to the lymphatic route, DPL exit the graft via blood vessels and traffic to the spleen where they encounter allo-specific T cells (52).

For skin graft recipients, splenectomy was performed seven days before skin transplantation. An incision was made on the ventral left side of the mouse, and a small portion of the bowel retracted upwards to allow visualisation of the spleen. The vessels supplying the spleen were ligated with 7/0 silk suture (Pearsalls, Ltd., Taunton, UK), and cut close to the spleen. The spleen was removed and the incision closed with 4/0 suture (Unik Surgical Sutures, Taipei, Taiwan). For heart and kidney transplant recipients splenectomy was performed at the time of transplantation.

2.4.3 Skin transplantation

Skin transplantation was performed as described by Billingham *et al.* (210). A section of tail skin was removed from the donor, trimmed to an approximate size of 1cm², and placed on saline-soaked gauze on ice whilst the recipient was prepared. A small section of skin, similar to the size of the graft, was removed from the dorsal aspect of the recipient. For double skin transplant recipients two sections of skin were removed, one on either side of the spine. The donor skin(s) was placed in the opening, and fixed in place with Germolene new skin (Bayer, Newbury, UK). The skin was covered with a paraffin-coated mesh dressing (Johnson and Johnson, New Brunswick, NJ, USA), dry gauze was placed on top and the animal was wrapped in Transpore tape (3M, Maplewood, MN, USA). The bandages were removed after seven days, and rejection of the graft monitored by observation. The graft was considered rejected when it was more than 90% necrotic.

2.4.4 Heart transplantation

Cardiac transplantation was performed as first described by Corry *et al.* (211). A large v-shaped incision was made in the donor, and the gut was removed to reveal the inferior vena cava (IVC) and the aorta. Heparinized saline (500µl; 200units/ml); (Leo Pharma, Hurley, UK) was injected into the IVC and allowed to circulate for 1 minute, then the aorta was cut to allow exsanguination of the animal. The rib cage was opened to reveal the heart; and the IVC, azygous veins and the superior vena cava were tied with 7/0 silk suture (Pearsalls, Ltd.) and cut. The aorta and the pulmonary artery were cut straight across using microscissors (Fine Science Tools, Heidelberg, Germany). A tie was then placed around the entire heart and it was removed from the animal and placed in sterile saline on ice whilst the recipient was prepared.

The anaesthetized recipient was shaved, the abdomen swabbed with povidine iodine, as Vetasept (Animalcare, York, UK), and a sterile drape placed over the operating area. A midline incision was made, and the bowels and bladder retracted and covered in saline-soaked sterile gauze. The IVC and aorta were exposed, and the lumbar veins which drain into the IVC were tied with 7/0 silk suture. Microvessel clamps (Fine Science Tools) were placed at the top and bottom of the IVC and aorta. A venotomy and aortotomy were made using a 21 gauge needle (Terumo UK Ltd., Bagshot, UK), and extended with microscissors. Anchor stitches were placed at the top and bottom of the donor and recipients aorta, and the left-hand walls were anastomosed with a running stitch using 10/0 nylon suture (Unik Surgical Sutures). This was tied to the top anchor stitch; then the heart was flipped over to complete anastomosis of the right-hand wall. The pulmonary artery was anastomosed to the recipient IVC in the same way, except that the right wall was completed first. A small piece of Spongostan (Ferrosan Medical Devices, Soborg, Denmark) was placed over the anastomoses before removal of the clamps. The midline incision was closed with 4/0 suture (Unik Surgical Sutures).

Cardiac grafts were monitored by palpation of the abdomen, and the strength of beating assessed according to the scale developed by Superina *et al.* (212). Rejection was defined as absence of a palpable heartbeat on 2 consecutive days.

2.4.5 Kidney transplantation

Renal transplantation was performed as described by Han *et al.* (213). A v-shaped incision was made in the donor and the gut removed to reveal the left kidney. The gonadal and adrenal veins, which branch off the renal vein were tied twice with 7/0 silk suture and cut between the ties. A loose tie was placed on the aorta above the junction with the renal artery, and the ureter was cut close to the bladder. Heparinised saline (200µl; 200units/ml) was injected into the IVC and allowed to circulate for 1 minute. The tie on the aorta was tightened, and the needle was removed to allow exsanguination of the animal. The renal vein was cut at its junction with the IVC, and the aorta was cut obliquely below the renal artery and above the tie made earlier. The kidney was removed and kept in sterile saline on ice whilst the recipient was prepared.

The anaesthetized recipient was shaved, the abdomen swabbed with povidone iodine, and a sterile drape placed over the operating area. A midline incision was made, and the bowels and bladder retracted and covered in saline-soaked sterile gauze. A tie was placed around the left renal vein and artery, and the left kidney removed. The IVC and aorta were exposed, and the lumbar veins which drain into the IVC were tied with 7/0 silk suture. Microvessel clamps were placed at the top and bottom of the IVC and aorta. A venotomy and aortotomy were made using a 21 gauge needle, and extended with microscissors. Anchor stitches were placed at the top and bottom of the donor and recipients aorta, and the left-hand walls were anastomosed with a running stitch using 10/0 nylon suture. This was tied to the top anchor stitch, then the kidney was flipped over to complete anastomosis of the right-hand wall. The renal vein was anastomosed to the IVC in the same manner except that the left-hand wall was stitched from inside the lumen.

A small piece of Spongostan was placed over the anastomoses before removal of the clamps. The midline incision was closed with a 4/0 suture.

Seven days following transplantation, the right native kidney was removed. From this point the renal graft became life-sustaining and renal function was monitored weekly by measuring blood urea nitrogen (BUN). Rejection was defined as death of the recipient due to kidney failure or the requirement for it to be culled due to uraemia, as defined by BUN of ≥ 30 mmol/L, causing ill health.

2.5 Blood urea nitrogen measurement (BUN)

BUN was used as a measure of kidney function in kidney transplant recipients. Blood was taken from the tail vein of mice, and centrifuged at 1300RPM for 30 minutes. The serum was removed by pipetting and stored at -20°C . For analysis, $5\mu\text{l}$ of serum was added to $500\mu\text{l}$ Infinity Urea (Clindia Benelux B.V, Leusden, The Netherlands), and the absorbance at 340nm read on a spectrophotometer (Beckman Coulter (UK), Ltd., High Wycombe, UK). BUN was then calculated according to the manufacturer's instructions.

2.6 Monoclonal antibody therapy

A number of EYFP recipients of BALB/c kidney grafts were treated with a rat anti-mouse ICAM-1 blocking antibody (IgG2b isotype); (Bioxcell, West Lebanon, NH, USA). The antibody was administered to kidney transplant recipients intravenously (IV) via the tail vein at a dose of $200\mu\text{g}$ per mouse 30 minutes before transplantation.

2.7 Tamoxifen treatment

Ephrin B2^{-/-} mice to be used as organ donors were injected intraperitoneally (IP) with 5µg tamoxifen (Sigma-Aldrich; Merck KGaA) dissolved in corn oil (Sigma-Aldrich; Merck KGaA) eight days prior to transplantation.

2.8 Tissue harvesting

2.8.1 Mediastinal lymph nodes

Following heterotopic heart transplantation into the abdomen of a mouse (as described above), lymph flows from the organ into the peritoneal cavity and enters the diaphragmatic lymphatics which drain into the mediastinal lymph nodes (Figure 2.3) (176).

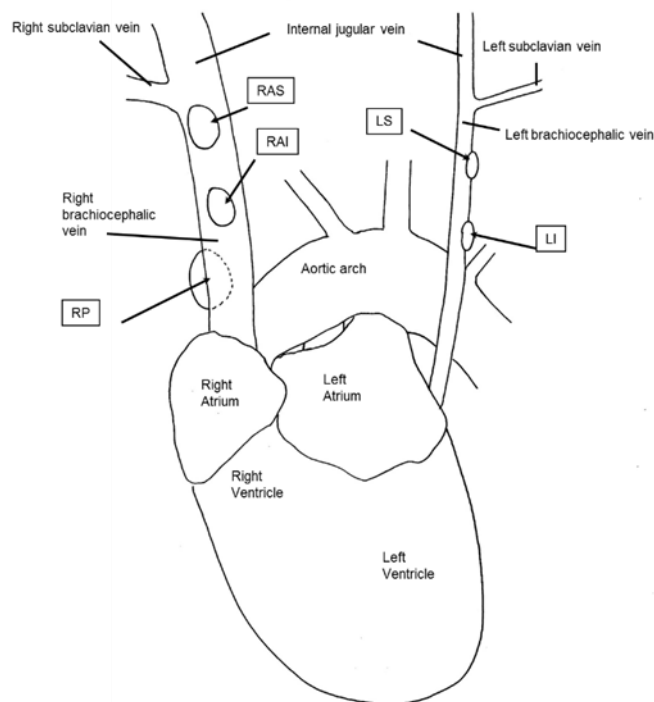


Figure 2.3- Location of the mediastinal lymph nodes in the mouse.

Numbers and exact positions of these lymph nodes vary slightly between individual mice, but normally consist of: the right anterior superior (RAS) and right anterior inferior (RAI) mediastinal lymph nodes, located on top of the right brachiocephalic vein; the right posterior (RP) mediastinal lymph node, located underneath the right brachiocephalic vein; and the left superior (LS) and left inferior (LI) mediastinal lymph nodes, located on top of the left brachiocephalic vein (176).

This has been demonstrated by our group in published experiments (176). These lymph nodes can be visualised following IP administration of 0.5% Evans Blue (Sigma-Aldrich; Merck KGaA) (Figure 2.4).

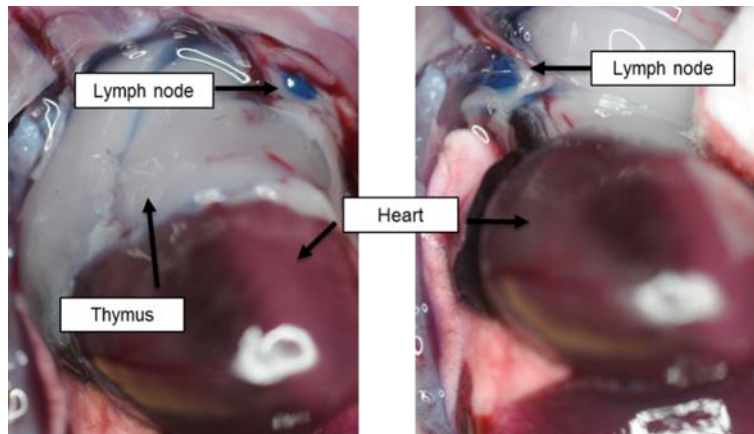


Figure 2.4- Location of mediastinal lymph nodes. Photograph of the chest cavity of a mouse following intraperitoneal injection of Evans Blue, showing mediastinal lymph nodes which have been stained blue. Original magnification 10x (177).

2.8.2 Immunohistochemistry

Skin, hearts and kidneys were harvested in PLP. PLP-fixed tissue was kept at 4°C for 4 hours, then transferred to a 13% sucrose solution overnight at 4°C. Tissue was embedded in OCT (Thermo Fisher Scientific, Inc.), gradually cooled on dry ice, and stored at -80°C. Sections (5µm) were cut using a cryostat (Bright, Luton, UK), air dried overnight, and fixed in ice cold acetone for 5 minutes. Endogenous peroxidase activity within the tissue was quenched with 3% H₂O₂ in PBS (Oxoid Ltd.), and avidin/biotin was blocked using a kit (Vector Laboratories, Peterborough, UK) according to manufacturer's instructions. Tissue was incubated with anti-lymphatic vessel endothelial hyaluronan receptor 1 (LYVE-1) polyclonal antibody (Abcam, Cambridge, UK) at a 1:500 dilution with PBS containing 5% bovine serum albumin (Sigma-Aldrich; Merck KGaA), overnight at 4°C. After washing with PBS, a biotin conjugated anti-rabbit secondary (Biolegend, San Diego, CA, USA) at a 1:100 dilution was added for 30 minutes at room temperature. This

was followed by incubation with Streptavidin horseradish peroxidase solution (BD Biosciences, Franklin Lakes, NJ, USA) for 30 minutes at room temperature. LYVE-1 staining was detected using a Novared detection kit (Vector Laboratories) according to manufacturer's instructions. For counter-staining of nuclei, sections were incubated in Mayer's haematoxylin (VWR, Lutterworth, UK) for 3 minutes, followed by washing in running tap water for 10 minutes. Sections were then dehydrated through dips in 90% followed by 100% ethanol and xylene. Slides were mounted in DPX (VWR). LYVE-1 staining was quantified using ImageJ software.

For intracellular Foxp3 staining in PLP fixed kidney sections, the same protocol was followed, except slides were incubated with anti-Foxp3 antibody (Biolegend) at a 1:400 dilution, overnight at 4°C.

2.8.3 Histology

Renal grafts were harvested in 10% formalin. Formalin fixed tissue was processed using a Leica ASP200 tissue processor; and embedded in wax. Sections (4µm) were cut using a microtome (Leica, Wetzlar, Germany), and baked overnight at 60°C. Periodic acid Schiff's staining (PAS) was performed by removing wax in xylene and rehydration through dips in 100% followed by 90% ethanol, and washing in running tap water for 5 minutes. Sections were incubated in 1% periodic acid for 10 minutes followed by washing with distilled water. Sections were then incubated in Schiff's reagent (VWR) for 10 minutes followed by washing in running tap water for 5 minutes. Sections were then incubated in Mayer's haematoxylin (VWR) for 3 minutes, followed by washing in running tap water for 10 minutes. Sections were then dehydrated through dips in 90% followed by 100% ethanol and xylene. Slides were mounted in DPX (VWR).

2.9 Real-time PCR

In order to quantify the amount of DPL that had trafficked from the graft to the DLN of the recipient, a real-time PCR assay for a donor-specific gene was used. To calculate the copy number of the donor-specific gene from unknown samples, a mean was calculated from triplicate ct values, applied to a standard curve generated from donor strain DNA, and corrected for the total amount of DNA in the sample.

2.9.1 Genomic DNA extraction

Mediastinal lymph nodes were harvested from cardiac and renal transplant recipients and stored at -20°C. DNA was extracted using the DNeasy mini kit from Qiagen, Inc., according to the manufacturer's protocol. The quantity of total DNA within samples was assayed using a NanoDrop™ spectrophotometer according to manufacturer's instructions.

2.9.2 *zfy1* PCR

A PCR assay for *zfy1* was used to quantify donor DNA in recipient DLN of mice receiving male BALB/c kidney grafts. *Zfy1* encodes a zinc finger protein located in the testes determining region of the Y chromosome (214), and is therefore in this case a donor-specific gene as only male mice were used as donors. This assay has previously been used by our laboratory to quantify DPL in a heart transplantation model (177).

PCR reactions were made up to a final volume of 20µl in white hard-shell 96-well PCR plates. The PCR reaction was set up as previously described (215). Data was analysed using the Bio-Rad CFX software.

2.9.3 *cre* PCR

A PCR assay for *cre* was used to quantify donor DNA in recipient DLN of mice receiving either wild-type or ephrin B2^{-/-} heart grafts; as the donor mice had been transduced with the *cre* gene, and therefore DPL within the grafts contained a copy of the gene.

PCR reactions were made up to a final volume of 20µl in white hard-shell 96-well PCR plates (Bio-Rad Laboratories, Inc., Hercules, CA, USA). PCR reactions consisted of: 10µl Taqman (Invitrogen; Thermo Fisher Scientific, Inc.), 1µl primer mix (assay Mr00635245, FAM conjugated probe); (Applied Biosystems; Thermo Fisher Scientific, Inc.), and genomic DNA (extracted from DLN as above) diluted to a volume of 9µl in DNase free water (Qiagen, Inc.). After addition of reaction mixtures to wells of the plate, the plate was spun for 1 minute at 1500RPM. The PCR conditions were as follows: an initial hold step of 50°C, then heating to 95°C, and 40 cycles of 15 seconds at 95°C followed by annealing for 1 minute at 60°C. Data was analysed using the Bio-Rad CFX software.

2.9.4 Calculation of cell number

The CFX software calculates the amount of target DNA (i.e. *zfy1* or *cre*) in samples by comparing ct values to a standard curve. As the copy number of the *cre* transgene in donor mice was unknown, individual standard curves using DNA from each donor mouse were run at the same time as the recipient DLN DNA samples. For the *zfy1* assay this was not necessary as all male donor mice have one copy of the gene per cell (214).

In order to calculate the number of donor cells within recipient DLN DNA samples from the PCR assays the c value was used. The c value denotes the size of an organism's genome in terms of the mass of DNA (in picograms) in a haploid cell, i.e. a gamete, or half the amount of DNA in a diploid cell. The c-value for *mus musculus* is 2.45 (216).

Therefore, the number of donor cells was determined by calculating the percentage of the total sample DNA which was donor specific (i.e. the proportion value), converting this to a concentration (picograms of DNA) and dividing by 4.9 (double the c-value).

2.10 Tissue digestion for flow cytometry

2.10.1 Heart

Mice were anaesthetised with isoflurane, and exsanguination was achieved by drawing blood from the abdominal IVC. The rib cage was then opened to reveal the heart. The heart was perfused with 1ml cold sterile saline through the aorta and removed from the animal. The heart was placed in a 40mm petri dish and sliced in half using a blade. Any remaining blood was flushed from the ventricles using saline, and the tissue placed in a fresh petri dish containing 1ml heart digestion media. The tissue was minced to 1mm pieces using microscissors and transferred to a 5ml polypropylene tube, which was placed on ice.

Tissue was allowed to settle at the bottom of the tube and supernatant aspirated to a 50ml Falcon tube with 100µm nylon mesh attached. The mesh was washed with heart digestion media, and the tube placed on ice. To the heart tissue, 1ml digestion mix (heart digestion media plus 10µg/ml type 1 collagenase (Sigma-Aldrich; Merck KGaA) and 10µg/ml DNase 1) pre-warmed to 37°C was added, and the tube incubated at 37°C for 15 minutes. The tube was vortexed for 1 minute half way through the incubation.

This process was repeated, and after the final incubation the remaining undigested tissue was mashed through a 100µm nylon mesh with the plunger of a 1ml syringe. The tube containing the digested heart tissue was centrifuged at 1100RPM for 5 minutes at 4°C. The supernatant was discarded and the tissue re-suspended in 3ml 0.01M EDTA in FCS at room temperature. The suspension was then layered over 3ml Histopaque-1077 (Sigma-Aldrich; Merck KGaA) at room temperature, and centrifuged for 30 minutes at 900RPM at room temperature with no brake.

Leukocytes form an opaque layer between the Histopaque-1077 and the FCS. Due to low yields of leukocytes from heart tissue, the FCS and leukocyte layer were carefully removed to a 15ml Falcon tube and topped up to 10ml with PBS. The tube was spun at 1100RPM for 10 minutes at 4°C. The supernatant was discarded and the heart leukocytes were re-suspended in FACS buffer.

2.10.2 Kidney

Mice were anaesthetised with isoflurane, and exsanguination was achieved by drawing blood from the abdominal IVC. The kidney was removed and placed in heart digestion media on ice for transportation. Leukocytes were extracted according to a published protocol (217).

2.10.3 Lymph nodes

Stromal cells were isolated from mediastinal lymph nodes of mice receiving heart grafts using a technique described by Broggi *et al.* (218) with some modifications. Lymph nodes were harvested into a 40mm petri dish containing 1ml LEC digestion media, and the capsules disrupted using a 27G needle attached to a 1ml syringe. The tissue was then transferred to a 5ml polypropylene round-bottomed tube, and washed with a further 1ml LEC digestion media to ensure all tissue was transferred. The tubes containing lymph node tissue were kept on ice for transportation between the biological services unit and laboratory.

Tissue was allowed to settle at the bottom of the tube and the supernatant was aspirated using a sterile pastette to a sterile 50ml Falcon tube with 100µm nylon mesh attached. The mesh was washed with LEC digestion media, and the tube placed on ice. To the lymph node tissue, 750µl digestion mix 1 (LEC digestion media plus 1mg/ml collagenase IV (Worthington Biochemical Corporation, Lakewood, NJ, US) and 40µg/ml DNase 1

(Roche Diagnostics, Basel, Switzerland)) pre-warmed to 37°C was added, and the tube incubated at 37°C for 30 minutes with 30 seconds gentle vortexing every 10 minutes.

Tissue was again allowed to settle at the bottom of the tube and supernatant aspirated to the 50ml Falcon tube with 100µm nylon mesh attached. The mesh was washed with LEC digestion media, and the tube placed on ice. To the lymph node tissue, 750µl digestion mix 2 (LEC digestion media plus 3.5mg/ml collagenase D (Roche Diagnostics) and 40µg/ml DNase 1) pre-warmed to 37°C was added, and the tube incubated at 37°C for 10 minutes.

The tissue was further disaggregated by pipetting up and down using a 1000µl pipette set at 700µl for approximately 2 minutes or until no visible tissue fragments remained. The digested tissue was then transferred to the 50ml Falcon with 100µm mesh attached. The mesh was washed 5 times with 1ml LEC digestion media, and the tube placed on ice.

The tube containing digested lymph node tissue was centrifuged at 1500RPM for 5 minutes at 4°C. The supernatant was discarded and the lymph node cells were re-suspended in FACS buffer.

2.11 Flow cytometry

Table 2- Table showing antibodies used for flow cytometry. All antibodies were supplied by Biolegend.

Target	Clone	Function	Fluorochrome	Dilution
CD45	30-F11	Leukocyte antigen common	Alexa Fluor 700	1:100
Podoplanin	8.1.1	Lymphatic endothelial cell marker	PE	1:200
CD3	17A2	T cell marker	APC	1:100
CD4	GK1.5	T cell marker (helper)	PE	1:100
CD8	53-6.7	T cell marker (cytotoxic)	FITC	1:100
CD44	IM7	T cell activation maker	PE-Cy7	1:100
CD31	MEC13.3	Lymphatic endothelial cell marker	APC	1:200
PDL1	10F.9G2	Co-inhibitory molecule	PE/Cy7	1:100
I-A^b	AF6-120.1	MHC class II molecule specific to mice of C57Bl/6 background	PE PE/Cy7	1:50 1:100
CD11c	N418	Dendritic cell marker	FITC	1:100
CD11b	M1/70	Macrophage marker	APC-Cy7	1:100
Dead cells	Sytox blue	Nucleic acid stain	BV405	1:1000
CD16/CD32	2.4g2	Fc Block		1:50

2.11.1 Lymphatic endothelial cells

One million cells were added to each tube for staining. FACS buffer (1ml) was added and the tubes centrifuged at 1100RPM for 5 minutes at 4°C. The supernatant was discarded and the cells re-suspended in 100µl FACS buffer. Fluorochrome-conjugated antibodies specific for LEC markers and co-inhibitory/co-stimulatory molecules were added according to the dilutions in Table 2 and the tubes incubated in the dark on ice for 30 minutes.

The stained cells were washed in FACS buffer as before to remove unbound antibodies. The supernatant was discarded and the stained cells re-suspended in 500µl Sytox blue dead cell stain (Thermo Fisher Scientific, Inc.). Cells were analysed on a Fortessa flow cytometer (BD Biosciences).

2.11.2 Kidney and heart leukocytes

For heart leukocytes the total amount of recovered leukocytes from each heart was added to a 5ml polypropylene tube. For kidney leukocytes one million cells were added. FACS buffer (1ml) was added and the tubes were centrifuged at 1100RPM for 5 minutes at 4°C. The supernatant was discarded and the cells re-suspended in 100µl Fc block (BD Biosciences) diluted in FACS buffer. The tubes were incubated for 20 minutes in the dark on ice. Fluorochrome-conjugated antibodies specific for DC markers and co-stimulatory molecules were added according to the dilutions in Table 2, and the tubes incubated in the dark on ice for 30 minutes.

The stained cells were washed in FACS buffer as before to remove unbound antibodies. The supernatant was discarded and the stained cells re-suspended in 1ml Sytox blue dead cell stain. Cells were analysed on a Fortessa flow cytometer.

2.11.3 Splenocytes

Naïve splenocytes from the same strain were used as a control for leukocyte markers in flow cytometry experiments. Splenocytes were isolated by; disaggregation of tissue through a 70µm sieve attached to a 50ml Falcon tube, followed by washing in PBS. Red blood cells were lysed by addition of 5ml RBC lysis buffer and incubation on ice in the dark for 10 minutes. Cells were washed in PBS, re-suspended in FACS buffer, and stained according to the protocol for the experimental sample.

2.11.4 Analysis of flow cytometry data

All flow cytometry analysis was carried out using Flowjo software (Tree Star, Inc., Ashland, OR, USA). Absolute numbers of specific cell types were calculated using the proportion value of the appropriate gate and multiplying this by the total amount of cells counted at the end of the digestion protocol. This was then expressed in terms of the weight of the tissue (whenever possible). For all samples in a particular experiment the same number of cells were added to the tube for staining. In addition the same number of events was collected for each sample analysed.

2.12 Statistics

All data was analysed using Graphpad Prism software (Graphpad Software Inc., La Jolla, CA, USA). Un-paired t tests with two-tailed *p* values were used for all data. Data are expressed as mean values with error bars representing standard error of the mean. For graft survival data, the log-rank sum test was used to compare survival across different groups.

Chapter 3 Using anti-ICAM-1 antibody therapy to block post-transplantation lymphatic trafficking of DPL

3.1 Background

The immune response to an allograft is initiated when donor-derived allo-antigens are recognised by the host immune system, leading to the priming of graft-destructive T cells. This can occur via three distinct pathways: the direct, indirect and semi-direct. Each relies on efficient trafficking of donor and recipient immune cells between the graft and SLO, i.e. the local DLN and spleen, via lymph and blood, respectively. SLO provide the perfect niche for interactions between APCs and allo-specific T cells and thus are crucial for an effective immune response (90, 91), as both DPL and host allo-reactive T cells are present in low numbers. Such niches provide a physical locality to facilitate effective interactions between them.

During the transplantation procedure the donor lymphatic vessels are not reconnected to the recipient lymphatics because of their small size. Therefore, they are left open-ended in the initial post-transplantation period. They do eventually reconnect to the recipient lymphatic vasculature (173); however, studies in this field are limited and the timing and dynamics of the process still remain largely unknown. Our laboratory has previously used SPECT/CT to demonstrate leakage of lymph from the donor organ and tracked the pathway of flow. Following injection of the radioactive tracer Nanocoll, which is used to visualise lymphatic flow in humans, into the heart graft; full body imaging allowed visualisation of the pattern of lymphatic flow from the graft. Results from this study demonstrated that in the murine heterotopic heart transplant model, where the donor heart is placed in the peritoneal cavity, lymph that leaks from the severed ends of donor lymphatics enters the peritoneal cavity and is picked up by the diaphragmatic lymphatics which drain into the mediastinal lymph nodes. Allo-specific CD8⁺ T cells were found in the mediastinal lymph nodes after transplantation, which further confirms these lymph nodes as the destination of DPL which have left the graft via the severed lymphatics. This route of lymph flow is maintained even after connection of donor

lymphatics with those of the recipient, which happens several weeks after transplantation (176).

It has been demonstrated *in vitro* that in response to inflammatory cytokines (in particular TNF α), LECs upregulate expression of key adhesion molecules (ICAM-1, vascular cell adhesion protein (VCAM) -1 and E-selectin) and secrete specific chemokines which enable transmigration of DC across the lymphatic endothelium (129, 130). The authors of these papers also used monoclonal antibodies *in vivo* to demonstrate reduced mobilization of DC to the DLN when this pathway is blocked. Chemokine gradients produced by the lymphatic vessel also guide DC towards the DLN (219). Interactions between donor-derived APCs and recipient T cells within the lymph node principally contribute to the induction of allo-immunity via the direct pathway of allo-recognition. This relies on efficient trafficking of DPL from the graft to the DLN via afferent lymphatic vessels.

It was hypothesised that blockade of the ICAM-1 pathway would hinder trafficking of DPL into recipient lymph nodes and, therefore prolong graft survival. Anti-ICAM-1 antibody therapy is known to have a beneficial effect on allograft survival, and has been used to demonstrate the importance of co-stimulation blockade in tolerance induction (220, 221). Anti-ICAM-1 in conjunction with anti-LFA1 can prolong survival of mouse cardiac allografts, but it was used in the context of blocking T cell infiltration into the grafts (222, 223). Its effect on migration of DPL out of the graft has not been studied. Here, an anti-ICAM-1 antibody was used in a mouse kidney allograft model, to assess the contribution to the allo-response of immediate post-transplantation trafficking of DPL via the lymphatic route to recipient lymph, where the spleen of the recipient is removed to eliminate this alternative site of allo-sensitisation.

3.2 Quantification of DPL trafficking using real-time PCR

To determine the effect of ICAM-1 blockade on DPL trafficking, female EYFP (H-2^b) recipients of male BALB/c (H-2^d) kidney grafts were treated with either anti-ICAM-1 antibody or vehicle control (saline) 30 minutes before transplantation surgery, and also received a splenectomy at the time of transplantation (Figure 3.1). EYFP recipients were used here because they had been used in a previous study by our laboratory that assessed post-transplantation lymphatic flow (177). A dose of 200µg per mouse was chosen after examination of the literature. Studies by others on the effect of anti-ICAM-1 antibody therapy on allograft survival used doses of antibody between 100 and 200µg per mouse (224-226). The proportion and absolute number of donor cells in the mediastinal lymph nodes 24 hours post-transplantation was determined by real-time PCR for the donor-specific male gene *zfy1*. The time point of 24 hours after transplantation was chosen as the time to quantify DPL in recipient DLN after examination of the literature as the study by Benichou and colleagues showed that DPL were undetectable in heart transplant recipient DLN past day 1 (58). It is also known that DPL are rapidly killed by recipient NK cells (32).

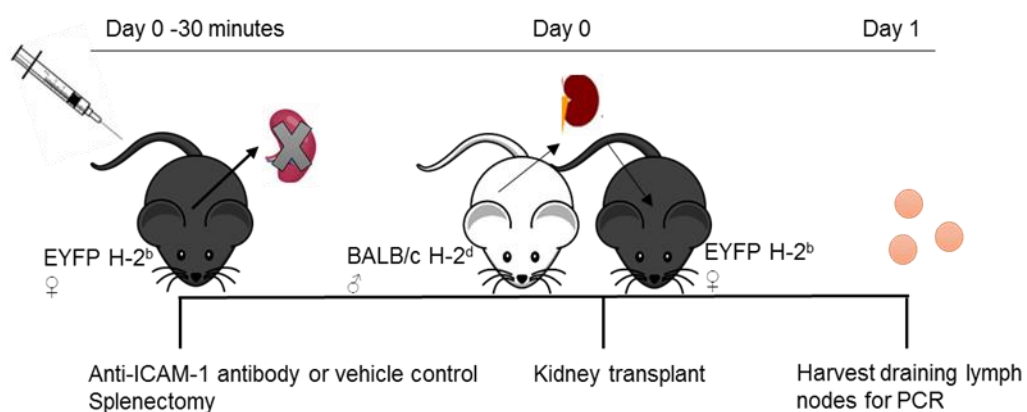


Figure 3.1- Experimental design of quantification of DPL trafficking after anti-ICAM-1 antibody therapy

Quantitative real-time PCR was used to quantify donor cells in recipient lymph nodes because of its sensitivity and accuracy. The genomic target to be amplified was the male-specific gene, *zfy1*, which is located on the Y chromosome, and thus only male (donor) DNA would be amplified. A standard curve was generated with DNA isolated from male BALB/c mediastinal lymph nodes (Figure 3.2) and the proportion of male DNA in transplant recipient DLN was quantified from the standard curve. This data could then be converted to the number of cells of donor origin in the recipient sample by using the c-value which refers to the total amount of DNA in each diploid cell of the organism (227).

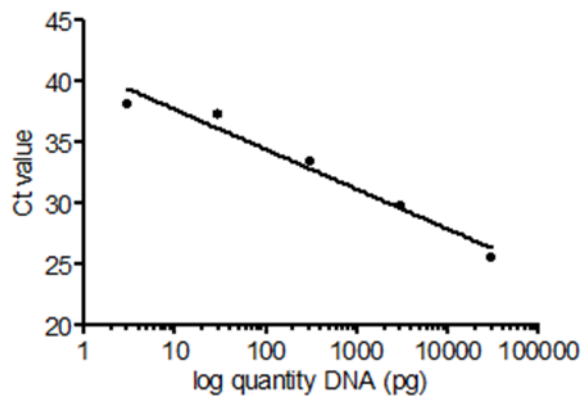


Figure 3.2- Real-time PCR standard curve for *zfy1* using male BALB/c genomic DNA. The ct value formed a linear relationship with the amount of male DNA in the reaction ($R^2=0.9654$), allowing for reliable quantification of male DNA within experimental samples. Ct value refers to the PCR cycle number where the fluorescent signal rises above background.

The proportion of donor-derived DNA within recipient DLN 24 hours after transplantation was significantly reduced in anti-ICAM-1 antibody-treated recipients compared with vehicle controls ($0.03\pm 0.01\%$ vs. $0.07\pm 0.02\%$, $p=0.0375$); (Figure 3.3). When the data for donor-derived DNA as a proportion of the total DNA was converted to values corresponding to the number of donor-derived cells within recipient lymph nodes (according to the calculations described in section 2.9.4) there was no significant difference between the two groups (658 ± 225 vs. 879 ± 243 cells, $p=0.2787$); (Figure 3.4).

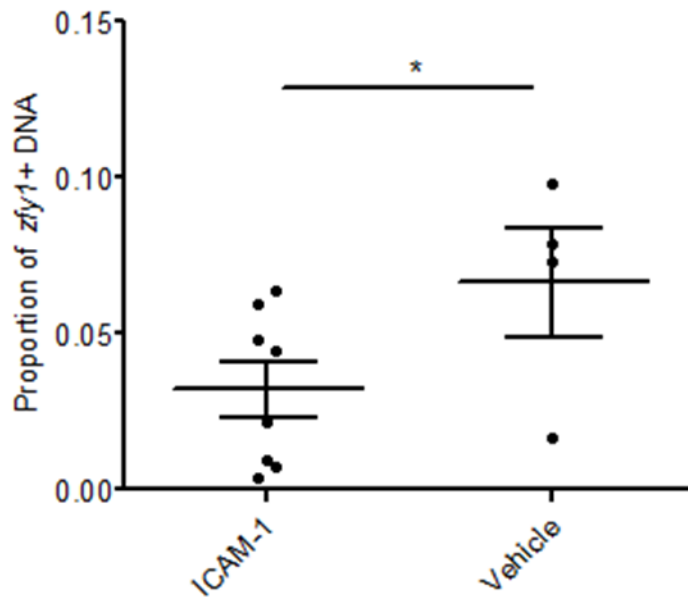


Figure 3.3- Quantification of donor DNA within recipient DLN 24 hours post-transplantation. Male BALB/c kidneys were transplanted into female EYFP recipients and 24 hours later the mediastinal lymph nodes were harvested, subjected to DNA extraction and analysed using a real-time quantitative PCR assay for a the donor specific gene, *zfy1*. The proportion of the total amount of recipient draining lymph node DNA that was of donor origin was calculated by comparing ct values to the standard curve in Figure 3.2. The proportion of recipient DLN DNA that was donor-derived 24 hours post-transplantation was reduced in anti-ICAM-1 antibody-treated recipients compared with vehicle control-treated recipients, $p=0.0375$. Each data point represents the average of triplicate readings from one mouse.

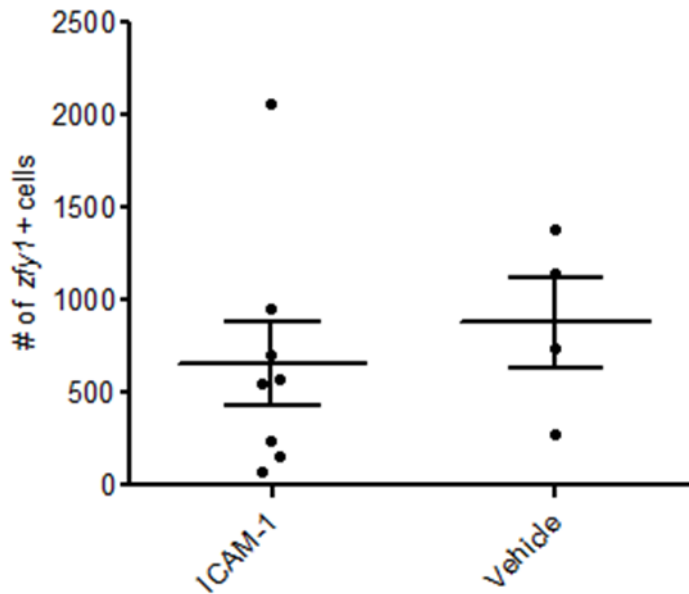


Figure 3.4- Quantification of donor cells within recipient DLN 24 hours post-transplantation. Male BALB/c kidneys were transplanted into female EYFP recipients and 24 hours later the mediastinal lymph nodes were harvested, subjected to DNA extraction and analysed using a real-time quantitative PCR assay for the donor specific gene, *zfy1*. The proportion of the total amount of recipient draining lymph node DNA that was of donor origin was calculated by comparing ct values to the standard curve in Figure 3.2. The number of donor-derived cells was calculated using the c-value which corresponds to the total amount of DNA per cell. There was no difference in the number of donor-derived cells in recipient DLN between anti-ICAM-1 antibody-treated and vehicle control-treated recipients, $p=0.2787$. Each data point represents the average of triplicate readings from one mouse.

3.3 Survival of allogeneic kidney graft in anti-ICAM-1 antibody-treated recipients

Rejection of allografts depends on presentation of donor antigen to recipient T cells, and recipient lymph nodes provide the perfect niche for this interaction. Therefore, having demonstrated that treatment with anti-ICAM-1 antibody before transplantation led to a reduction in donor cell trafficking from the graft to the DLN, it was investigated whether this would affect graft survival, as a result of reduced priming of allo-reactive T cells, in the same model of mouse kidney transplantation.

To this end, BALB/c kidneys were transplanted into EYFP recipients injected with either anti-ICAM-1 antibody or vehicle 30 minutes before transplantation. Recipients were also splenectomised to remove alternative locations for T cell priming. The remaining native kidney was removed at day 7, rendering the transplanted kidney life-sustaining. Graft function was monitored by regular assessment of BUN (Figure 3.5).

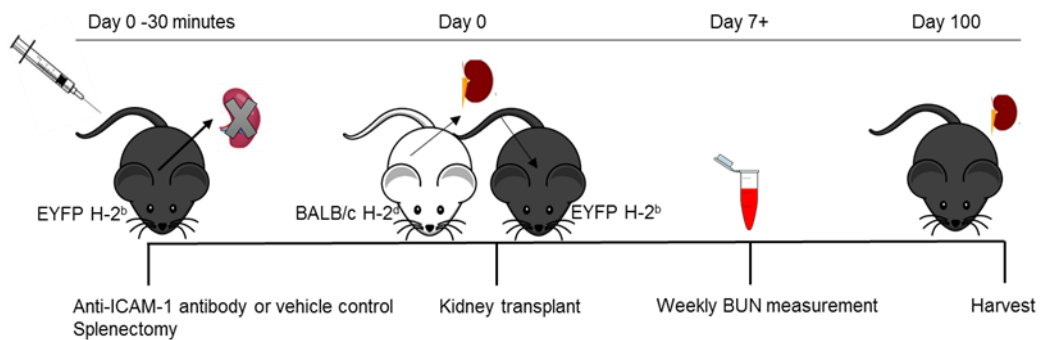
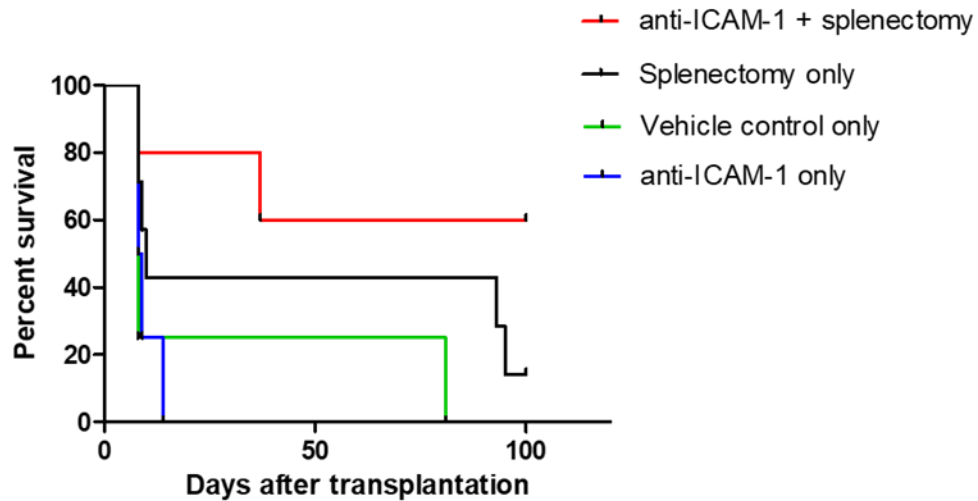


Figure 3.5- Experimental design of assessment of survival of kidney allografts in anti-ICAM-1 antibody-treated recipients

Anti-ICAM-1 antibody treatment in splenectomised recipients resulted in indefinite graft survival of fully allogeneic donor grafts in some recipients (median survival time (MST)>100 days). By contrast, splenectomy only and anti-ICAM-1 antibody treatment only had reduced beneficial effects (MST=10 days, $p=0.1676$; and MST=8.5 days, $p=0.0276$ respectively); (Figure 3.6).



Group	Antibody treatment	Splenectomy	MST	N	<i>p</i> (compared to antibody+splenectomy)
	Yes	yes	>100	5	NA
	No	yes	10	7	0.1676
	No	no	8	4	0.0712
	Yes	no	8.5	4	0.0276

Figure 3.6- Survival of kidney allografts in recipients treated with anti-ICAM-1 antibody. Kidneys from BALB/c mice were transplanted into splenectomised or non-splenectomised recipients treated with either anti-ICAM-1 antibody or vehicle control. Splenectomised recipients treated with anti-ICAM-1 antibody survived longer than non-splenectomised recipients treated with anti-ICAM-1 antibody, $p=0.0276$.

Kidney function was measured at weekly intervals after transplantation using an assay for BUN (Figure 3.7). In the anti-ICAM-1 antibody plus splenectomy group BUN from all long-term surviving recipients was within the normal range until the end of the experiment (100 days); (Figure 3.7 d). Conversely, in the splenectomy only group, although three recipients survived long-term, the BUN steadily increased with time until the mice succumbed to rejection (Figure 3.7 c).

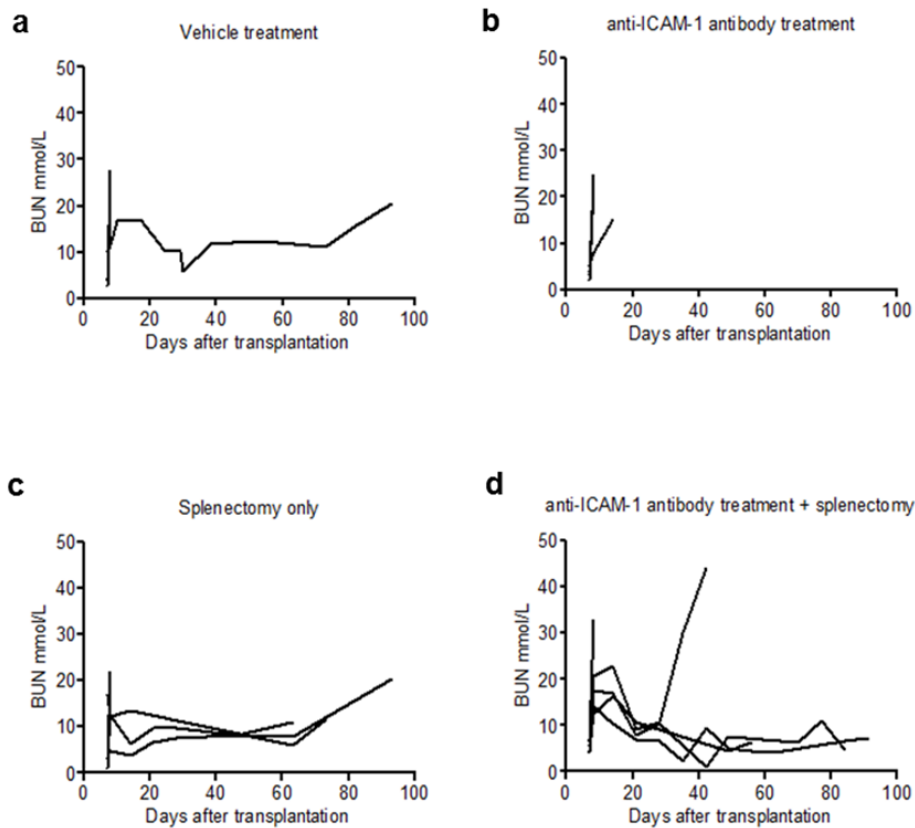


Figure 3.7- Blood urea nitrogen (BUN) measurements from kidney allograft recipients. (a) BUN of mice receiving vehicle treatment only with no splenectomy where most recipients were sacrificed at an early time point due to poor graft function with high BUN. (b) BUN of mice receiving anti-ICAM-1 antibody-treatment only and no splenectomy where all recipients were sacrificed at an early time point due to poor graft function with high BUN. (c) BUN of mice receiving splenectomy only where those surviving past day 10 had increasing BUN. (d) BUN of mice receiving anti-ICAM-1 antibody-treatment and splenectomy where 60% of recipients survived until the end of the experiment with normal graft function and BUN within normal range. Normal range is 0-10 mmol/L.

Histological examination of donor grafts transplanted into anti-ICAM-1 antibody-treated splenectomised recipients showed well preserved tubules. Areas of dense mononuclear cell infiltration, suggestive of tertiary lymphoid organs, were also found (Figure 3.8), in accordance with our previous description of histological changes in tolerant murine kidney allografts (186). Thus, reducing DPL trafficking via lymphatics in the early post-transplantation period improved graft function and survival, but only if the recipient spleen was removed before transplantation.

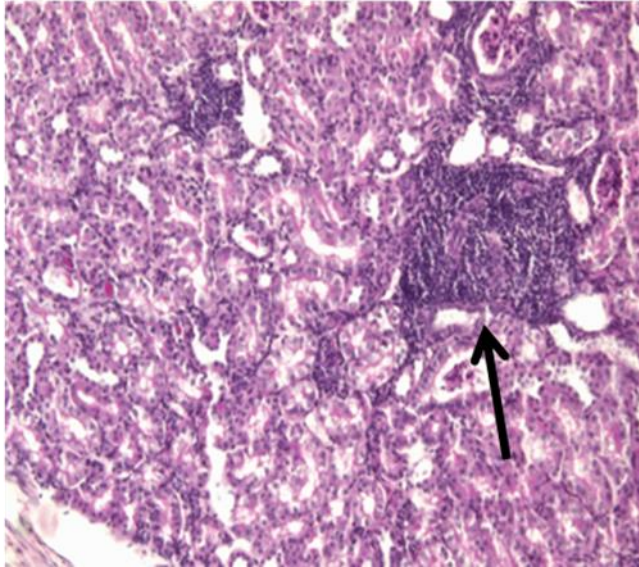


Figure 3.8- Histology of long-term surviving kidney grafts. Kidney grafts were harvested 100 days after transplantation and stained with periodic acid Schiff's (PAS) to demonstrate tissue structure and cellular infiltration. Representative PAS staining on long-term surviving kidney allograft from splenectomised anti-ICAM-1 antibody-treated recipient, showing presence of dense mononuclear cell infiltration, suggestive of tertiary lymphoid organs (arrow). Original magnification 100x.

3.4 Quantification of T cell infiltrate in anti-ICAM-1 antibody-treated allogeneic kidney grafts

Rejection and tolerance of allografts is mediated by T cells which have encountered donor antigen. Donor-specific T cells that have been activated in recipient SLO traffic back to the graft to exert their effector functions. In order to clarify whether the positive effects of anti-ICAM-1 antibody treatment in splenectomised recipients was due to a reduction in T cell priming in DLN as a result of reduced trafficking of DPL; the graft T cell response was analysed.

Kidney grafts were harvested from recipients having either received anti-ICAM-1 antibody therapy plus splenectomy or vehicle plus splenectomy, 5 days following transplantation, and the T cell infiltrate was quantified using flow cytometry (Figure 3.9).

Day 5 was chosen as it was around the time of heavy T cell infiltration, but before the entire kidney was destroyed, making it impossible to perform histological analysis.

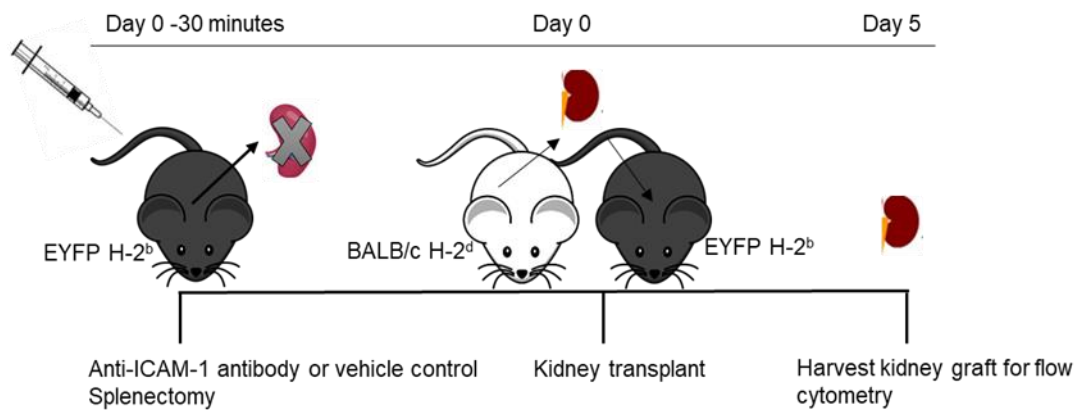


Figure 3.9- Experimental design of assessment of T cell infiltration of kidney allografts in anti-ICAM-1 antibody-treated recipients.

Kidney grafts were digested and the leukocytes obtained by density centrifugation. T cells were gated as presented in Figure 3.10; lymphocytes were broadly gated in the forward vs. side scatter plot and then further defined as single cells. These cells were further defined as CD45⁺ and dead cells were excluded. They were further categorized by CD3 positivity and then the CD4⁺ and CD8⁺ populations quantified and expression of CD44 assessed.

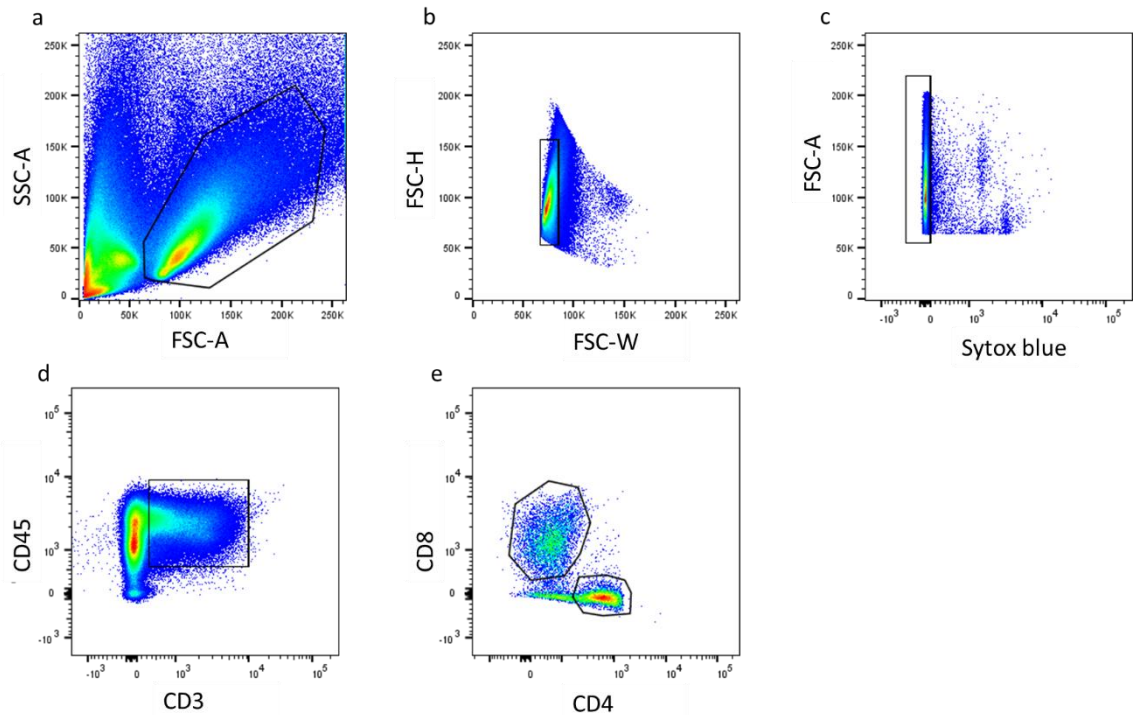


Figure 3.10- Gating strategy for T cells.

Kidney grafts were harvested at day 5 post-transplantation, digested and the leukocytes recovered. Cells were gated according to (a) scatter properties, (b) single cells, (c) dead cell stain exclusion, (c) CD45 and CD3 expression (e) CD8 or CD4 expression.

Grafts from recipients treated with anti-ICAM-1 before transplantation had a similar degree of T cell infiltration as grafts from those that received vehicle treatment. There was no difference in the size of the T cell population (CD45 CD3 double positive population) as a proportion of the total between anti-ICAM-1 antibody-treated recipients and vehicle control-treated recipients ($6.37 \pm 1.822\%$ vs. $4.63 \pm 0.7\%$, $p=0.4717$); (Figure 3.11 a). In addition, there was no difference in the size of the CD4+ and CD8+ T cell populations as a proportion of the total between anti-ICAM-1 antibody-treated and vehicle control-treated recipients (CD4+, 2.560 ± 0.86 vs. $2.613 \pm 0.35\%$, $p=0.9617$; CD8, 2.96 ± 0.89 vs. $1.47 \pm 0.33\%$, $p=0.2299$); (Figure 3.11 b and c).

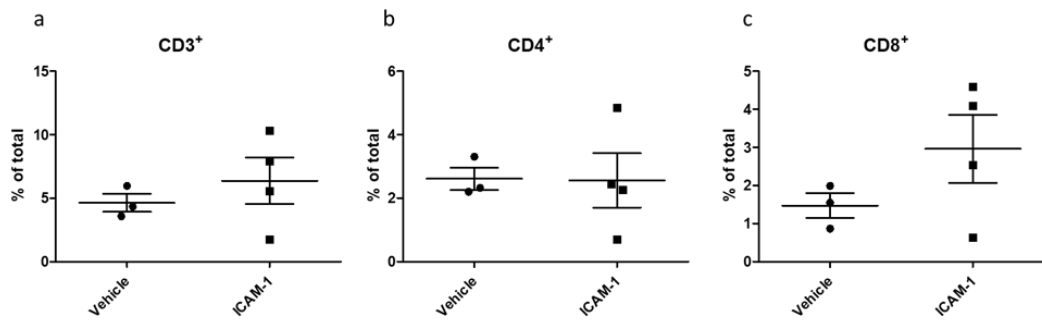


Figure 3.11- Size of T cell populations within kidney grafts at day 5 post-transplantation (proportion).

Kidney grafts were harvested at day 5 post-transplantation, digested and the leukocytes recovered. Cells were analysed for expression of CD3, CD4 and CD8 by flow cytometry. There were no differences in the size of the (a) total T cell populations, $p=0.4717$ (b) CD4⁺ T cell populations, $p=0.9617$ and (c) CD8⁺ T cell populations, $p=0.2299$ as a proportion of the total between anti-ICAM-1 antibody-treated and vehicle control-treated recipients. Each data point represents one mouse.

These results were confirmed by calculation of the number of CD3⁺, and CD3⁺CD4⁺, and CD3⁺CD8⁺ cells per gram of tissue in each sample. Absolute numbers were calculated using the weight of the portion of the kidney used for analysis. There was no difference in the number of CD3⁺, CD3⁺CD4⁺ or CD3⁺CD8⁺ cells between grafts from anti-ICAM-1 antibody-treated and vehicle control-treated recipients (CD3⁺, 11214±2676 vs. 6114±13967 cells/gram, $p=0.2143$; CD4⁺, 4517±1164 vs. 3647±781 cells/gram, $p=0.5930$; CD8⁺, 4924±1202 vs. 2016±539 cells/gram, $p=0.1087$); (Figure 3.12 a-c).

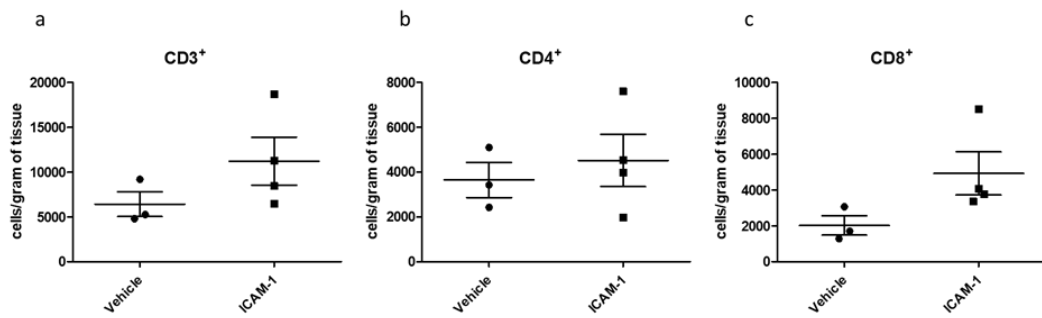


Figure 3.12- Size of T cell populations within kidney grafts at day 5 post-transplantation (absolute number).

Kidney grafts were harvested at day 5 post-transplantation, digested and the leukocytes recovered. Cells were analysed for expression of CD3, CD4 and CD8 by flow cytometry. There were no differences in the number of (a) total T cells, $p=0.2143$ (b) CD4⁺ T cells, $p=0.5930$ and (c) CD8⁺ T cells, $p=0.1087$ between anti-ICAM-1 antibody-treated and vehicle control-treated recipients. Each data point represents one mouse.

The activation status of the T cells infiltrating kidney allografts in anti-ICAM-1 antibody-treated and vehicle control-treated recipients was then assessed. CD44 is frequently used as a marker of T-cell activation because T cells upregulate expression of this molecule following activation (228). There was no difference in expression levels of CD44 on CD4⁺ and CD8⁺ T cells from anti-ICAM-1 treated grafts compared with vehicle control-treated graft, (MFI (median fluorescence intensity) of CD44 on CD4⁺ T cells, 8140 ± 361 vs. 6287 ± 838 , $p=0.0737$; MFI of CD44 on CD8⁺ T cells, 5931 ± 207 vs. 4886 ± 499 , $p=0.0832$); (Figure 3.13 a and b).

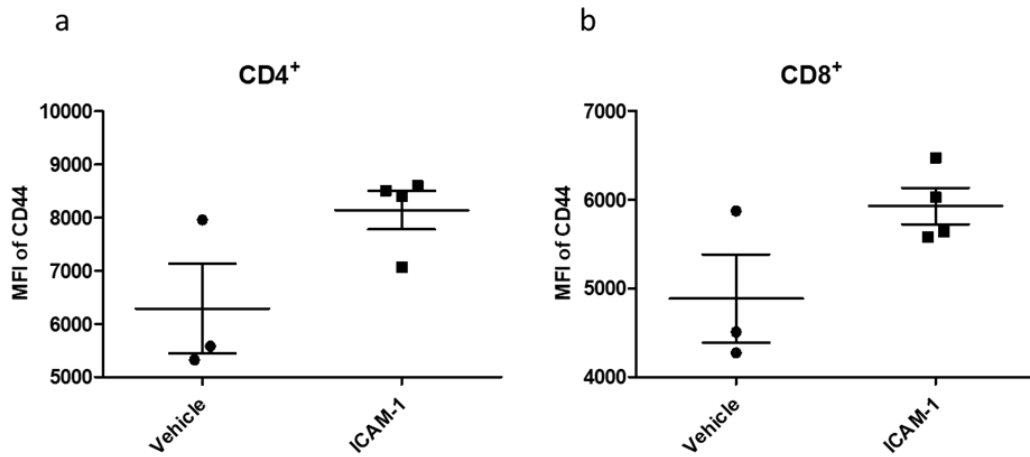


Figure 3.13- Activation status of T cells infiltrating kidney grafts at day 5 post-transplantation. Kidney grafts were harvested at day 5 post-transplantation, digested and the leukocytes recovered. T cells were analysed by flow cytometry for expression of the activation marker, CD44. There was no difference in expression of CD44 on graft-infiltrating (a) CD4⁺, $p=0.0737$ and (b) CD8⁺ T cells, $p=0.0832$ between anti-ICAM-1 antibody-treated and vehicle control-treated recipients. Each data point represents one mouse. MFI (median fluorescence intensity).

In addition, the numbers of Foxp3⁺ cells within the grafts from both groups at day 5 were investigated. The expression of the Treg-specific transcription factor, Foxp3, was examined histologically and no difference in number of Foxp3-expressing cells was found between the anti-ICAM-1-treated and vehicle-treated groups (13.55 ± 2.32 vs. 15.83 ± 3.75 positive cells per medium powered field, $p=0.6072$); (Figure 3.14 a and b).

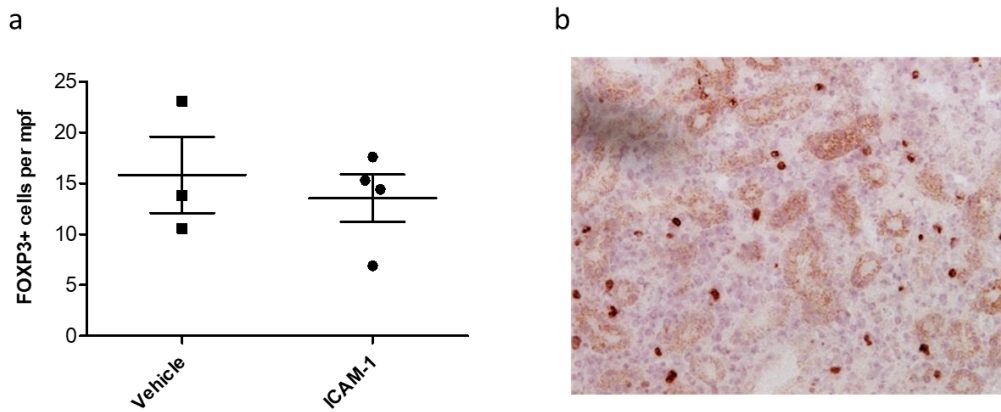


Figure 3.14- Foxp3 expression within kidney grafts at day 5 post-transplantation. Kidney grafts were harvested at day 5 post-transplantation and snap frozen sections were stained immunohistochemically for expression of the Treg specific transcription factor, Foxp3. (a) There was no difference in the average number of Foxp3 positive cells per medium powered field within graft tissue between anti-ICAM-1 antibody-treated and vehicle control-treated recipients, $p=0.6072$. (b) Representative image showing Foxp3 positive cells distributed throughout the parenchyma of a kidney graft. Original magnification 200x. At least 10 random fields of view were analysed per section. Each data point represents one tissue section from one mouse.

In conclusion, there was no difference in the T cell infiltration of kidney allografts between recipients that received anti-ICAM-1 antibody treatment compared with those that received vehicle control treatment. The proportions and absolute numbers of the CD4⁺ and CD8⁺ T cell populations were similar between the two groups. In addition, there was no significant difference in expression levels of CD44 on T cells between anti-ICAM-1-treated and vehicle control-treated recipients. And finally the numbers of Tregs were the same between the two groups, as assessed by immunohistochemical analysis of Foxp3 expression.

3.5 Summary

This chapter presents results from an experiment using anti-ICAM-1 antibody treatment in a murine kidney transplant model in order to test the contribution of post-transplantation trafficking of DPL via the lymphatic route. Recipient mice were treated with an anti-ICAM-1 antibody or saline before transplantation and their spleens removed

so that the lymphatic route could be assessed in isolation. Treatment with anti-ICAM-1 antibody led to a reduction in donor-derived DNA in the recipient DLN 24 hours post-transplantation; and long-term graft survival with normal function in some recipients. The T cell infiltrate within the graft was also assessed at day 5 after transplantation, and no significant differences in proportions and numbers of CD4⁺ and CD8⁺ T cells were found between anti-ICAM-1-treated and vehicle control-treated animals.

3.6 Discussion

Efficient trafficking of immune cells is essential for the induction of the allo-immune response in solid organ transplantation; in particular the movement of DPL from the graft to the local DLN, where they encounter and activate cognate T cells, is the driving force of acute rejection.

Previous work from our group has visualised lymph flow from the graft to DLN in heterotopic murine heart transplantation, and has demonstrated the presence of donor specific allo-reactive T cells in these lymph nodes, but not in other non-draining lymph nodes (176). Here, the aim was to establish whether blocking the traffic of cells from the graft to the DLN via the lymphatic route would affect the survival of allografts.

Studies on the fate of DPL after transplantation are limited by technical difficulties in tracing these cells *in vivo* in an accurate and quantitative manner. This is in part due to the small population size, and the lack of reliable markers. Most *in vivo* tracking studies rely on the use of the CD45.1/CD45.2 alloantigen system, and employ flow cytometry to quantify cells of donor origin (229). This often means that tissue from multiple recipient mice are pooled together so that the donor population can be seen reliably on the flow cytometry plot. Quantitative real-time PCR, amplifying genomic DNA targets, is more sensitive for quantification of small populations as in theory only one copy of the target

gene is needed for amplification to occur and be visualised by fluorescence. Indeed, this technique is successfully used for the assessment of haematological disease (230), and for diagnosis of viral infection in the clinic (231). This technique has been used here to accurately quantify the number of donor cells that have trafficked to the DLN of recipients.

An ICAM-1-dependant mechanism for immune cell trafficking via the lymphatic system, in inflammatory conditions has been confirmed by others (129), but whether or not this pathway is important in the immune response following transplantation has not yet been investigated. Here, it is shown that treatment with an ICAM-1 blocking antibody immediately prior to transplantation reduced trafficking of DPL to the DLN. When used in recipients of kidney allografts with intact spleens, this did not result in graft prolongation. This is not surprising as donor passenger leukocytes can leave donor organs via the blood and traffic to the spleen of recipient where they can prime T cells (88), indicating that the blood and lymphatic routes of antigen trafficking to SLO can compensate for each other. Removal of the spleen of the recipient removed this route and resulted in significant prolongation of graft survival in this model. One recipient in the vehicle only group rejected the donor graft later, at 81 days rather than around 8 to 10 days. This is not unusual; late rather than early rejection in a small percentage of recipients has been described in this model (232).

These results point to an active role for ICAM-1 in trafficking of DPL following transplantation; blocking of this pathway resulting in a dampened allo-immune response and long-term survival of allografts. This is consistent with observations by Ziegler and colleagues, who demonstrated suppression of antigen-induced T-cell proliferation when trafficking was reduced following CCL19-IgG treatment to block lymphatic chemokine gradients (233).

Other pathways, in addition to the direct antigen presentation pathway, such as the indirect and semi-direct pathways of antigen presentation, are important in the rejection response. The demonstration here that blocking the direct pathway resulted in prolonged graft survival does not mean that the other pathways of antigen presentation are not important. This would be particularly true in human organ transplantation where the rejection response is expected to be more pronounced than that seen in laboratory animals (234).

Anti-ICAM-1 antibody treatment may have other effects in addition to blockade of DPL trafficking; and therefore, the beneficial effect of anti-ICAM-1 antibody treatment seen here may not be solely attributed to its effect on DPL trafficking. ICAM-1 is a known molecule involved in T-cell transmigration into tissue during inflammation (235), as well as a co-stimulator of T cells (reviewed in (236)), and indeed blocking studies have previously been performed in transplantation models to confirm the role of ICAM-1 in this context (226). However, the focus of this work was to assess the role of ICAM-1-mediated lymphatic trafficking in the immediate post-transplant period, and thus treatment was restricted to one pre-transplantation injection, rather than repeat injections for the duration of the experiment. Anti-ICAM-1 antibody treatment was not expected to have any significant effect on T cell infiltration into the graft, which happens later after transplantation.

If indeed, reduced DPL trafficking and therefore reduced T-cell activation was the sole mechanism responsible for the graft prolongation effect seen, then one would expect reduced T cell infiltration into the anti-ICAM-1-treated donor grafts. However this was not the case. The T cell infiltrate at day 5 following transplantation was the same in anti-ICAM-1-treated recipients compared with vehicle control-treated recipients. Accumulation of lymphocytes in renal allografts that eventually survive long-term is a well described phenomenon, where they have been postulated to play an active role in the graft-protective effect (186). It is also important to note that assessing T-cell infiltration

using flow cytometry, although resulting in a more accurate quantification of cell numbers than using standard immunohistochemistry, does not give any information on the location of the cells within the kidney graft. The presence of mononuclear cells within the interstitium does not always correlate with poor graft function; lymphocytes need to be present within the tubules for the diagnosis of tubulitis and therefore rejection. Without this information, it is difficult to make assumptions on the impact of the T cell infiltrate on graft function and rejection. The superior graft survival in the anti-ICAM-1 antibody-treated recipients could be because the reduction in DPL trafficking to DLN in the immediate post-transplantation period led to sub-optimal priming of T cells in this location; however, more work is needed to fully elucidate the mechanism.

In addition, blockade of the ICAM-1/LFA-1 axis has been postulated to result in T cells being released from the DLN more readily (237). Indeed, Reichardt *et al.* showed that interactions between T cells and lymphatic vessels in the lymph node via LFA-1 and ICAM-1 respectively, are essential for retention of T cells in the lymph node; and concluded that LFA-1/ICAM-1 interactions within the lymph node enhance antigen-specific responses because of increased likelihood of T cell encounter of cognate antigen (237). Therefore, it is possible that by blocking this interaction with an anti-ICAM-1 antibody in this model, sub-optimally primed T cells leave the DLN more readily and traffic to the graft.

Additionally, the anti-ICAM-1 antibody administered to the recipient has, in theory, two locations of potential action; the graft lymphatics and the recipient lymphatics. More detailed analysis would be needed to assess the contribution of these two locations of DPL trafficking to the allo-immune response.

This chapter highlights the importance of the lymphatic route of DPL trafficking in the induction of the allo-immune response, and reveals ICAM-1-mediated lymphatic trafficking as a potential therapeutic target for the prevention of acute transplant rejection.

Chapter 4 Effects of disruption to donor lymphatics on the allo- response

4.1 Background

Lymphatic vessels within the graft parenchyma are the point of entry of DPL into the recipient lymphatic system. We have previously demonstrated the route of lymph flow from here to the DLN in a murine model of heterotopic heart transplantation (176). The previous chapter explored the contribution of the lymphatic system to the allo-response by pharmacologically blocking ICAM-1, a key molecule involved in the transmigration of immune cells across the lymphatic endothelium.

In this chapter, an alternative approach was used to investigate whether hindering lymphatic vessel function would improve graft outcome due to altered trafficking of DPL in the immediate post-transplantation period. Various agents are available to target lymphatic function systemically such as anti-CCL21 (179) and anti-VEGFR3 (178); however, their effects are limited to the treatment period and they target mainly the development of new lymphatic vessels, rather than lymphatic vessels that are already within the donor grafts. Here, a specific mouse strain which has a spatially and temporally conditional knock-out of ephrin B2 was used. The eph/ephrin signalling pathway controls multiple cell functions including migration and cytoskeletal organisation (238). Particularly in LECs, ephrin B2 signalling via ephB4 controls lymphangiogenesis and lymphatic valve maintenance (117). The mouse strain used here has a cre recombinase linked to the *Prox1* transcription factor and a floxed *ephrin B2* gene, thus allowing specific deletion of ephrin B2 in LECs. According to the original publication using this strain, following tamoxifen administration efficient ephrin B2 deletion is observed in the lymphatic endothelium within 1 week (102); and these mice lack the capacity to grow new functional lymphatic vessels and existing lymphatic vessels become functionally ineffective, dilate and disintegrate *in situ*.

When using these mice for the work presented here, it was observed that from day ten following tamoxifen administration ephrin B2 deficiency becomes fatal. Therefore, it was

decided that for all experiments ephrin B2^{-/-} mice would be harvested at day eight following tamoxifen treatment to ensure that the knockout had no effect on the function of organs to be used in transplantation models.

Using the ephrin B2^{-/-} mouse as an organ donor in transplantation therefore allowed the study of the effect of the disruption of donor lymphatics on graft survival.

4.2 Deletion of ephrin B2 following tamoxifen treatment

Mice from the ephrin B2 colony were genotyped before and after tamoxifen treatment to assess the status of the floxed *ephrin B2* gene and to demonstrate successful deletion. At weaning ear samples were taken and PCR performed using primer sequences **a** and **b** (as outlined in section 2.3.1), yielding a 380 bp product if the mice were homozygous for floxed *ephrin B2*. In addition, 8 days after tamoxifen treatment, another ear sample was taken and PCR performed using primer sequences **a** and **c**, yielding a 320 bp product if the *ephrin B2* gene had been successfully deleted (Figure 4.1).

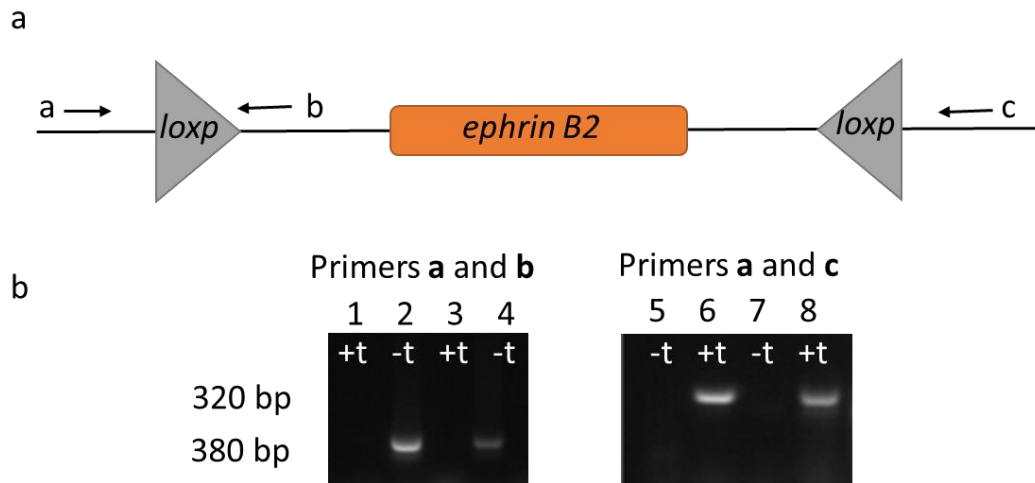


Figure 4.1- PCR to demonstrate successful deletion of *ephrin B2*. PCR was performed on DNA of cre positive mice homozygous for the floxed *ephrin B2* gene before and after tamoxifen treatment. Before tamoxifen treatment (-t), PCR using primer sequences **a** and **b** yields a 380 bp product, demonstrating that both *ephrin B2* alleles are floxed. PCR using primer sequences **a** and **c** after tamoxifen treatment (+t) yields a 320 bp product demonstrating deletion of the *ephrin B2* gene. (a) Schematic of floxed *ephrin B2* gene showing location of primer sequence binding (b) Representative images of DNA products from both PCR assays on agarose gels. Lanes 2 and 4 show a 380 bp band demonstrating that the mice are homozygous for floxed *ephrin B2*; this band is not present after tamoxifen treatment (lanes 1 and 3). Lanes 6 and 8 show a 320 bp product demonstrating that floxed *ephrin B2* has been deleted after tamoxifen treatment; this band is not present before tamoxifen treatment (lanes 5 and 7).

4.3 Effect of ephrin B2 deficiency on lymphatic morphology within organs

In order to investigate the effect of ephrin B2 deficiency in lymphatic endothelial cells the gross appearance of the lymphatic networks within organs that would subsequently be used as donor organs in transplantation models was studied. For the experiments discussed in this chapter control mice were either: wild-type for both *ephrin B2* alleles (i.e. non-floxed) and cre positive (referred to as wild-type), or had floxed *ephrin B2* alleles but were cre negative (referred to as control). The term *ephrin B2*^{-/-} refers to donor mice which have floxed *ephrin B2* alleles, are cre positive and treated with tamoxifen, meaning that the *ephrin B2* gene has been deleted in LECs. *ephrin B2*^{-/-} and wild-type mice were

treated with tamoxifen; and eight days later skin, heart and kidney tissue was harvested and analysed by immunohistochemistry. Frozen tissue sections were stained for the lymphatic marker LYVE-1, and lymphatics analysed in terms of density and size.

The density and size of lymphatic vessels in each organ was quantified. There was no difference between the ephrin B2^{-/-} and wild-type groups, in terms of lymphatic density (skin, 1.00±0.17 vs. 0.92±0.17 vessels per medium powered field, $p=0.7216$; heart, 0.64±0.13 vs. 0.69±0.01, $p=0.7372$; kidney, 0.40±0.05 vs. 0.27±0.06, $p=0.2784$); (Figure 4.2). In addition, there was no difference in average vessel size between the two groups (skin, 8656±2388 vs. 4794±563.2 arbitrary values, $p=0.1541$; heart, 7833±1867 vs. 9063±2887, $p=0.7299$; kidney, 4720±1146 vs. 3554±806, $p=0.3582$); (Figure 4.3).

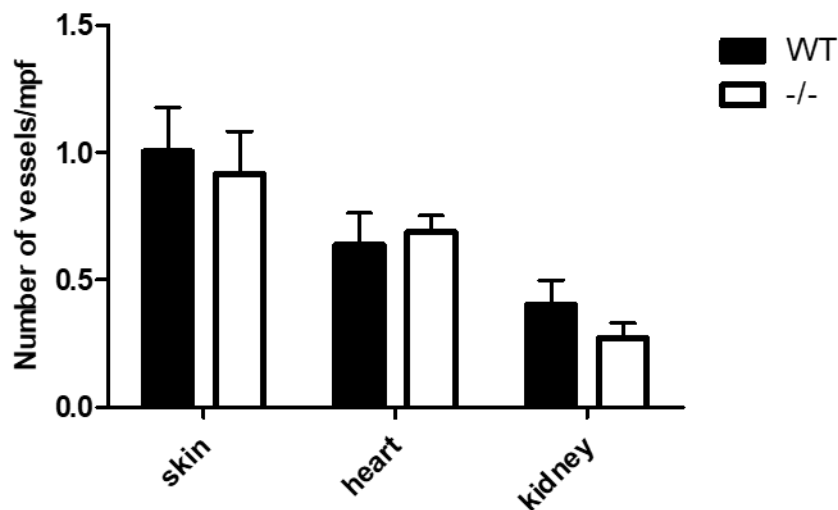


Figure 4.2- Quantification of lymphatic vessel density in skin, heart and kidney. Skin, heart and kidney tissue was harvested from ephrin B2^{-/-} and wild-type mice 8 days following tamoxifen treatment and stained for the lymphatic marker, LYVE-1. There were no differences in the number of vessels in skin ($p=0.7216$), heart ($p=0.7372$) and kidney ($p=0.2784$) tissue after tamoxifen treatment between wild-type (WT) and ephrin B2^{-/-} (-/-). At least 5 random fields of view were analysed per section. Bars represent the average number of vessels per section. One section of tissue was analysed per mouse. n=5 mice in each group.

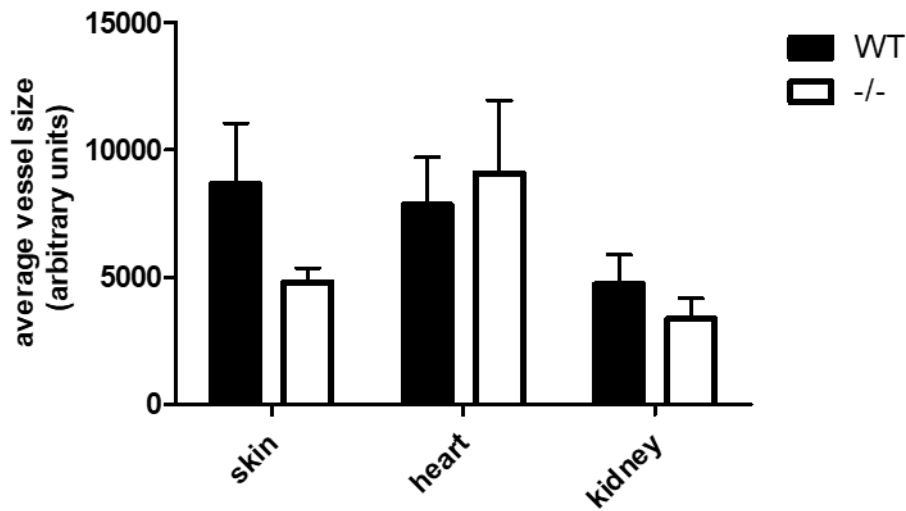


Figure 4.3- Quantification of lymphatic vessel size in skin, heart and kidney. Skin, heart and kidney tissue was harvested from ephrin B2^{-/-} and wild-type mice 8 days following tamoxifen treatment and stained for the lymphatic marker, LYVE-1. There were no differences in skin ($p=0.1541$), heart ($p=0.7299$) and kidney ($p=0.3582$) lymphatic vessel size after tamoxifen treatment between ephrin B2^{-/-} and wild-type (WT) mice. At least 5 random fields of view were analysed per section. Bars represent the average size of vessel per section. One section of tissue was analysed per mouse. n=5 mice in each group.

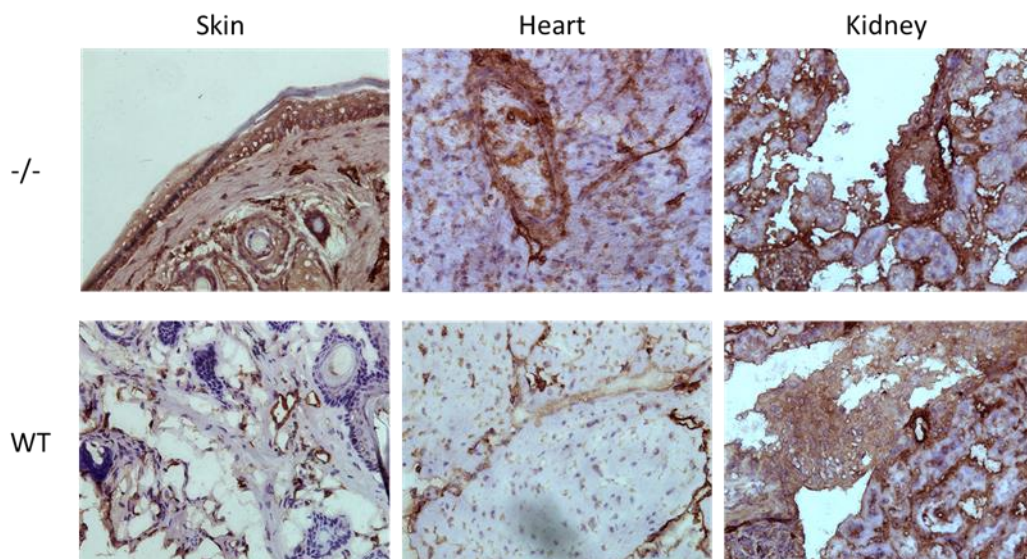


Figure 4.4- LYVE-1 staining of skin, heart and kidney tissue from tamoxifen-treated wild-type (WT) and ephrin B2^{-/-} mice. Skin, heart and kidney tissue was harvested from ephrin B2^{-/-} and wild-type mice 8 days following tamoxifen treatment and stained for the lymphatic marker, LYVE-1. Representative images of LYVE-1 staining from all tissues demonstrates no difference in size or density of lymphatics between wild-type and ephrin B2^{-/-} tissue. Original magnification 200x.

Collectively, these observations suggested that despite the fact that following deletion of *ephrin B2*, mice eventually die as a result of lymphatic dysfunction, the gross appearance of the lymphatic vasculature in skin, heart and kidney at day eight is normal in comparison to wild-type mice, and the knock-out of *ephrin B2* had no effect on lymphatic vessel density and size.

4.4 Phenotype of graft antigen presenting cells after tamoxifen treatment

As the aim was to use *ephrin B2*^{-/-} mice as organ donors in transplantation models, it was essential to confirm that the knockout of *ephrin B2* in LECs had no effect on the leukocyte composition of the donor organs being used in these models. The reason for this being that a reduction in number or antigen presenting capacity could lead to enhanced survival of *ephrin B2*^{-/-} grafts. To this end, cardiac leukocytes from tamoxifen treated wild-type and *ephrin B2*^{-/-} mice were isolated and analysed by flow cytometry (Figure 4.5).

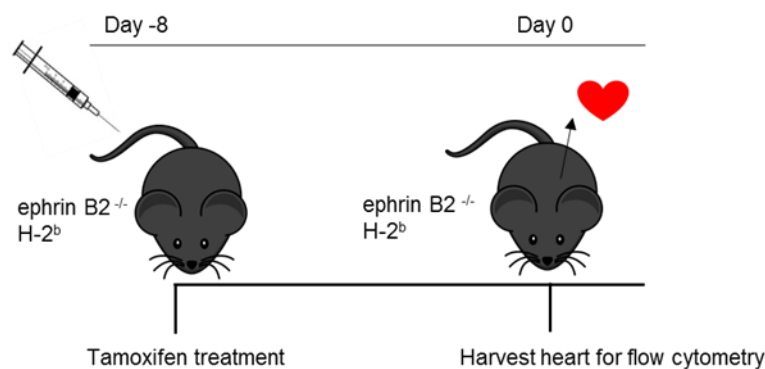


Figure 4.5- Experimental design for assessment of antigen presenting cell numbers and phenotype in *ephrin B2*^{-/-} and wild-type mice.

Hearts from wild-type and *ephrin B2*^{-/-} mice were digested and the leukocytes obtained by density centrifugation; these cells were then analysed by flow cytometry. The CD45⁺

leukocytes from each sample were analysed by first gating out debris from the digested tissue using the forward and side scatter properties of the sample. Subsequently any doublets were excluded from analysis and the CD45⁺ live population gated on for further analysis. Within the live CD45⁺ gate the proportions of CD11b⁺ and CD11c⁺ cells were calculated (Figure 4.6 a to e).

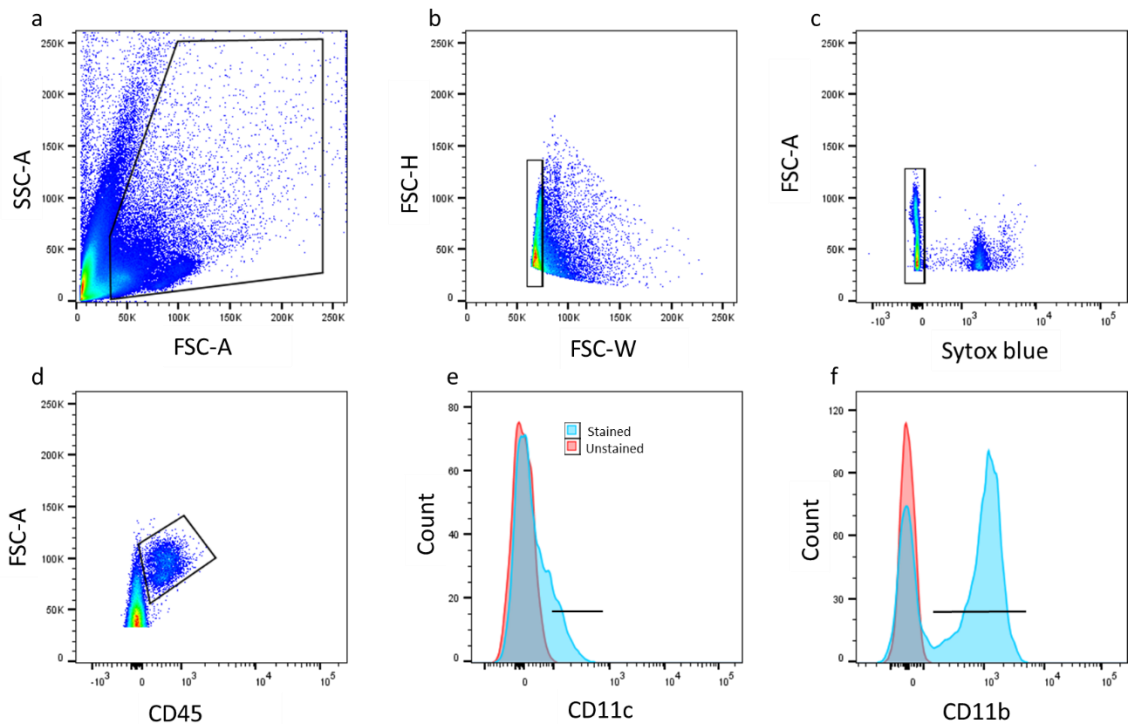


Figure 4.6- Gating strategy for heart antigen presenting cells.

Hearts were harvested 8 days after tamoxifen treatment; digested and the leukocytes recovered. Cells were gated according to (a) scatter properties, (b) single cells, (c) dead cell stain exclusion, (d) CD45 expression, and either; (e) CD11c or (f) CD11b expression. Solid black lines indicate where positive gates were placed.

The proportions of CD11b⁺ and CD11c⁺ cells within the CD45⁺ gate were analysed and no significant differences were found between the two groups in the proportions of these two APC populations. The proportion of CD11b⁺ cells in the CD45⁺ gate was 33.6±2.8% in ephrin B2^{-/-} hearts, compared with 50.52±8.93% in wild-type hearts ($p=0.1089$); (Figure 4.7 a). The proportion of CD11c⁺ cells in the CD45⁺ gate was 8.21±1.5% in ephrin B2^{-/-} hearts, compared with 15.78±5.21% in wild-type hearts ($p=0.2001$); (Figure 4.7 b).

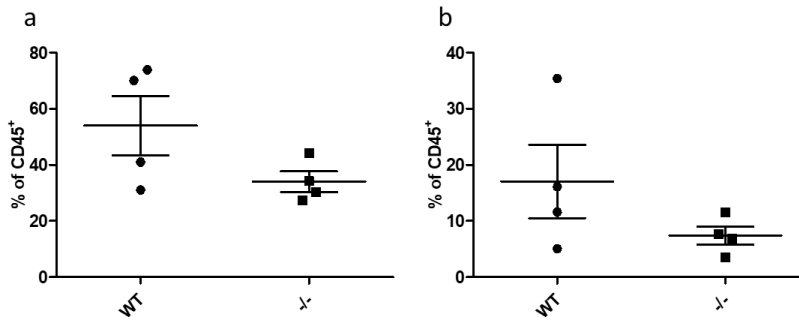


Figure 4.7- Proportions of antigen presenting cells in heart tissue from ephrin B2^{-/-} (-/-) and wild-type (WT) mice after tamoxifen treatment. Hearts were harvested 8 days after tamoxifen treatment, digested and the leukocytes recovered. Cells were gated according to Figure 4.6 and analysed for expression of CD11c and CD11b. There were no differences in the size of (a) the CD11b⁺ population, $p=0.1089$, and (b) the CD11c⁺ population, $p=0.2001$ as a proportion of the total CD45⁺ leukocyte population between ephrin B2^{-/-} and wild-type mice. Each data point represents one mouse.

In order to confirm the above finding, the absolute numbers of CD11b⁺ and CD11c⁺ cells within the heart leukocyte preparations were calculated using the values calculated when counting the cells during preparation of the sample at the stage following density centrifugation. There was no significant difference in the numbers of CD11b⁺ cells between ephrin B2^{-/-} and wild-type heart leukocytes (3245 ± 3799 vs. 10743 ± 3642 , $p=0.0910$); (Figure 4.8 a). Similarly, there was no significant difference in the numbers of CD11c⁺ cells between ephrin B2^{-/-} and wild-type heart leukocytes (689 ± 222 vs. 3069 ± 1735 , $p=0.2225$); (Figure 4.8b).

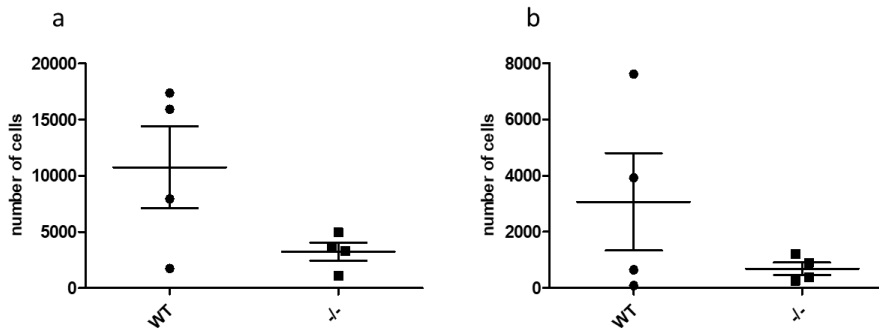


Figure 4.8- Absolute numbers of antigen presenting cells in heart tissue from ephrin B2^{-/-} (-/-) and wild-type (WT) mice after tamoxifen treatment.

Hearts were harvested 8 days after tamoxifen treatment, digested and the leukocytes recovered. Cells were gated according to Figure 4.6, analysed for expression of CD11c and CD11b, and the absolute numbers calculated based on the total cells recovered from the tissue. There were no differences in the numbers of (a) CD11b⁺ cells, $p=0.0910$, and (b) CD11c⁺ cells, $p=0.2225$ between ephrin B2^{-/-} and wild-type mice. Each data point represents one mouse.

DCs become activated by local inflammation leading them to adopt a 'mature' phenotype. Following maturation, DCs upregulate expression of MHC class II and co-stimulatory molecules, such as CD80, to enhance antigen presentation to T cells, and migratory molecules, such as CCR7, to aid trafficking to SLO. Therefore, the CD11c⁺ and CD11b⁺ populations within heart tissue of wild-type and ephrin B2^{-/-} mice were studied to examine whether or not the absence of ephrin B2 on LEC had affected the phenotype of heart resident DCs. As expected, MHC class II expression by DCs (both CD11c⁺ and CD11b⁺) was low, and there was no statistically significant difference in the proportion of CD11c⁺ and CD11b⁺ cells that were MHC II⁺ between cells isolated from ephrin B2^{-/-} hearts compared with wild-type hearts (CD11c⁺: 9.93 ± 2.64 vs. 9.80 ± 4.35 , $p=0.9793$, CD11b⁺: 0.51 ± 0.42 vs. 0.83 ± 0.56 , $p=0.6588$); (Figure 4.9 e and Figure 4.10 e respectively). The heart resident antigen presenting cell populations were compared to those recovered from transplant recipient spleens, where the CD11c and MHC class II expression are both high (Figure 4.9 b); to demonstrate that heart resident CD11c⁺ and CD11b⁺ leukocyte populations are immature, and that this is unchanged by deletion of ephrin B2.

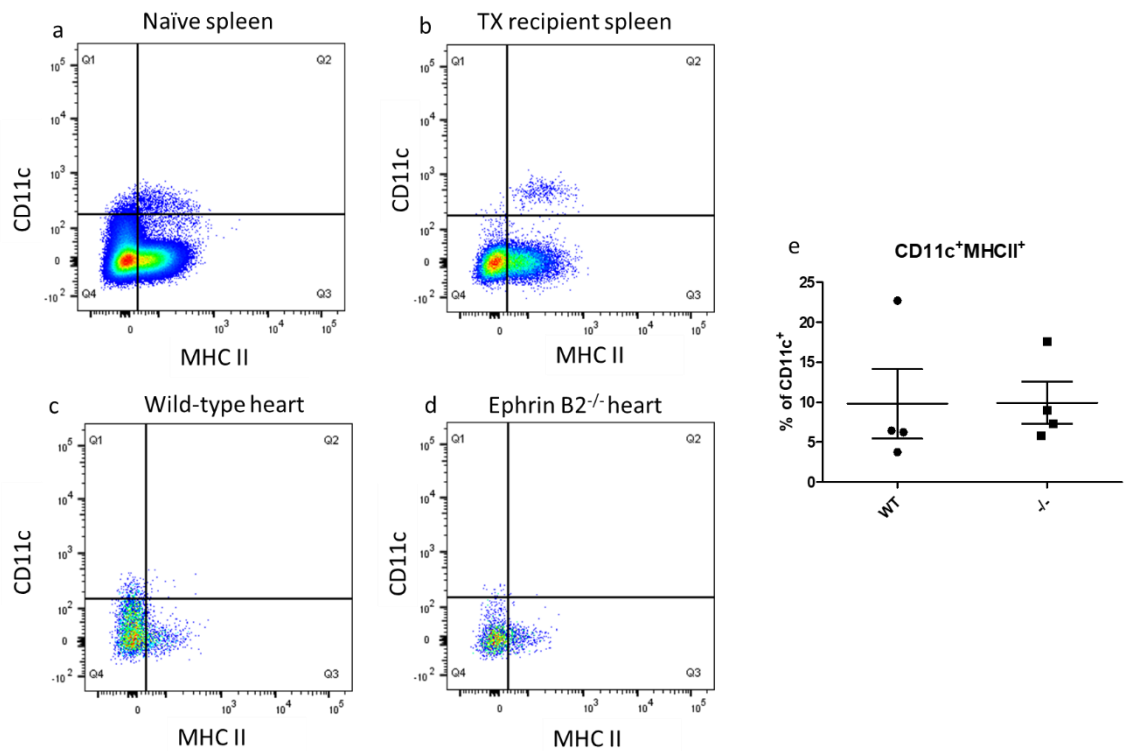


Figure 4.9- Phenotype of heart resident CD11c⁺ cells wild-type (WT) and ephrin B2^{-/-} hearts following tamoxifen treatment.

Hearts were harvested 8 days after tamoxifen treatment, and spleen were harvested 1 days after allogeneic heart transplantation, digested and the leukocytes recovered. Cells were gated according to Figure 4.6 and analysed for expression of CD11c and MHC class II. Heart leukocytes were compared to (a) naïve spleen leukocytes and (b) spleen leukocytes recovered from a heart transplant recipient to demonstrate immature status of CD11c⁺ dendritic cells. There was no difference in the proportion of CD11c⁺ MHC II⁺ double positive cells between (c and e) wild-type and (d and e) ephrin B2^{-/-} hearts following tamoxifen treatment. (e) Each data point represents one mouse. $p=0.6588$

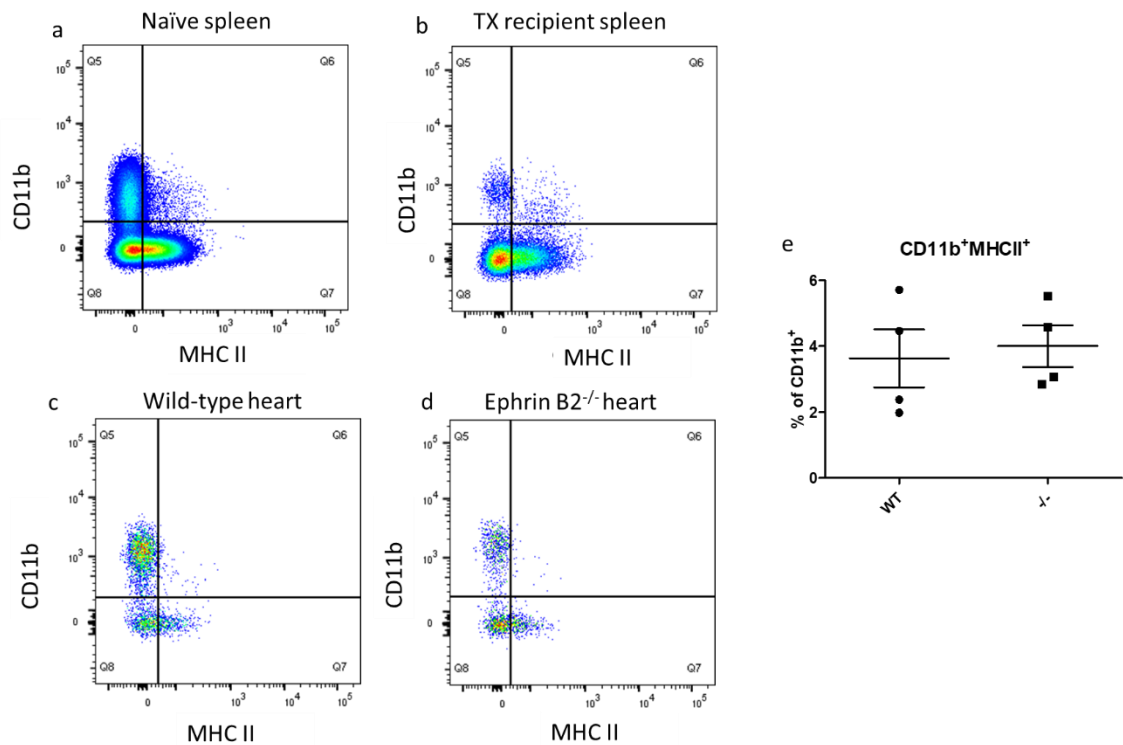


Figure 4.10- Phenotype of heart resident CD11b⁺ cells wild-type (WT) and ephrin B2^{-/-} hearts following tamoxifen treatment.

Hearts were harvested 8 days after tamoxifen treatment, digested and the leukocytes recovered. Cells were gated according to Figure 4.6 and analysed for expression of CD11b and MHC class II. Heart leukocytes were compared to (a) naïve spleen leukocytes and (b) spleen leukocytes recovered from a heart transplant recipient to demonstrate immature status of CD11b⁺ antigen-presenting cells. There was no difference in the proportion of CD11b⁺ MHC II⁺ double positive cells between (c and e) wild-type and (d and e) ephrin B2^{-/-} hearts following tamoxifen treatment. (e) Each data point represents one mouse. $p=0.9793$

Therefore, deficiency of ephrin B2 in LECs within heart tissue had no discernible impact on the phenotype of resident populations of APC; cells that would become DPL following transplantation.

4.5 Survival of ephrin B2^{-/-} grafts in allogeneic recipients

Lymphatic vessels in the donor organ serve as an entry point for DPL into the recipient, as from here it is hypothesised that they leave the graft and are eventually picked up by recipient lymphatics and traffic to the DLN. Therefore, it was decided to assess the effect of knocking out ephrin B2, an essential molecule in lymphatic vessel function, in graft lymphatics, on the allo-immune response.

Donor mice were administered 5µg tamoxifen intraperitoneally, and after 8 days skin, hearts and kidneys were transplanted into fully allogeneic BALB/c recipients (Figure 4.11).

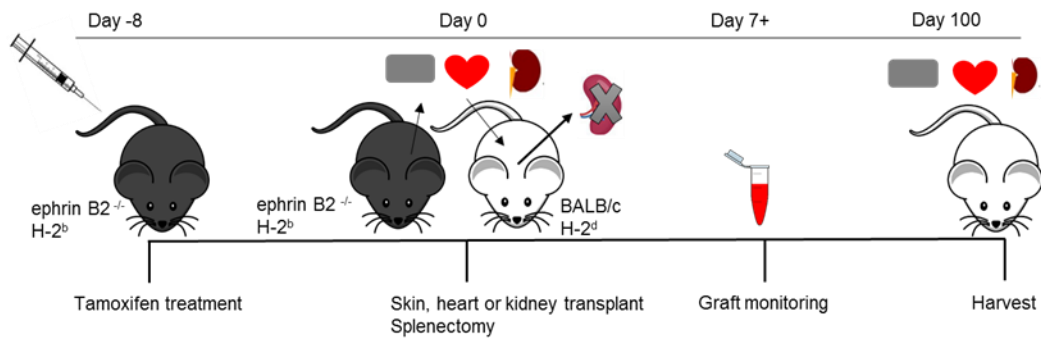
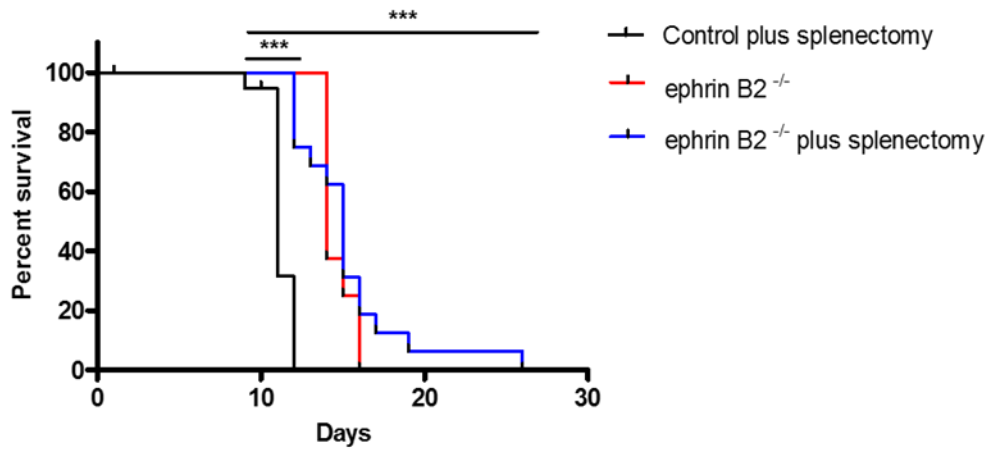


Figure 4.11- Experimental design for assessment of survival of ephrin B2^{-/-} grafts in allogeneic recipients.

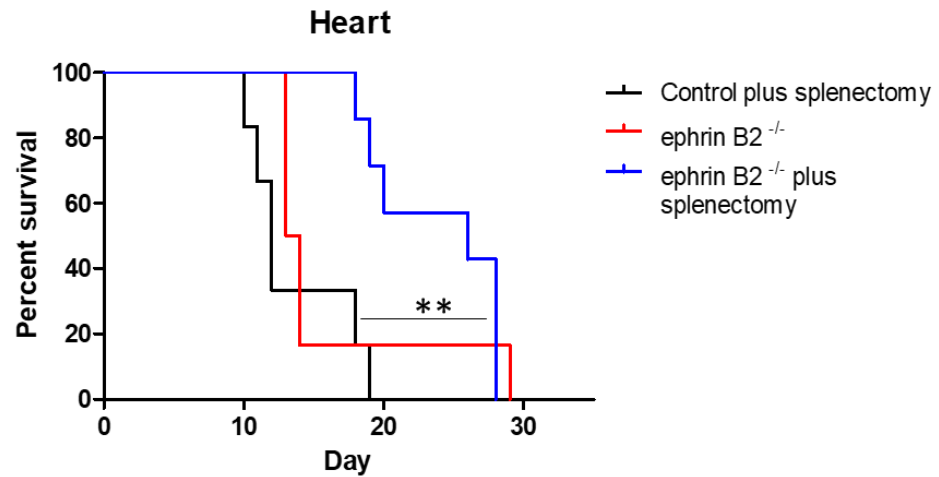
Whilst skin allografts from control donors transplanted onto BALB/c splenectomised recipients were rejected acutely (MST=10 days), skin from ephrin B2^{-/-} donors survived significantly longer on BALB/c recipients with or without intact spleens (splenectomy: MST=15 days, $p<0.0001$, non-splenectomy: MST=14 days, $p<0.0001$); (Figure 4.12).



Group	Phenotype	Splenectomy	MST	N	<i>p</i> (Compared to control+splenectomy)
—	Wild-type	yes	10	11	NA
—	Ephrin B2 ^{-/-}	no	14	8	<0.0001
—	Ephrin B2 ^{-/-}	yes	15	16	<0.0001

Figure 4.12- Survival of ephrin B2^{-/-} skin on allogeneic recipients. Skin from ephrin B2^{-/-} and control mice was transplanted onto BALB/c recipients that had either received a splenectomy or had intact spleens. Ephrin B2^{-/-} skin survived significantly longer than control skin. *** *p*<0.0001

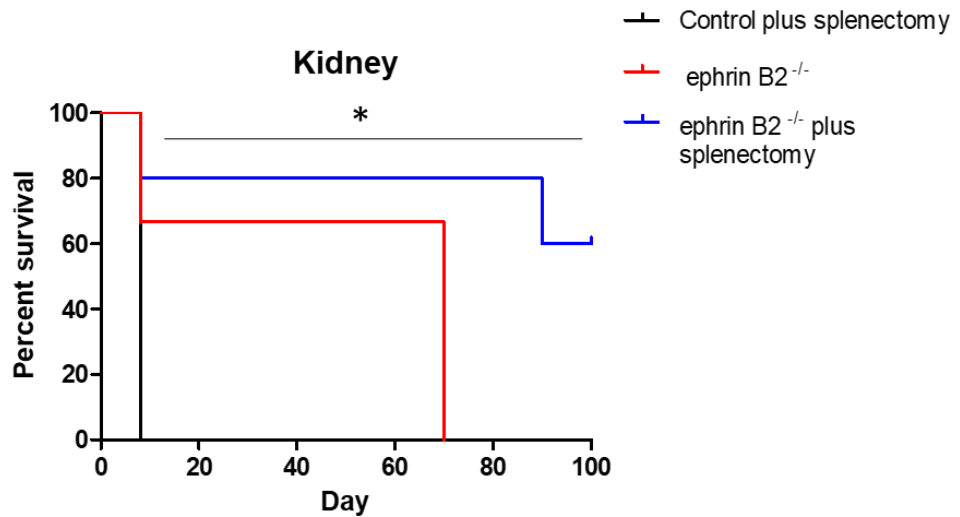
Heart allografts from ephrin B2^{-/-} donors also survived significantly longer in splenectomised BALB/c recipients (MST=26 days) than control hearts (MST=12 days, *p*=0.0021) and ephrin B2^{-/-} hearts in non-splenectomised recipients (MST=13.5 days, *p*=0.2981); (Figure 4.13).



Group	Phenotype	Splenectomy	MST	N	<i>p</i> (Compared to control+splenectomy)
—	Wild-type	yes	12	6	NA
—	Ephrin B2 ^{-/-}	no	13.5	6	0.2981
—	Ephrin B2 ^{-/-}	yes	26	7	0.0021

Figure 4.13- Survival of ephrin B2^{-/-} hearts in allogeneic recipients. Hearts from ephrin B2^{-/-} and control mice were transplanted into BALB/c recipients that had either received a splenectomy or had intact spleens. Ephrin B2^{-/-} hearts survived significantly longer than control hearts. ** $p < 0.01$

Kidneys from ephrin B2^{-/-} donors survived indefinitely in splenectomised BALB/c recipients (MST > 100 days) whereas control kidneys rejected acutely (MST = 8 days, $p = 0.0237$). Ephrin B2^{-/-} kidneys in non-splenectomised recipients has an MST of 70 ($p = 0.0736$); (Figure 4.14). Therefore, disruption of donor lymphatics had a significant impact on graft survival, with all organs assessed (skin, heart, and kidney) surviving longer in allogeneic recipients if the *ephrin B2* gene was knocked out prior to transplantation.



Group	Phenotype	Splenectomy	MST	N	p (Compared to control+splenectomy)
—	Wild-type	yes	8	4	NA
—	Ephrin B2 ^{-/-}	no	70	3	0.0736
—	Ephrin B2 ^{-/-}	yes	>100	5	0.0237

Figure 4.14- Survival of ephrin B2^{-/-} kidneys in allogeneic recipients. Kidneys from ephrin B2^{-/-} and control mice were transplanted into BALB/c recipients that had either received a splenectomy or had intact spleens. Ephrin B2^{-/-} kidneys survived significantly longer than control kidneys when the recipient was splenectomised. * $p < 0.05$

Ephrin B2^{-/-} kidneys that survived long-term in splenectomised recipients had normal kidney function, as demonstrated by a mean BUN of 9.45 ± 2.9 mmol/L at the end of the experiment (100 days, normal range 0-10 mmol/L). In addition, histological analysis of sections from long-term surviving ephrin B2^{-/-} kidneys showed small well defined areas of dense mononuclear cell infiltration, suggestive of TLOs, well preserved tubular structure, and mild lymphocyte infiltration of tubules (Figure 4.15). These histological changes have previously been shown in a model of kidney allograft tolerance in our laboratory (186).

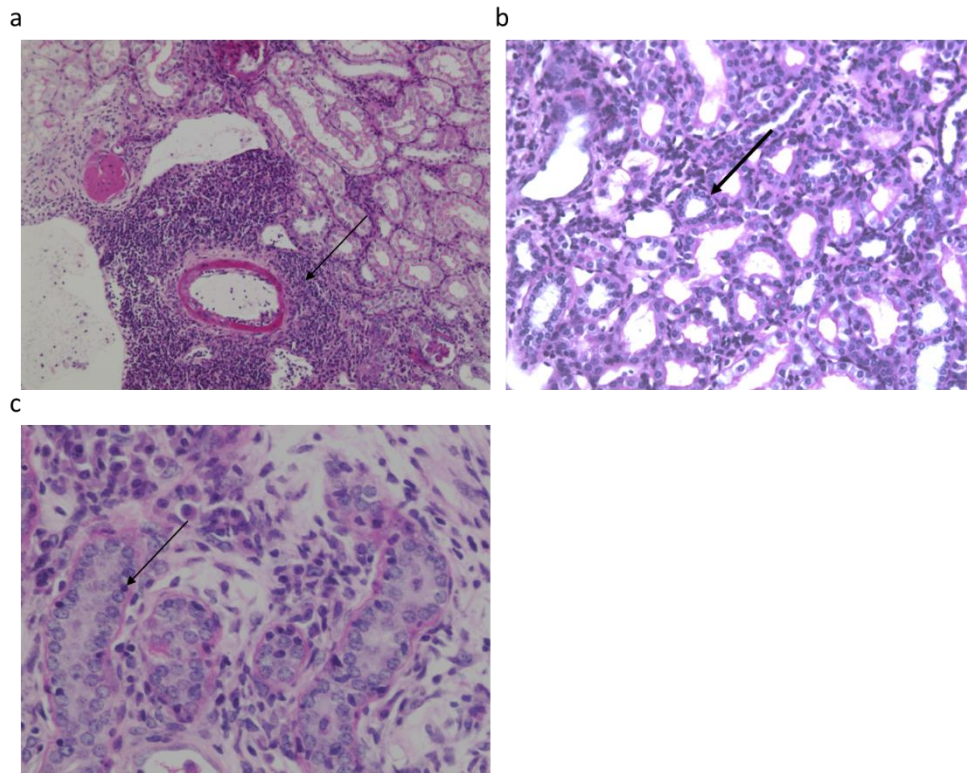


Figure 4.15- Histology of long-term surviving ephrin B2^{-/-} kidney grafts. Kidney grafts were harvested 100 days after transplantation and stained with PAS to demonstrate tissue structure and cellular infiltration. Representative images showing (a) presence of dense mononuclear infiltrates suggestive of TLOs (arrow), (b, c) good preservation of tubular structure with mild lymphocyte infiltration into tubules (arrows). Original magnification (a) 40x, (b) 200x, (c) 400x

In addition, immunohistochemical analysis of long-term surviving ephrin B2^{-/-} kidney grafts revealed the presence of lymphatic vessels (Figure 4.16). Lymphatic vessels were observed in all ephrin B2^{-/-} kidney grafts that survived to 100 days.

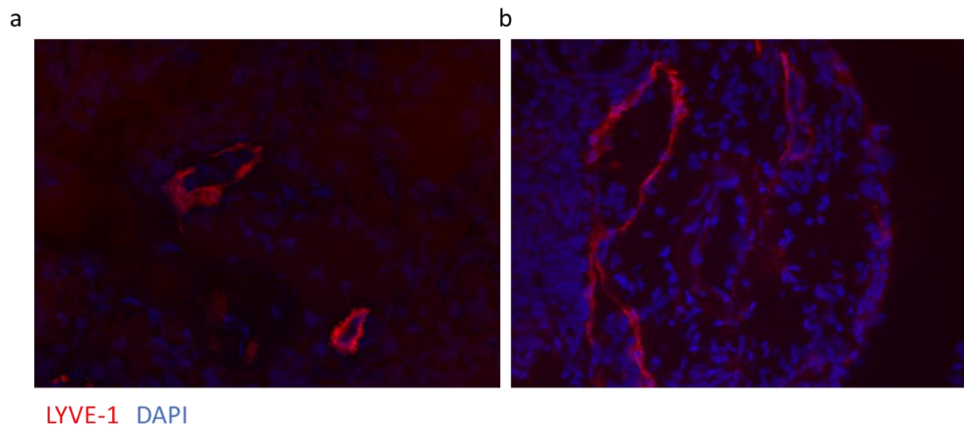


Figure 4.16- LYVE-1 staining of long-term surviving ephrin B2^{-/-} kidney grafts. Kidney grafts were harvested 100 days after transplantation and stained for the lymphatic marker LYVE-1. Representative images showing presence of lymphatic vessels in ephrin B2^{-/-} kidney grafts. Original magnification (a and b) 200x

4.6 Quantification of DPL trafficking using real-time PCR

Having demonstrated that organs with the ephrin B2 knockout in LECs survived longer after transplantation than organs without the knockout, the effect of this on post transplantation trafficking of DPL was assessed. As ephrin B2 is essential for lymphatic function, it was hypothesised that the knockout would result in a different trafficking pattern of cells out of the graft in the immediate post-transplantation period.

To determine the effect of the ephrin B2 knockout on DPL trafficking, ephrin B2^{-/-} hearts or wild-type cre positive hearts were transplanted into BALB/c recipients, and the mediastinal lymph nodes (DLN for heterotopic cardiac transplantation) were harvested after 24 hours (Figure 4.17).

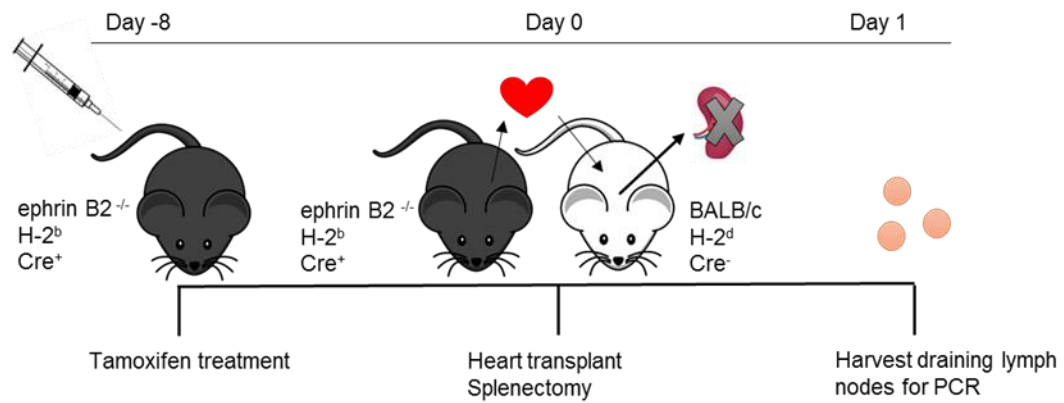


Figure 4.17- Experimental design for quantification of DPL trafficking from ephrin B2^{-/-} and wild-type heart grafts.

The proportion and absolute number of donor cells in the mediastinal lymph nodes 24 hours post-transplantation was determined by real-time PCR for the donor-specific gene, *cre*. Quantitative real-time PCR was used to quantify donor cells in recipient lymph nodes because of its sensitivity and accuracy. The genomic target to be amplified was the donor specific gene, *cre*, which is inserted into the genome of the donor mice as a transgene, and thus only donor DNA would be amplified. A standard curve was generated for each data point with DNA isolated from the specific *cre* positive donor's mediastinal lymph nodes and the proportion of DNA in transplant recipient DLN that was donor-derived was quantified from the standard curve. This data could then be converted to the number of cells of donor origin in the recipient sample by using the c-value.

There was no significant difference in the absolute number of donor-derived cells (140.0 ± 32.34 vs. 169.6 ± 52.67 , $p=0.6409$); (Figure 4.19) or density of donor-derived DNA (0.012 ± 0.004 vs. 0.016 ± 0.005 , $p=0.5830$); (Figure 4.18) in recipient DLN from animals that received a wild-type graft compared with those that received an ephrin B2^{-/-} graft. Thus, knock-out of ephrin B2 in LECs of the graft had no impact on the kinetics of donor cell trafficking between the graft and DLN in the immediate post-transplantation period.

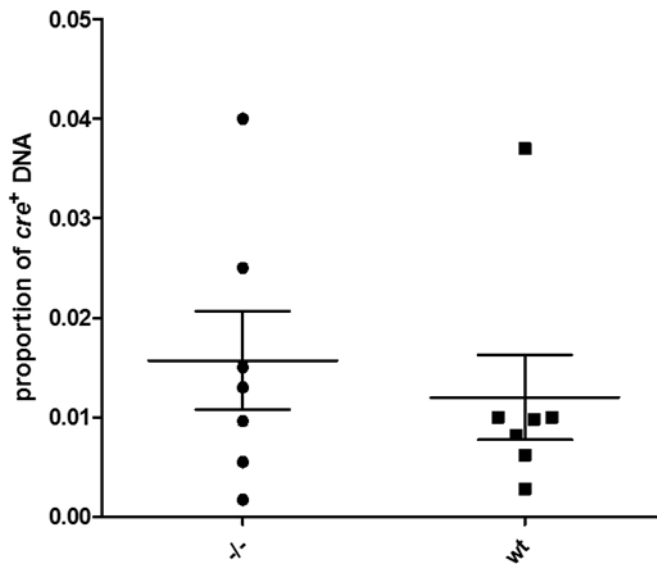


Figure 4.18- Quantification of donor DNA within recipient DLN 24 hours post-transplantation. Hearts from tamoxifen-treated wild-type (wt) or ephrin B2^{-/-} (-/-) were transplanted into splenectomised BALB/c recipients and 24 hours later the mediastinal lymph nodes were harvested, subjected to DNA extraction and analysed using a real-time quantitative PCR assay for the donor specific gene, *cre*. The proportion of the total amount of recipient draining lymph node DNA that was of donor origin was calculated by comparing ct values to standard curves generated from donor lymph node DNA. There was no difference in the proportion of donor-derived DNA within recipient DLN DNA between recipients receiving wild-type and ephrin B2^{-/-} grafts, $p=0.5830$. Each data point represents the average of triplicate readings from one mouse.

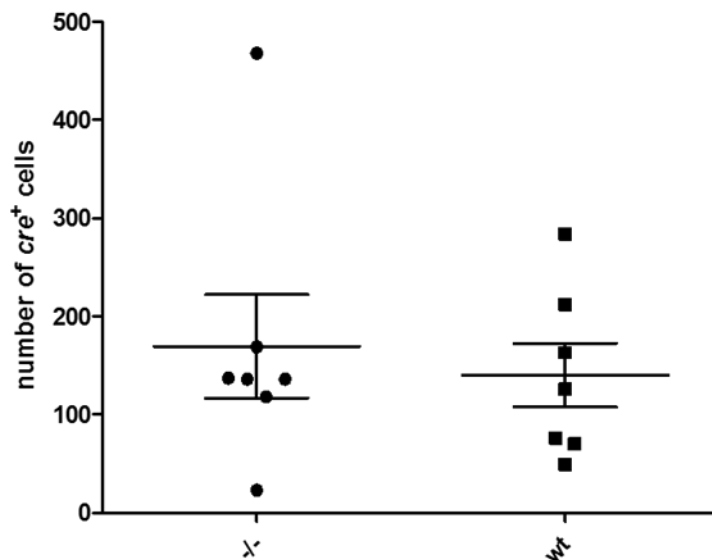


Figure 4.19- Quantification of donor cells within recipient DLN 24 hours post-transplantation. Hearts from tamoxifen-treated wild-type (wt) or ephrin B2^{-/-} (-/-) were transplanted into splenectomised BALB/c recipients and 24 hours later the mediastinal lymph nodes were harvested, subjected to DNA extraction and analysed using a real-time quantitative PCR assay for a the donor specific gene, *cre*. The proportion of the total amount of recipient draining lymph node DNA that was of donor origin was calculated by comparing ct values to a standard curve. The number of donor-derived cells was calculated using the c-value which corresponds to the total amount of DNA per cell. There was no difference in the number of donor-derived cells in recipient DLN between recipients receiving wild-type and ephrin B2^{-/-} grafts, $p=0.6409$ Each data point represents the average of triplicate readings from one mouse.

4.7 Further evaluation of ephrin B2 deficiency on DPL trafficking

The previous experiment confirmed that there was no difference in donor cell trafficking from the graft to the recipient DLN in the immediate post-transplantation period between ephrin B2^{-/-} and wild-type heart grafts, despite the prolongation of survival observed in recipients of ephrin B2^{-/-} grafts. To further understand the mechanism for the graft prolongation effect observed, a double skin transplant experiment was performed, where recipient mice received both an ephrin B2^{-/-} and wild-type graft at the same time. This experiment would demonstrate whether or not the effect on survival of the ephrin B2 knockout was limited to the area of the graft, or if the ephrin B2^{-/-} graft was able to exert a dominant protective effect systemically. The experiment in the previous section was limited to one time point after transplantation (24 hours) after transplantation. Indeed, if there was reduced trafficking of DPL from ephrin B2^{-/-} grafts, in this experiment the ephrin

B2^{-/-} graft may reject at a faster tempo because of the presence of the wild-type graft. As both grafts will elicit the same allogeneic response because they originate from the same strain, T cells activated by DPL from either skin graft can carry out the rejection of both skins. The T cells activated in the DLN will enter the blood and have the ability to traffic to either of the grafts to elicit effector functions.

To this end, recipient BALB/c mice were transplanted with two skin grafts: either two wild-type grafts, two ephrin B2^{-/-} grafts, or one wild-type and one ephrin B2^{-/-} graft. Both wild-type and ephrin B2^{-/-} donor mice were treated with tamoxifen eight days before transplantation (as in previous experiments), and tail skin was harvested and grafted onto the dorsal aspect of splenectomised recipient BALB/c mice (Figure 4.20).

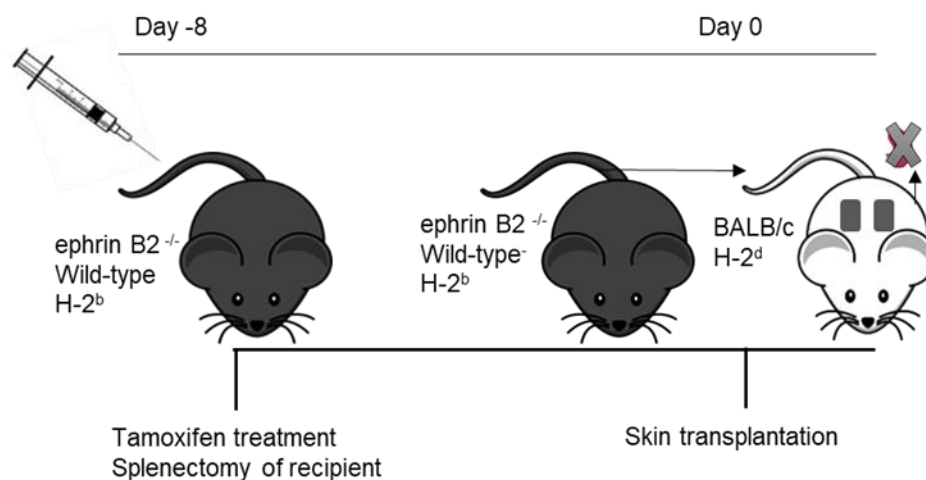
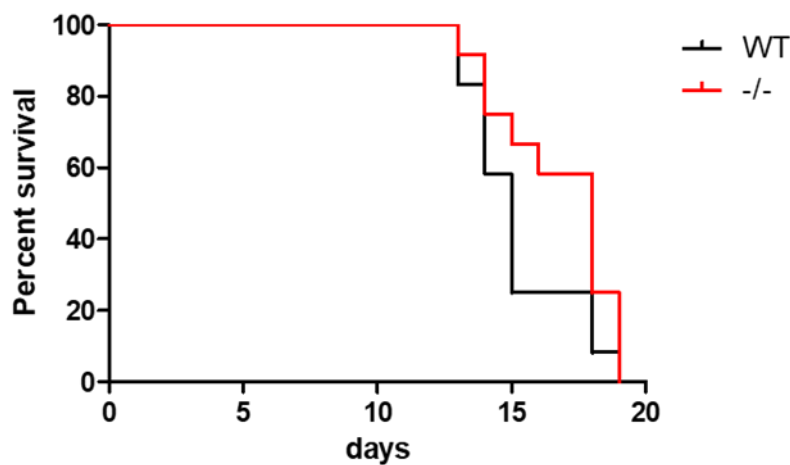


Figure 4.20- Experimental design for double skin transplantation. Recipient BALB/c mice received two skin transplants, one from an ephrin B2^{-/-} donor and one from a wild-type donor, both having received tamoxifen treatment. Recipients also received a splenectomy before skin transplantation.

Firstly, in order to assess whether or not ephrin B2^{-/-} grafts retain their survival advantage over wild-type grafts when two skin grafts are transplanted onto one recipient, BALB/c

recipients were transplanted with two grafts of the same type i.e. either two wild-type grafts or two ephrin B2^{-/-} grafts.

When either two wild-type or two ephrin B2^{-/-} grafts were transplanted onto the same recipient the rate of rejection was similar to that observed in the single transplant experiment (section 4.4), with ephrin B2^{-/-} skin surviving longer (MST=18 days) than wild-type skin (MST=15 days, $p=0.1179$) on allogeneic BALB/c splenectomised recipients (Figure 4.21). The prolongation of survival of ephrin B2^{-/-} grafts compared to the wild-type grafts in this experiment was less pronounced than in the previous experiment (section 4.4). This may be due to the fact that in these experiments recipient mice received two grafts simultaneously which increases the overall antigen load.

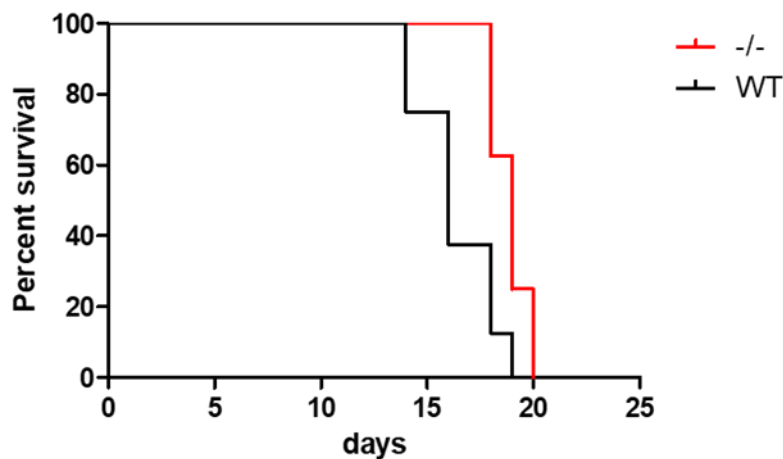


Group	Phenotype	Splenectomy	MST	N	<i>p</i>
—	Wild-type	yes	15	12	NA
—	Ephrin B2 ^{-/-}	yes	18	12	0.1179

Figure 4.21- Survival of double ephrin B2^{-/-} skin grafts compared with double wild-type skin grafts in allogeneic BALB/c recipients.

Either, two ephrin B2^{-/-} or two wild-type skin grafts were transplanted onto splenectomised BALB/c recipients and survival monitored. Ephrin B2^{-/-} grafts survived longer with an MST of 18 days compared to wild-type grafts with an MST of 15 days. N=12 in each group. $p=0.1179$.

Following this result, BALB/c recipients were transplanted with both a wild-type and an ephrin B2^{-/-} graft simultaneously. When BALB/c recipients received one wild-type and one ephrin B2^{-/-} graft simultaneously, there was still a survival advantage of ephrin B2^{-/-} grafts compared with wild-type grafts. Ephrin B2^{-/-} grafts survived longer (MST=19 days) than the wild-type grafts (MST=16 days, $p=0.0076$); (Figure 4.22).



Group	Phenotype	Splenectomy	MST	N	<i>p</i>
—	Wild-type	yes	16	6	NA
—	Ephrin B2 ^{-/-}	yes	19	6	0.0076

Figure 4.22- Survival of double ephrin B2^{-/-} skin grafts compared with double wild-type skin grafts on allogeneic BALB/c recipients.

Splenectomised BALB/c mice were transplanted with one ephrin B2^{-/-} and one wild-type graft, and survival was monitored. Ephrin B2^{-/-} grafts survived longer with an MST of 19 days compared to wild-type grafts with an MST of 16 days. N=6 in each group. $p=0.0076$.

Therefore, rejection of ephrin B2^{-/-} grafts compared with wild-type grafts followed the same pattern in the case of co-transplantation onto the same recipient (Figure 4.22), as when two of the same type were transplanted onto one recipient (Figure 4.21). This data suggests that the beneficial effect on survival seen in ephrin B2^{-/-} grafts is limited to the local environment of the graft, and that the presence of an ephrin B2^{-/-} graft cannot prolong the survival of a wild-type graft on the same recipient. This provides

circumstantial evidence for a direct effect of ephrin B2 deficiency in LECs on graft survival, rather than what was originally hypothesised, i.e. a downstream effect on lymphatic trafficking of DPL from the grafts to the DLN.

4.8 Summary

The results presented in this chapter further confirm the role of lymphatics in the immune response to a transplanted organ. Mice with a conditional lymphatic-specific knockout of ephrin B2, a molecule known to be essential for lymphatic function, were used as organ donors in allogeneic skin, heart and kidney transplantation models. There were no gross differences in the lymphatic networks within ephrin B2^{-/-} grafts before transplantation, nor did they have reduced immunogenicity due to the knock-out. However, when transplanted into allogeneic recipients they survived significantly longer than their wild-type counterparts. This effect was consistent across all organs studied; skin, heart and kidney. Trafficking of donor cells from the graft to the DLN in the immediate post-transplantation period was assessed by PCR, and no difference was found between ephrin B2^{-/-} and wild-type transplants, meaning that the observed effect on survival could not be attributed to diminished trafficking of DPL from ephrin B2^{-/-} grafts. This was further confirmed by assessing survival of ephrin B2^{-/-} skin grafts in the presence of a wild-type graft. If there was in fact diminished trafficking of DPL from ephrin B2^{-/-} grafts, the improvement in survival would be reversed because trafficking of DPL from the co-transplanted wild-type graft would overcome the defect. However, this wasn't the case and ephrin B2^{-/-} grafts maintained their survival advantage over wild-type grafts even in the presence of canonical trafficking from the wild-type graft.

In conclusion, grafts with ephrin B2 deficiency in LECs reject at a significantly slower rate than wild-type grafts in allogeneic recipients; and this effect cannot be attributed to a defect in trafficking of DPL out of the graft or reduced immunogenicity of the graft. It is

therefore likely that the effect on survival is due to a direct effect of ephrin B2 deficiency, rather than a downstream effect on lymphatic function.

4.9 Discussion

In order to build on evidence from chapter 3 that the lymphatic system plays a role in the immune response to a transplanted organ, particularly in the trafficking of cells between the graft and the DLN, a mouse with a lymphatic deficiency was used. Research in the field of lymphatic biology is limited by the availability of knock-out mice models. Most mice models with a defect in the lymphatic vasculature do not survive to adulthood, as the lymphatic system is vital for drainage of fluid from the peripheral organs and transportation of this fluid back into the blood circulation. Without functional lymphatics, fluid either builds up in the organs themselves or fluid draining from the periphery fails to drain into the thoracic duct and builds up in the chest cavity leading to the fatal condition chylothorax. The model available to our laboratory at the time was a conditional knockout of ephrin B2 in LECs. This removes the obstacle of lethality as the knockout can be induced in adulthood at the time of the experiment. It did however limit the use of the knockout to the donor in the transplantation models presented here, as this knockout is still lethal eventually and therefore was not suitable to induce in recipient mice which would need to remain alive for assessment of graft survival.

The eph/ephrin signalling molecules are best known for their function in development, particularly for the role they play in neuronal guidance (reviewed in (239)); however, it is now clear that this pathway is active in many cell types in adult organisms and has been implicated in pathologies such as oncogenesis (240). The eph/ephrin pathway is used by cells for repulsion and adhesion during patterning processes and thus there is an interest in targeting this pathway for anti-cancer therapy to inhibit communication between tumour cells. This pathway is also recognised as highly important during

development of the blood and lymphatic vasculature, in particular the ephrin B2 ligand. Hence why it was chosen for study here. Although much of the research into the role of ephrin B2 in lymphatic function has been carried out in developmental models, where it is important for lymphatic valve formation in collecting vessels, it has also been shown to be crucial for VEGF-C-induced lymphangiogenesis. Ephrin B2 is critical for internalization of the VEGF-C receptor VEGFR3, and in its absence signalling downstream of VEGFR3 is halted, which in turn inhibits growth of new lymphatic vessels (117). Ephrin B2 blocking antibodies have been used successfully to block growth of new vessels in experimental tumour models (164).

Taking this evidence from the literature for the role of ephrin B2 in lymphatic function and lymphangiogenesis, it was hypothesised that a lymphatic-specific deletion of ephrin B2 in donor organs would impact graft survival. The results presented in this chapter confirm this hypothesis; ephrin B2^{-/-} grafts survived significantly longer in allogeneic recipients than control grafts. Survival of all organs studied (skin, heart and kidney) was significantly prolonged when ephrin B2 was knocked out in LECs compared with controls. Removal of the spleen was essential for the prolongation of survival in heart and kidney but not skin allografts. This is likely to be because the spleen is not an important location for allo-antigen recognition in skin transplantation, as skin grafts are not vascularised, making it more difficult for DPL to traffic via blood to the spleen of the recipients. Ephrin B2^{-/-} kidney grafts in splenectomised recipients survived indefinitely, with good kidney function and histological features previously seen in tolerant grafts (186). This is probably due to the reduced immunogenicity of kidney grafts compared with skin and heart, rather than as a result of a stronger or different immunological effect of knocking out the ephrin B2 gene in the donor kidney.

Prolonged survival of ephrin B2^{-/-} grafts could not be attributed to a defect in DPL trafficking from the ephrin B2^{-/-} grafts to the DLN in the immediate post-transplantation period, as there was no difference in the number of donor cells trafficking to recipient

DLN from ephrin B2^{-/-} compared with wild-type grafts at 24 hours after transplantation. In addition, there were no microscopic differences in lymphatic structure and density between ephrin B2^{-/-} and wild-type organs before transplantation. Furthermore, long-term surviving ephrin B2^{-/-} kidney grafts had lymphatic vessels which could be observed after LYVE-1 staining at day 100, indicating that in this model lymphatic vessels are not completely ablated. Although it would be essential to confirm that these lymphatics are not of recipient origin which would indicate that they are a result of post-transplantation lymphangiogenesis rather than donor lymphatics unaffected by tamoxifen treatment. The proportions and absolute numbers of CD11c⁺ and CD11b⁺ cells within ephrin B2^{-/-} hearts before transplantation was also unaffected. This suggests that lymph and cells are still able to leak from the severed graft lymphatics of ephrin B2^{-/-} organs in the same manner as in the wild-type. Therefore, it is likely that knocking out ephrin B2 in LECs of the graft has a direct impact on the immune response following transplantation, rather than affecting downstream events such as trafficking of cells via lymphatics between the graft and DLN.

As ephrin B2 signalling has also been implicated in immune regulation and activation, this may be a possible explanation for the prolonged survival of ephrin B2 knockout grafts. Ephrin B2 has been shown to be able to act as a co-stimulator of T cells (121), and as LECs have the ability to present antigen to T cells (241), deletion of ephrin B2 in this model and the subsequent effect on survival of allografts could be explained by this mechanism.

Ephrin B2 has also been associated with endothelial transmigration of cells, particularly monocytes (242). Although no difference was found in the kinetics of DPL trafficking in the immediate post-transplantation period in the model presented here, it's possible that by investigating in more detail different time points and phenotypes of trafficking cells, this could be uncovered as the mechanism for the improvement in survival of ephrin B2^{-/-} grafts.

Lastly, there is evidence that ephrin B2 can activate monocytes in disease settings such as atherosclerosis (119). Braun *et al.* showed that ephrin B2 is located on the luminal side of arteries and interacts with the ephB4 receptor on monocytes aiding their trans-differentiation into inflammatory macrophages. This could explain the reduced immunogenicity of ephrin B2^{-/-} grafts in the model presented here.

Therefore, there are multiple possible mechanisms to explain the effect, on allograft survival, of lymphatic-specific deletion of ephrin B2 in the models presented in this chapter. By investigating in more detail the specific interactions between LECs in the graft and leukocytes trafficking between the graft and secondary lymphoid organs, a role for ephrin B2 in the allo-immune response could be uncovered, which would pave the way for more targeted treatment of transplant rejection in the clinic.

Chapter 5 Draining lymph node LEC response to transplantation

5.1 Background

Lymph nodes are highly organized structures that are essential for optimal encounters between APCs and T cells required to mount an effective immune response. In addition to cells of the immune system, lymph nodes possess an intricate network of stromal cells that act to guide leukocytes to different compartments, ensuring optimal interactions for an immune response. Lymph node stromal cells consist of: blood endothelial cells, which line the blood vessels within the lymph node including high endothelial venules; follicular dendritic cells, which reside in follicles and aid B cell survival; fibroblastic reticular cells (FRCs), which are present throughout the cortex and T cell areas and help in the support of HEVs and promotion of T-cell survival; and finally LECs, which line the afferent and efferent lymphatic vessels, the medullary sinuses and the subcapsular sinuses, and guide leukocytes through the lymph node by secretion of CCL21. Although originally thought of as purely structural, these stromal cell types are now known to play active roles in the co-ordination of immune cell trafficking and survival (reviewed in (187)).

LECs line lymphatic vessels within lymph nodes and in peripheral organs. The recent development of techniques to isolate this cell population from human and mouse tissue has led to a wealth of information regarding their role in the immune response (122). LECs are characterised by expression of podoplanin, an integral membrane glycoprotein, and CD31 (also known as platelet endothelial cell adhesion molecule 1), an endothelial cell marker. They constitutively secrete the chemokine CCL21 for homeostatic migration of APC from the periphery to the lymph nodes and movement of leukocytes within the lymph node (243). Upon inflammation they upregulate expression of CCL21 and other chemokines for active recruitment of leukocytes from tissue parenchyma (244). They also express danger sensing receptors such as TLRs (139).

In addition to actively recruiting leukocytes to the lymphatic vessels and lymph nodes, LECs express a variety of molecules that have a direct impact on leukocyte function.

They upregulate ICAM-1, ICAM-2, VCAM-1 and CD62E in response to inflammation, which function to aid leukocyte adhesion and transmigration across the lymphatic endothelium, and thus entry to the lymph node. They are also known to express MHC class I and present antigen to CD8⁺ T cells. The function of antigen presentation by LECs is to induce tolerance of CD8⁺ T cells to self-antigen. Lymph node LEC express a range of peripheral tissue antigens, and present them to CD8⁺ T cells in the presence of high levels of PDL1, which engages PD1 on T cells and leads to their deletion (155, 196). LECs also express MHC class II and upregulate expression in response to inflammation. They lack the ability to load endogenous antigen onto MHC class II because they do not express H-2M, however they do acquire MHC class II-peptide complexes from dendritic cells (199). For some time the function of MHC II expression by LECs was unknown; however, it is now becoming clear that it plays a regulatory role. Work from the lab of Melody Swartz concluded that interactions between MHC class II-peptide-expressing LECs and CD4⁺ T cells led to deletion of the T cells by apoptosis; DC activation of CD4⁺ T cells was also inhibited when LECs were added to the culture (245). In addition to PDL1 and MHC class II, LECs express conventional co-stimulatory molecules such as CD80 and CD40, albeit at low levels (246).

Taking this evidence from the literature it is clear that LECs within lymph nodes do not just provide conduits for trafficking immune cells; they can also directly impact the cells they come into contact with via a range of mechanisms that are dependent on the inflammatory milieu. This led to the hypothesis that LEC in lymph nodes draining a transplanted organ would undergo phenotypic changes in response to transplantation. In order to test this hypothesis, LECs were isolated from DLN of mice that had received a heterotopic heart transplant, and analysed by flow cytometry.

5.2 Assessing changes in draining lymph node LEC phenotype following heart transplantation

In order to investigate phenotypic changes of DLN LEC in response to transplantation, heterotopic heart transplantation was performed between donor BALB/c and recipient C57BL/6 mice, and DLN were harvested at day three (Figure 5.1). This time point was chosen after examination of the literature, based on studies of LEC responses to inflammatory stimuli (246).

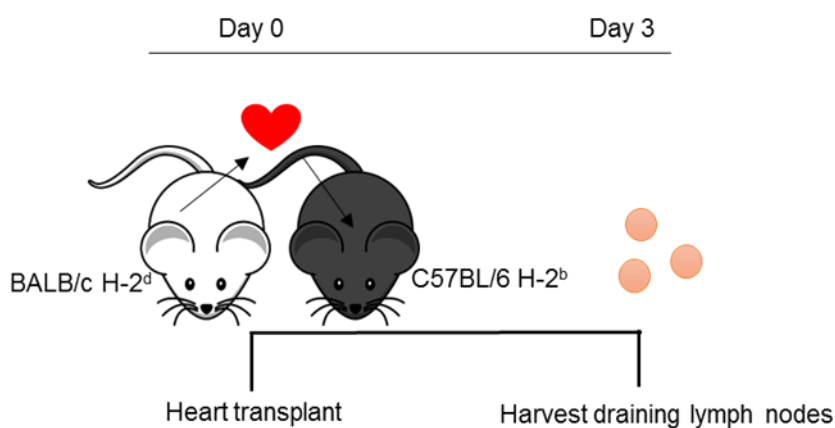


Figure 5.1- Experimental design for assessment of phenotypic changes in lymph node LECs after transplantation.

Fully allogeneic BALB/c donor heart grafts were transplanted into C57BL/6 recipients. Three days after transplantation, draining lymph nodes were harvested for analysis.

Mediastinal lymph nodes were harvested from heart transplant recipients at day three, digested according to a published protocol (218), and the LECs analysed by flow cytometry. In order to gate the LECs from the total lymph node sample, debris from the digestion process was first gated out on the forward vs. side scatter plot, and single cells gated. Subsequently, live CD45⁻ cells were gated on in order to analyse the stromal cell compartment and not the leukocytes. Lastly, a scatter plot of podoplanin vs. CD31 was created to identify the three stromal cell compartments: blood endothelial cells (CD31⁺ podoplanin⁻), fibroblastic reticular cells (CD31⁻ podoplanin⁺), double negative cells (CD31⁻ podoplanin⁻) and lymphatic endothelial cells (CD31⁺ podoplanin⁺); (Figure 5.2).

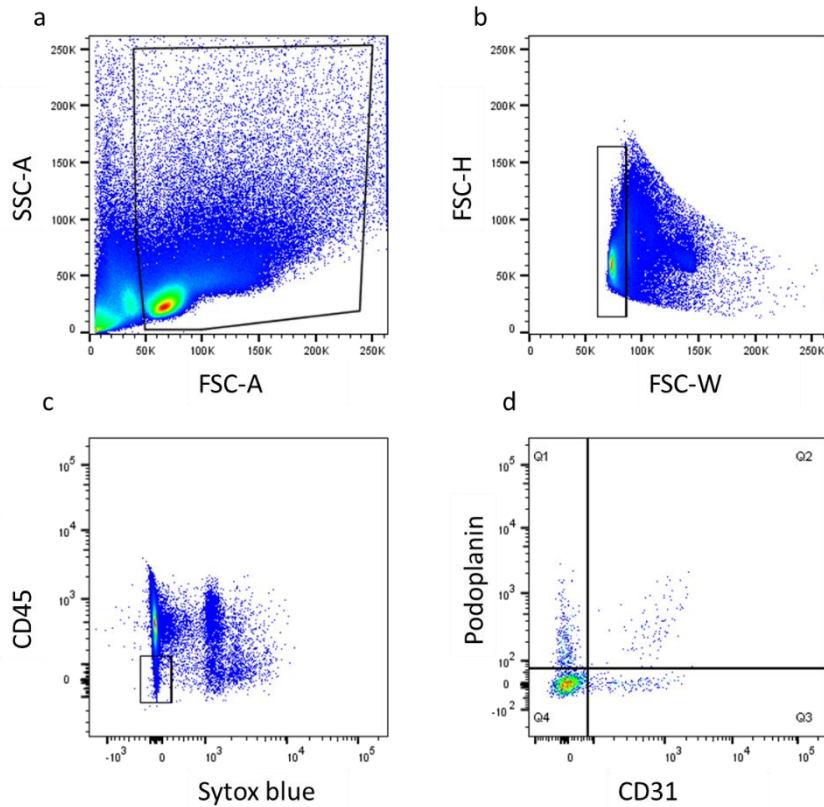


Figure 5.2- Gating strategy for lymph node LECs.

Draining lymph nodes were harvested from heart transplant recipients at day 3, digested and the cells isolated. Cells were gated according to (a) scatter properties, (b) single cells, and (c) dead cells stain exclusion and CD45 negativity. These cells were then analysed for expression of podoplanin and CD31 which results in identification of four distinct populations (d) double negative cells (Q4), blood endothelial cells (Q3), fibroblastic reticular cells (Q1), and LECs (Q2).

The LEC population from each lymph node sample was then analysed for expression of PDL1 and MHC class II, to find out if there was upregulation of these molecules in response to transplantation. In order to quantify any phenotypic changes in LECs from DLN of heart transplant recipients, LEC expression of the markers mentioned above was compared to naïve controls, i.e. lymph node LECs from mediastinal lymph nodes of mice that had not received a transplant. In addition to this, syngeneic transplantation was also performed between C57BL/6 donors and recipients in order to test whether any phenotypic changes observed in LECs were due to the inflammation caused by ischemia-reperfusion injury during transplantation or were a direct result of the allo-response.

There was no significant difference in expression of PDL1 or MHC class II between naïve lymph node LECs and LECs from DLN of transplant recipients; either syngeneic (PDL1, $p=0.8168$, MHC II, $p=0.4279$, or allogeneic (PDL1, $p=0.6754$, MHC II, $p=0.5304$); (Figure 5.3).

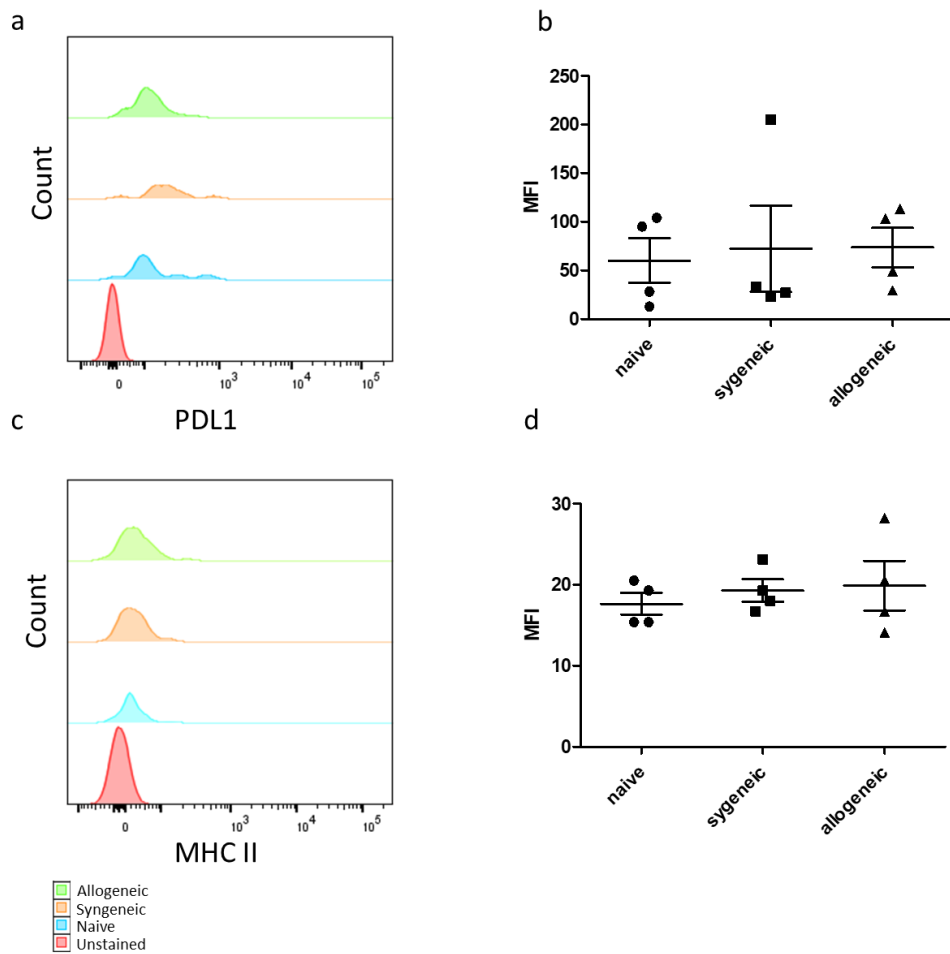


Figure 5.3- Phenotype of DLN LECs following transplantation. Draining lymph nodes were harvested from heart transplant recipients at day 3, digested and the cells isolated and analysed by flow cytometry. LECs were gated according to Figure 5.2 and the expression of (a and b) PDL1 and (c and d) MHC class II quantified. There was no difference in expression of PDL1 on LECs after syngeneic ($p=0.8168$) or allogeneic ($p=0.6754$), or MHC class II after syngeneic ($p=0.4279$) or allogeneic ($p=0.5304$). Each data point represents one mouse. MFI, median fluorescence intensity.

5.3 Assessing DLN lymphangiogenesis following transplantation

Lymph nodes draining areas where inflammation is present undergo lymphangiogenesis, whereby the lymphatic vessels expand to allow increased drainage from the inflamed area and to improve the chances of an encounter between APCs and T cells. This process is particularly prevalent in cancer, where it has been linked to progression of the disease via metastasis (247). Therefore, it was hypothesised that lymph node lymphatic vessels in draining lymph nodes would expand in response to transplantation, and that this results in an increase in the size of the LEC population recovered from DLN of heart transplant recipients when compared to lymph nodes from naïve mice. The proportion of LECs DLN samples was quantified using the samples from the experiment described above (Figure 5.2) There was no significant difference in the proportion of the total that were LECs within the DLN of transplant recipients compared with naïve controls ($0.006\pm 0.001\%$ (syngeneic) and $0.004\pm 0.0009\%$ (allogeneic) vs. $0.007\pm 0.002\%$, $p=0.6734$ and 0.2869 respectively); (Figure 5.4).

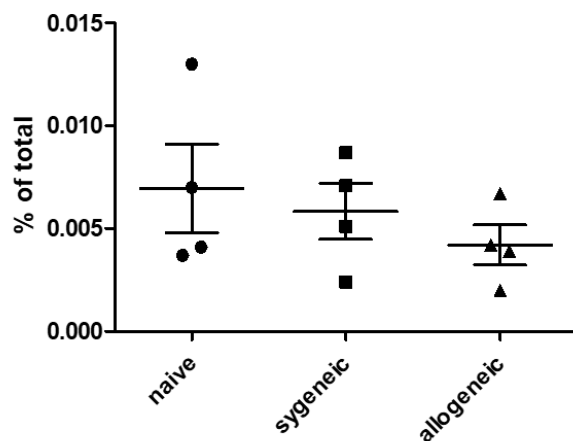


Figure 5.4- Quantification of DLN LECs after transplantation (proportion). Draining lymph nodes were harvested from heart transplant recipients at day 3, digested and the cells isolated and analysed by flow cytometry. LECs were gated according to Figure 5.2 and the size of the LEC population quantified as a proportion of the total. There was no difference in the size of the DLN LEC population after syngeneic ($p=0.6734$) or allogeneic ($p=0.2869$) when compared to the LEC population within naïve mediastinal lymph nodes. Each data point represents one mouse.

This result was confirmed by calculating the absolute number of LECs in each lymph node sample using the total number of cells recovered following the digestion protocol. Again, there was no significant difference in the total number of lymph node LEC between transplant recipients (both syngeneic and allogeneic) and naïve controls (190±68 (syngeneic) and 134±32 (allogeneic) vs. 162±58 cells, $p=0.7652$ and 0.6881 respectively); (Figure 5.5).

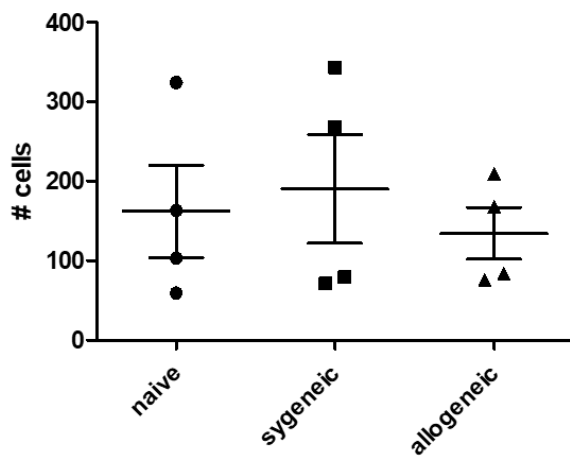


Figure 5.5- Quantification of DLN LECs after transplantation (absolute number). Draining lymph nodes were harvested from heart transplant recipients at day 3, digested and the cells isolated and analysed by flow cytometry. LECs were gated according to Figure 5.2 and the size of the LEC population quantified in terms of the number of cells in the sample. There was no difference in the size of the DLN LEC population after syngeneic ($p=0.7652$) or allogeneic ($p=0.6881$) when compared to the LEC population within naïve mediastinal lymph nodes. Each data point represents one mouse.

5.4 Summary

Taken together, these results show that following heterotopic heart transplantation there is no change in expression of PDL1 and MHC class II on DLN LECs three days after syngeneic or allogeneic cardiac transplantation. In addition, there is no expansion of the lymphatic network within these DLN as demonstrated by calculating the proportion and absolute numbers of LECs in each sample. In conclusion, there is no measurable

response of the DLN LECs to transplantation (both syngeneic and allogeneic) at day three.

5.5 Discussion

Lymph nodes draining areas of inflammation and tumours are known to undergo lymphangiogenesis. This process enhances APC migration from the inflamed region (248), and thus amplifies the immune response. In cancer, lymph node lymphangiogenesis allows for successful metastasis from the peripheral tumour to the local lymph nodes, and therefore disease progression. It is as yet unknown whether or not lymph node lymphangiogenesis occurs following solid organ transplantation.

Lymph node LEC are important mediators of the immune system as they can present self-antigen in the context of MHC class I for induction of CD8⁺ T cell tolerance. This occurs via a PDL1-dependent mechanism, in spite of the fact that LECs also express conventional co-stimulatory molecules. The function of MHC class II expression by LECs is less well understood, although emerging evidence points to a regulatory role.

Our group has identified the DLN in heterotopic heart transplantation in the mouse as the mediastinal lymph nodes. As these lymph nodes are one of the sites of induction of the T cell response to the allograft, it is expected that changes to the phenotype of LECs could affect the immune response. The experiment presented in this chapter aimed to assess the response of DLN LECs to transplantation, both in terms of lymphangiogenesis and phenotypic changes in the cells themselves.

Heterotopic heart transplants were performed between syngeneic and allogeneic strain combinations and the DLN were harvested at day three. LECs were obtained by careful digestion of the tissue and analysed by flow cytometry. The proportion and total numbers

of LECs in the samples were calculated, and no significant differences were found between transplant recipient lymph nodes and naïve controls. In addition, there was no difference in expression of PDL1 and MHC class II between transplant recipient lymph nodes and naïve controls.

Lymphatic remodelling and growth of new lymphatic vessels by lymphangiogenesis at tumour sites and in lymph nodes draining tumours is a well-studied process that plays a role in the progression of the disease (141). It is also known that lymphatic remodelling occurs in transplanted organs, although the outcome of the process in this case is less clear. As presented in chapter 1 there is evidence for both a positive and negative effect of lymphangiogenesis on graft outcome, with convincing data on both sides of the argument. Increased lymphatic vessel density within the graft could enhance DC migration to the DLN for activation of antigen-specific T cells, or could increase drainage of graft destructive T cells away from the graft; both cell types are known to traffic via the lymphatics. Although there have been studies on graft lymphangiogenesis, there is no evidence from the literature to show that lymphangiogenesis occurs in lymph nodes draining transplanted organs (172). The experiment presented here aimed to assess this. Following heterotopic heart transplantation, there was no expansion of DLN lymphatics by day 3 after transplantation. The DLN response to transplantation was measured by flow cytometry, which limits data to number of certain cell types based on expression of surface markers. Immunohistochemistry could be used in conjunction with flow cytometry to show the location of lymphatic vessels and whether or not there were any structural changes. In addition, for this experiment one time point was chosen. This was based on studies of lymph node phenotypic changes from the literature available at the time. Many of these studies look at LECs in culture, which are likely to respond differently to cells in a lymph node of a live mouse. Therefore, in the fullness of time a variety of time points following transplantation would be chosen and the phenotypic changes of LECs studied to see if these cell do respond to transplantation. It would also be beneficial to study DLN LECs from transplant recipients *in vitro* to test whether or not

they can prime allo-reactive T cells. An experiment using human primary LEC cultures has shown that LECs disrupt allogenic DC/T cell interactions via production of indoleamine 2,3 dioxygenase (246). Studying co-cultures of DLN LECs from transplant recipients with allogeneic DCs and T cells in the transplantation model presented here would help to provide evidence for a role of lymphatics outside of providing a passive conduit for immune cells.

Chapter 6 Discussion

6.1 Using anti-ICAM-1 antibody therapy to block post-transplantation lymphatic trafficking of DPL

6.1.1 Summary of findings

Trafficking of cells from the graft to SLO is essential for the initiation and maintenance of an immune response against the graft. The seminal paper by Lakkis *et al.* first demonstrated the importance of the SLO in transplantation. The direct pathway of allo-recognition is active in the immediate post-transplantation period and relies on efficient trafficking of DPL out of the graft towards the DLN and spleen. Although the involvement of the blood route to the spleen has been well studied, the lymphatic route out of the graft has received little attention.

Presented in chapter 3 are results from experiments that aimed to pharmacologically block the lymphatic route of DPL trafficking from the graft to the DLN in a mouse kidney transplantation model. Recipient female mice were treated with anti-ICAM-1 antibody or vehicle control before receiving a male kidney graft. They also received a splenectomy so that the lymphatic route of DPL trafficking could be studied in isolation.

Firstly, the kinetics of DPL trafficking to recipient DLN was assessed using a donor-specific real-time PCR assay. There was a reduction in the amount of donor DNA in recipient DLN after anti-ICAM-1 antibody treatment compared with vehicle control, suggesting that treatment with anti-ICAM-1 before transplantation reduced trafficking of DPL out of the graft towards the DLN in the immediate post-transplantation period.

Next, the effect of anti-ICAM-1 antibody therapy on the survival of allografts was assessed. Treatment with anti-ICAM-1 before transplantation in conjunction with a splenectomy did lead to prolonged, and in some cases indefinite, survival of the allograft. Long-term surviving anti-ICAM-1 antibody-treated grafts also benefited from normal graft

function. This indicated that the lymphatic route of trafficking of DPL out of the graft post-transplantation plays an important role in the rejection process.

In order to see if the prolonged survival observed in anti-ICAM-1 antibody-treated recipients was due to a reduction in T cells infiltrating the graft, the T cell infiltrate of recipients was assessed at day five after transplantation. Grafts from anti-ICAM-1 antibody-treated grafts had a similar degree of T cell infiltration, including Foxp3+ cells, than those from vehicle control treated-recipients.

6.1.2 Implications and limitations

The results from chapter 3 highlight the importance of post-transplantation trafficking of DPL out of the graft and towards the recipient DLN. When this pathway was blocked with anti-ICAM-1 antibody, there was a reduction in the proportion of donor DNA in recipient draining lymph nodes, most likely as a result of fewer DPL leaving the graft via the lymphatic route. This translated into improved survival of kidney allografts in anti-ICAM-1 antibody-treated, splenectomised recipients. These results demonstrate the potential for therapeutics targeting lymphatic trafficking in transplantation patients, as an adjunct to traditional immunosuppressive drugs.

It is important to bear in mind that the model used in these experiments is relatively 'soft' in terms of immunogenicity. Kidney transplants between BALB/c donor and C57BL/6 recipient mice can undergo spontaneous acceptance in a small number of recipients, albeit with poor graft function (186). Therefore, a vehicle control-treated and non-splenectomised control group was included. Indeed, in this group one out of four kidney allografts survived until day 81; however, the BUN increased over the course of the experiment indicating deteriorating kidney function. Although the case of this long-term surviving recipient wouldn't be referred to as spontaneous acceptance, it is clear from previous studies in our laboratory (186), and from the literature (249), that spontaneous

acceptance of kidney allografts in mice is a recognized phenomenon, and therefore any results pointing to prolonged survival in following anti-ICAM-1 antibody therapy should be interpreted with caution; although the much higher than control permanent acceptance rate and superior graft function is very strong evidence for the beneficial effect of anti-ICAM-1 treatment. In addition, there is a degree of heterogeneity in kidney transplant outcome within groups which is likely due to variations which occur in the transplant procedure, such as; differences in anatomy, differences in reaction to anaesthetics and analgesics, and differences in cold and warm ischemia times. All of these factors have the potential to affect DPL trafficking out of the graft. It is likely that this beneficial effect is only modest and is unlikely to replace the need for long term immunosuppressive treatment in the clinic, but may be able to reduce the total amount of immunosuppression required and or to reduce the frequency and severity of acute rejection.

In these experiments the anti-ICAM-1 antibody was administered IV and was therefore likely to have effects additional to blocking lymphatic trafficking of DPL. ICAM-1 is widely expressed on different cell types throughout the body, and functions in many biological processes. The half-life of the anti-ICAM-1 antibody used in these experiments is unknown and it would be important to determine this in order to fully rule out any effects of the antibody on rejection processes which occur after trafficking of DPL out of the graft. Particularly, the role of integrins such as LFA-1 (the receptor for ICAM-1) has been well studied in the context of T-cell migration, activation and memory function. Naïve T cells migrate from the blood to SLO in an integrin-dependent manner. In addition, interactions between T cells and DCs, necessary for T-cell differentiation, are dependent on the ICAM-1/LFA-1 axis. And finally migration of antigen-specific activated T cells into inflamed or infected tissue is integrin-dependent (reviewed in (250)). Activation and differentiation of antigen-specific T cells in SLO, and homing of these cells to the graft, are critical steps in the initiation of rejection. Therefore, by blocking ICAM-1 pharmacologically in these experiments, there may have been an effect on T-cell

activation and migration to the graft. The T-cell response was analysed at day five following transplantation, and infiltration of T cells into the anti-ICAM-1 antibody-treated grafts was observed. One dose of antibody was administered before transplantation, and is likely cleared from the system so that events following DPL migration out of the graft, such as T-cell activation and migration, are unaffected. However, this would have to be evaluated in this model to rule out effects of anti-ICAM-1 antibody on the T-cell response to the allograft. The fact that there were T cells infiltrating donor kidneys in anti-ICAM-1 antibody-treated recipients supports the notion that the dosing schedule used here has not hindered T cell infiltration and that the beneficial effect was more likely to be via its effect on DPL trafficking. Unfortunately, due to time constraints as a result of the technical challenges involved in mouse kidney transplantation, for the experiment presented in section 3.4 the numbers of mice would have to be increased in order to accept the null hypothesis that there are no differences between the two groups.

Therapies targeting both ICAM-1 (Enlimomab (251)) and LFA-1 (Efalizumab (252)) have been trialled in renal transplant patients with some success. The rationale for using these antibodies was mainly based on their influence on T-cell infiltration of the graft rather than prevention of DPL trafficking out, as was the case for the study presented here. Efalizumab was trialled for safety in combination with conventional immunosuppression (cyclosporin and mycophenolate mofetil), and the results showed no increase in the incidence of acute rejection; however, 8% of patients receiving a high dose of Efalizumab in conjunction with immunosuppression developed post-transplant lymphoproliferative disease. Enlimomab has shown efficacy in renal transplant patients; however, a subsequent trial raised concerns over the possible activation of neutrophils, leading to fever and leukopenia (253).

As ICAM-1 is an abundantly expressed molecule throughout the body and therefore pharmacological blocking is not specific to the lymphatic endothelium, more pronounced effects on post-transplant trafficking of DPL out of the graft may be seen with a more

lymphatic-specific target. LYVE-1, the lymphatic vessel hyaluronan receptor, is primarily expressed on lymphatic endothelium, and is an attractive target for blocking lymphatic trafficking of leukocytes. Initial studies on a LYVE-1 global knock-out mouse showed no defects in lymphatic development and function, including trafficking of DCs between the skin and draining lymph nodes (254). However, more evidence has emerged showing that expression of hyaluronan on the surface of monocyte-derived macrophages leads to engagement with LYVE-1 on lymphatic endothelium and subsequent transmigration (255). In addition, group A streptococcus, which has a hyaluronan capsule, rapidly disseminates through the body via the lymphatic system, and its entry into lymphatics has been shown to be LYVE-1-dependent (256). Taking this evidence from the literature, LYVE-1 would be a suitable target for blocking lymphatic trafficking of DPL post-transplantation, and an anti-LYVE-1 antibody could be used as an alternative to the anti-ICAM-1 antibody, to provide more specific targeting of lymphatic trafficking of DPL after transplantation.

The complex mechanisms involved in lymphatic trafficking of leukocytes are only now beginning to be elucidated. It is likely to be the case that many molecules and pathways are involved, and that different mechanisms will be used by diverse cell types depending on the microenvironment and inflammatory signals. Therefore, it will be important to study in more detail the mechanism of DPL migration via lymphatics in transplantation models, as this route provides a potential avenue for adjunctive immunosuppressive therapy for transplant patients.

6.2 Effects of disruption to donor lymphatics on the allo-response

6.2.1 Summary of findings

The lymphatic vessels within the graft are the point of entry of DPL, trafficking via this route, into the recipient. The role of graft lymphatics in this context has not previously been studied in transplantation models. Ephrin B2^{-/-} mice were used as donors to assess the contribution of donor lymphatics to the allo-response.

Firstly, the effect of ephrin B2 deficiency on the cellular composition of donor organs was assessed. There were no differences in the proportions and numbers of CD11c⁺ and CD11b⁺ from ephrin B2^{-/-} hearts compared with wild-type controls. CD11c⁺ and CD11b⁺ leukocytes from ephrin B2^{-/-} and wild-type hearts also displayed no differences in expression of molecules involved in antigen presentation: MHC class II and CD80. Therefore, ephrin B2 deficiency had not effected the density or phenotype of APCs within the donor organ before transplantation.

The gross structure of the lymphatic vessels within donor organs was also assessed, and there were no differences in lymphatic density and size of vessels within skin, heart and kidney tissue, between ephrin B2^{-/-} and wild-type animals.

All types of ephrin B2^{-/-} organs assessed (skin, heart and kidney) survived significantly longer in fully allogeneic recipients compared with control organs. This demonstrated that deficiency of ephrin B2 conferred a survival advantage on donor organs. In order to assess whether or not this survival advantage was due to reduced trafficking of DPL out of ephrin B2^{-/-} grafts as a result of dysfunctional lymphatics, as originally hypothesised, DPL within recipient DLN were quantified 24 hours after transplantation. There were no differences in proportion of donor DNA and number of donor cells within recipient draining lymph nodes at 24 hours after transplantation between recipients of ephrin B2^{-/-} and wild-type heart grafts.

In order to assess whether or not the survival advantage of ephrin B2^{-/-} grafts was a dominant effect, a double skin transplantation model was evaluated, whereby recipient mice received two skin grafts simultaneously, one from an ephrin B2^{-/-} donor and one from a wild-type donor. Survival of these mixed double skin transplants in allogeneic recipients was compared with survival of two grafts of the same type. The mixed double skin transplants behaved in the same way as the same type skin grafts, in that ephrin B2^{-/-} grafts survived longer than wild-type grafts, suggesting that the graft protective effect of knocking out the *ephrin B2* gene is exerted within the donor graft itself.

In conclusion, ephrin B2 deficiency in LECs provided a protective effect to transplanted organs, with all graft types surviving significantly longer in allogeneic recipients compared with control grafts. However, this effect is likely not due to a defect in lymphatic trafficking of DPL out of the graft in the immediate post-transplantation period, and is more likely to be due to a direct effect of ephrin B2 deficiency in the graft.

6.2.2 Implications and limitations

The results from chapter 4 provide evidence that ephrin B2 deficiency in LECs of grafts leads to significantly prolonged survival following allogeneic transplantation. Therefore, therapeutic targeting of graft lymphatics, especially via ephrin B2, in transplant patients could be used in addition to traditional immunosuppression to prolong graft survival. Although the original hypothesis for this experiment was that ephrin B2 deficiency would affect trafficking of DPL out of the graft towards the DLN via the lymphatics, this was not the case, and it is more likely that ephrin B2 deficiency provided a local protective effect. Due to technical difficulties in analysing small populations of DPL that have trafficked into the DLN, it was not possible to perform detailed phenotypic analyses to determine whether differences in the sub-populations of DPL trafficking out of ephrin B2^{-/-} grafts could be responsible for the graft prolongation effect. It is possible that cells trafficking

via defective lymphatics (i.e. ephrin B2^{-/-}) have an altered phenotype, providing an alternative explanation for the prolongation of survival of these grafts.

Antibodies targeting ephrin B2 are available and have been used to halt lymphangiogenesis in tumour models, with promising results in terms of reducing tumour size (164). In addition, there are clinical trials ongoing with drugs targeting a variety of eph/ephrin axes for anti-cancer and neurodegenerative therapies (257). The fact that therapeutic targeting of ephrins has proven to be efficacious and safe for patients, and there are agents available, suggests it could be a promising strategy for anti-rejection therapy in transplant recipients, based on the findings from chapter 4.

Studying the lymphatic system in transplantation models is limited by the availability of knock-out mice with a non-lethal defect in lymphatic function. Functional lymphatics are essential for survival, therefore many of the knockout mice available do not survive to adulthood. For these experiments a conditional knock-out was used so that adult mice were available; however, ephrin B2 deficiency in LECs is eventually lethal so these mice could not be used as recipients in the models presented here. This fact limited the use of ephrin B2^{-/-} mice to the donor strain in transplantation models; and they were used at a time point before showing any outward signs of lymphatic dysfunction. Since the experiments for chapter 4 were completed, a variety of novel mouse models for lymphatic dysfunction have been generated. Sugaya *et al.* have developed a mouse model of lymphatic dysfunction, in which, animals transgenically express the Kaposi's sarcoma herpes virus associated latency gene k-cyclin (*k-CYC*) under the control of the *VEGFR3* promoter. These mice display augmented primary tumour growth associated with a reduction of pro-inflammatory cytokine production in DLN, and decreased cytotoxic activity of tumour specific CD8⁺ T cells. However these mice do succumb to chylothorax eventually so their use is limited (258). Gardenier *et al.* have generated a mouse with a diphtheria toxin receptor (DTR) specifically expressed on LEC. Their model is also temporally and spatially conditional as it contains a *cre* recombinase gene linked to the

VEGFR3 promoter. After administration of tamoxifen, to induce DTR expression, and then diphtheria toxin specifically into the hind limb to ablate lymphatics in this region, the mice developed lymphedema identical to that seen in patients. They also defined a role for M2 macrophages in lymphatic regeneration following edema (259). This model would be useful to study the contribution of lymphatics to transplantation as lymphatics could be specifically ablated in the donor organ before transplantation, or systemically in the recipient. This would allow the contribution of both donor and recipient lymphatics to be assessed in parallel.

Although ephrin B2 deficiency had a significant impact on graft survival in the transplantation models presented here, this could not be attributed to a reduction in trafficking of DPL out of the graft via the lymphatics, or reduced antigen presenting capacity of the DPL. Unfortunately, due to time constraints as a result of the technical challenges involved in isolating cells from mouse tissue, and the unforeseen heterogeneity in proportions of heart antigen presenting cells between individual mice, the experiment presented in section 4.5 is not sufficiently powered to draw the conclusion that there are no differences in antigen presenting cell numbers within wild-type hearts compared with ephrin B2^{-/-} hearts. Numbers of mice would have to be increased in order to accept the null hypothesis that there are no differences between the two groups. Therefore, a mechanism for the effect on graft survival is yet to be elucidated. It is likely that prolongation of survival of ephrin B2^{-/-} grafts is due to a direct effect of ephrin B2 deficiency in LEC of the graft rather than a downstream effect on lymphatic trafficking. In order to investigate this further it would be beneficial to isolate LECs from ephrin B2^{-/-} mice and investigate whether or not they have reduced capacity for interactions with immune cells, which could explain the prolonged survival observed.

6.3 Draining lymph node LEC response to transplantation

6.3.1 Summary of findings

Lymph node stromal cells are becoming increasingly recognised as regulators of the immune system. LECs and fibroblastic reticular cells, in addition to providing specialised conduit systems for trafficking immune cells within the lymph node, play a role in the maintenance of peripheral tolerance. Studies have shown that MHC class II expression by LECs may have a regulatory effect on CD4⁺ T cells, halting their proliferation (199).

Lymph node expansion in response to inflammation is a well observed and characterized phenomenon. Expansion of lymphatic networks in DLN increases lymph flow from the affected area and increases the chance of antigen encounter by T cells, leading to a more effective immune response. Lymphangiogenesis in grafts is well described in kidney transplantation, although the contribution of this process to the immune response remains unclear.

Lymph node LECs were isolated from the mediastinal lymph nodes of heart transplant recipients three days after transplantation, and analysed by flow cytometry. Firstly, the expression profile of a range of co-stimulatory and co-inhibitory molecules (PDL1, MHC II, CD80 and CD40) was assessed. DLN LECs from transplant recipients did not upregulate expression of any of the molecules that were evaluated. In addition, lymph node lymphangiogenesis was evaluated by quantifying the proportion and numbers of LECs within DLN from transplant recipients. There was no significant difference in proportion or absolute number of LECs between transplant recipients (either syngeneic or allogeneic) and naïve lymph nodes.

In the fullness of time, a range of different time points after transplantation could be studied to see if lymph node lymphatics respond to transplantation either in the immediate post-transplantation period (i.e. before day 3), or later.

6.3.2 Implications and limitations

Results from chapter 5 investigating the response of DLN lymphatics to transplantation did not find any phenotypic or structural changes following transplantation. These results should be interpreted with caution because only one time point after transplantation was assessed. Day three after transplantation was chosen as the time point as studies by others on the effects of inflammation on LEC phenotype had used this time point (196, 201). However, these were studies on *in vitro* cultured LEC, and the inflammatory stimulus was directly applied to the cells in culture. The experiment presented here used primary LECs isolated from lymph nodes of mice that had received a heart transplant. It is currently unknown when exactly the inflammatory cytokines from a rejecting graft reach the DLN, although as DPL are present and detectable by 24 hours, it is likely that inflammatory cytokines arrive at the draining lymph nodes via the lymph at the same time or earlier. However, unlike in the case of DPL that are in a limited supply within the graft, inflammatory cytokines are constantly present within rejecting grafts and therefore the DLN will receive a constant supply of cytokines from the graft. This means that DLN LEC phenotype could vary throughout the lifetime of the graft, rather than just responding to inflammatory cytokines delivered to the DLN in the initial post-transplantation period. A range of time points would need to be studied to fully understand the response of DLN LECs to transplantation. It would also be interesting to measure the cytokine levels within the DLN at different time points to see if this correlates with LEC phenotype, and determine which cytokines are responsible for the changes observed.

In terms of lymph node lymphangiogenesis in response to transplantation, this has yet to be studied by others. Therefore, it was difficult to determine which time point after transplantation to study. A study assessing the contribution of immune complexes to autoimmune disease progression looked at the DLN lymphatic response three days following immunization (260), and found differences in lymphatic density between control and experimental mice. As with LEC phenotype, lymphangiogenesis of draining lymph

node lymphatics following transplantation is likely to be a dynamic process with many factors involved at different time points. A comprehensive study of DLN lymphatics looking at LEC phenotype, cytokine composition of lymph nodes and molecules involved in lymphangiogenesis would be needed to fully understand the response to transplantation.

6.4 Concluding remarks

A wealth of research in the past decade has led to the realisation that the lymphatic system plays a crucial role in immunity. Originally thought to simply provide a passive conduit system for removal of extra-cellular fluid and cells from tissue for return to the blood, the lymphatic system is now known to provide regulation of the immune response by: direct presentation of self-antigen by lymph node stromal cells to T cells, and orchestrated secretion of chemokines to guide immune cells out of tissue, and into and out of lymph nodes, in order to deliver a targeted adaptive immune response. This highly flexible system responds to disease caused by inflammation with the growth of new vessels within affected tissue and DLN exacerbating disease, and aids the spread of tumours by metastatic growth.

Despite the vast knowledge of the role that the lymphatic system plays in the immune response to pathogens and the progression of cancer, there is limited information available in the literature about the function of the lymphatic system in transplantation. Transplantation provides a unique model for lymphatic research because there are donor and recipient lymphatics to consider, with the former expressing foreign antigens. Furthermore, the donor lymphatics are not directly connected to the recipient lymphatics during the initial post-transplantation period. Studies in this area have provided conflicting results. Some researchers have concluded that the lymphatic system,

particularly the lymphangiogenic response in graft tissue, has a negative impact on graft outcome, whereas others have provided evidence to the contrary.

Transplantation saves the lives of patients living with end-stage organ failure. However, in order to protect grafts from the patient's own immune system, immunosuppressive drugs have to be administered. These drugs have unwanted side effects due to their lack of specificity, and often diminish the life expectancy of the patient. Targeted therapy for transplant patients is needed, and therefore better understanding of the allo-immune response is required.

This thesis aimed to investigate some of the roles of the lymphatic system in the immune response following transplantation. Mouse models of organ transplantation were used as they closely resemble the clinical situation and enable manipulation of the lymphatic system to decipher how this system functions during the allo-response. Some promising results have been presented here, with pharmacological blocking or genetic deletion of key molecules involved in lymphatic function leading to prolongation of graft survival. The results presented here have failed to support the original hypothesis that interfering with lymphatic function, either in the graft or the recipient, would reduce trafficking of DPL out of the graft towards the DLN and that in turn this would lead to sub-optimal priming of allo-specific T cells. As genetic modification of animals causing universal deletion of lymphatic vessels is embryonically lethal, it is not possible to use such models to study the effect of the absence of donor or recipient lymphatics in organ transplantation. Here a donor mouse with a conditional knockout of ephrin B2, which is crucial for lymphatic valve formation and function, was used as an alternative. However, in this model DPL trafficking was not affected as originally predicted. Therefore, the original hypothesis that interfering with lymphatic flow from the donor graft would prolong survival can neither be proved nor disproved with this model. Nonetheless, this model has provided evidence that suggests that dysfunctional graft lymphatics provide a local protective effect against rejection. Despite these interesting findings, more in depth analysis is needed to fully

elucidate the mechanisms of the prolonged survival seen in both models; the anti-ICAM-1 antibody model and the ephrin B2^{-/-} model. In addition, the results on lymph node LEC phenotypic and structural changes following transplantation were inconclusive and more time points need to be analysed.

In conclusion, the lymphatic system of both the donor and recipient contribute to the immune response following transplantation, in ways beyond providing a conduit for trafficking immune cells. Lymphatic-specific therapies have the potential for use as adjunctive immunosuppression in transplant recipients. However, more research is needed to reveal in detail the dynamic roles of the lymphatic system in the immune response to transplantation, in order to harness these for therapies.

References

1. NHS. www.nhsbt.nhs.uk 2017.
2. Nashan B, Moore R, Amlot P, Schmidt AG, Abeywickrama K, Souillou JP. Randomised trial of basiliximab versus placebo for control of acute cellular rejection in renal allograft recipients. CHIB 201 International Study Group. *Lancet* (London, England). 1997;350(9086):1193-8.
3. Lawen JG, Davies EA, Mourad G, Oppenheimer F, Molina MG, Rostaing L, et al. Randomized double-blind study of immunoprophylaxis with basiliximab, a chimeric anti-interleukin-2 receptor monoclonal antibody, in combination with mycophenolate mofetil-containing triple therapy in renal transplantation. *Transplantation*. 2003;75(1):37-43.
4. Ponticelli C, Yussim A, Cambi V, Legendre C, Rizzo G, Salvadori M, et al. A randomized, double-blind trial of basiliximab immunoprophylaxis plus triple therapy in kidney transplant recipients. *Transplantation*. 2001;72(7):1261-7.
5. Kahan BD, Rajagopalan PR, Hall M. Reduction of the occurrence of acute cellular rejection among renal allograft recipients treated with basiliximab, a chimeric anti-interleukin-2-receptor monoclonal antibody. United States Simulect Renal Study Group. *Transplantation*. 1999;67(2):276-84.
6. Hardinger KL. Rabbit antithymocyte globulin induction therapy in adult renal transplantation. *Pharmacotherapy*. 2006;26(12):1771-83.
7. Hanaway MJ, Woodle ES, Mulgaonkar S, Peddi VR, Kaufman DB, First MR, et al. Alemtuzumab induction in renal transplantation. *The New England journal of medicine*. 2011;364(20):1909-19.
8. Margreiter R. Efficacy and safety of tacrolimus compared with ciclosporin microemulsion in renal transplantation: a randomised multicentre study. *Lancet* (London, England). 2002;359(9308):741-6.
9. Johnson C, Ahsan N, Gonwa T, Halloran P, Stegall M, Hardy M, et al. Randomized trial of tacrolimus (Prograf) in combination with azathioprine or mycophenolate mofetil versus cyclosporine (Neoral) with mycophenolate mofetil after cadaveric kidney transplantation. *Transplantation*. 2000;69(5):834-41.
10. Ekberg H, Tedesco-Silva H, Demirbas A, Vitko S, Nashan B, Gurkan A, et al. Reduced exposure to calcineurin inhibitors in renal transplantation. *The New England journal of medicine*. 2007;357(25):2562-75.

11. Weir MR, Mulgaonkar S, Chan L, Shidban H, Waid TH, Preston D, et al. Mycophenolate mofetil-based immunosuppression with sirolimus in renal transplantation: a randomized, controlled Spare-the-Nephron trial. *Kidney Int.* 2011;79(8):897-907.
12. Budde K, Becker T, Arns W, Sommerer C, Reinke P, Eisenberger U, et al. Everolimus-based, calcineurin-inhibitor-free regimen in recipients of de-novo kidney transplants: an open-label, randomised, controlled trial. *Lancet (London, England).* 2011;377(9768):837-47.
13. Aboujaoude W, Milgrom ML, Govani MV. Lymphedema associated with sirolimus in renal transplant recipients. *Transplantation.* 2004;77(7):1094-6.
14. Huber S, Bruns CJ, Schmid G, Hermann PC, Conrad C, Niess H, et al. Inhibition of the mammalian target of rapamycin impedes lymphangiogenesis. *Kidney Int.* 2007;71(8):771-7.
15. Kunzendorf U, Ziegler E, Kabelitz D. FTY720—the first compound of a new promising class of immunosuppressive drugs. *Nephrology Dialysis Transplantation.* 2004;19(7):1677-81.
16. Hoitsma AJ, Woodle ES, Abramowicz D, Proot P, Vanrenterghem Y. FTY720 combined with tacrolimus in de novo renal transplantation: 1-year, multicenter, open-label randomized study. *Nephrology Dialysis Transplantation.* 2011;26(11):3802-5.
17. Miller J, Mendez R, Pirsch JD, Jensik SC. Safety and efficacy of tacrolimus in combination with mycophenolate mofetil (MMF) in cadaveric renal transplant recipients. FK506/MMF Dose-Ranging Kidney Transplant Study Group. *Transplantation.* 2000;69(5):875-80.
18. Mathew TH. A blinded, long-term, randomized multicenter study of mycophenolate mofetil in cadaveric renal transplantation: results at three years. Tricontinental Mycophenolate Mofetil Renal Transplantation Study Group. *Transplantation.* 1998;65(11):1450-4.
19. Halloran P, Mathew T, Tomlanovich S, Groth C, Hooftman L, Barker C. Mycophenolate mofetil in renal allograft recipients: a pooled efficacy analysis of three randomized, double-blind, clinical studies in prevention of rejection. The International Mycophenolate Mofetil Renal Transplant Study Groups. *Transplantation.* 1997;63(1):39-47.
20. Steiner RW, Awdishu L. Steroids in kidney transplant patients. *Seminars in Immunopathology.* 2011;33(2):157-67.
21. Kaisho T, Akira S. Critical roles of Toll-like receptors in host defense. *Critical reviews in immunology.* 2000;20(5):393-405.
22. Pratt JR, Basheer SA, Sacks SH. Local synthesis of complement component C3 regulates acute renal transplant rejection. *Nature medicine.* 2002;8(6):582-7.

23. Peng Q, Li K, Anderson K, Farrar CA, Lu B, Smith RA, et al. Local production and activation of complement up-regulates the allostimulatory function of dendritic cells through C3a-C3aR interaction. *Blood*. 2008;111(4):2452-61.
24. Strainic MG, Liu J, Huang D, An F, Lalli PN, Muqim N, et al. Locally produced complement fragments C5a and C3a provide both costimulatory and survival signals to naive CD4+ T cells. *Immunity*. 2008;28(3):425-35.
25. Morita K, Miura M, Paolone DR, Engeman TM, Kapoor A, Remick DG, et al. Early chemokine cascades in murine cardiac grafts regulate T cell recruitment and progression of acute allograft rejection. *Journal of immunology (Baltimore, Md : 1950)*. 2001;167(5):2979-84.
26. El-Sawy T, Belperio JA, Strieter RM, Remick DG, Fairchild RL. Inhibition of polymorphonuclear leukocyte-mediated graft damage synergizes with short-term costimulatory blockade to prevent cardiac allograft rejection. *Circulation*. 2005;112(3):320-31.
27. Grau V, Herbst B, Steiniger B. Dynamics of monocytes/macrophages and T lymphocytes in acutely rejecting rat renal allografts. *Cell Tissue Res*. 1998;291(1):117-26.
28. Walch JM, Zeng Q, Li Q, Oberbarnscheidt MH, Hoffman RA, Williams AL, et al. Cognate antigen directs CD8+ T cell migration to vascularized transplants. *The Journal of clinical investigation*. 2013;123(6):2663-71.
29. Zecher D, van Rooijen N, Rothstein DM, Shlomchik WD, Lakkis FG. An innate response to allogeneic nonself mediated by monocytes. *Journal of immunology (Baltimore, Md : 1950)*. 2009;183(12):7810-6.
30. Ochando J, Conde P, Bronte V. Monocyte-Derived Suppressor Cells in Transplantation. *Current transplantation reports*. 2015;2(2):176-83.
31. Benichou G, Yamada Y, Aoyama A, Madsen JC. Natural killer cells in rejection and tolerance of solid organ allografts. *Curr Opin Organ Transplant*. 2011;16(1):47-53.
32. Yu G, Xu X, Vu MD, Kilpatrick ED, Li XC. NK cells promote transplant tolerance by killing donor antigen-presenting cells. *The Journal of experimental medicine*. 2006;203(8):1851-8.
33. Goldstein DR, Tesar BM, Akira S, Lakkis FG. Critical role of the Toll-like receptor signal adaptor protein MyD88 in acute allograft rejection. *The Journal of clinical investigation*. 2003;111(10):1571-8.
34. Tesar BM, Zhang J, Li Q, Goldstein DR. TH1 immune responses to fully MHC mismatched allografts are diminished in the absence of MyD88, a toll-like receptor signal adaptor

- protein. *American journal of transplantation : official journal of the American Society of Transplantation and the American Society of Transplant Surgeons*. 2004;4(9):1429-39.
35. Mauiyyedi S, Colvin RB. Humoral rejection in kidney transplantation: new concepts in diagnosis and treatment. *Current opinion in nephrology and hypertension*. 2002;11(6):609-18.
36. Le Moine A, Goldman M, Abramowicz D. Multiple pathways to allograft rejection. *Transplantation*. 2002;73(9):1373-81.
37. Barbara JA, Turvey SE, Kingsley CI, Spriewald BM, Hara M, Witzke O, et al. Islet allograft rejection can be mediated by CD4+, alloantigen experienced, direct pathway T cells of TH1 and TH2 cytokine phenotype. *Transplantation*. 2000;70(11):1641-9.
38. Atalar K, Afzali B, Lord G, Lombardi G. Relative roles of Th1 and Th17 effector cells in allograft rejection. *Curr Opin Organ Transplant*. 2009;14(1):23-9.
39. Feng G, Gao W, Strom TB, Oukka M, Francis RS, Wood KJ, et al. Exogenous IFN-gamma ex vivo shapes the alloreactive T-cell repertoire by inhibition of Th17 responses and generation of functional Foxp3+ regulatory T cells. *Eur J Immunol*. 2008;38(9):2512-27.
40. Mills KH. Induction, function and regulation of IL-17-producing T cells. *Eur J Immunol*. 2008;38(10):2636-49.
41. Loong CC, Hsieh HG, Lui WY, Chen A, Lin CY. Evidence for the early involvement of interleukin 17 in human and experimental renal allograft rejection. *The Journal of pathology*. 2002;197(3):322-32.
42. Antonysamy MA, Fanslow WC, Fu F, Li W, Qian S, Troutt AB, et al. Evidence for a role of IL-17 in alloimmunity: a novel IL-17 antagonist promotes heart graft survival. *Transplantation Proceedings*. 31(1):93.
43. Martinez OM, Ascher NL, Ferrell L, Villanueva J, Lake J, Roberts JP, et al. Evidence for a nonclassical pathway of graft rejection involving interleukin 5 and eosinophils. *Transplantation*. 1993;55(4):909-18.
44. VanBuskirk AM, Wakely ME, Orosz CG. Transfusion of polarized TH2-like cell populations into SCID mouse cardiac allograft recipients results in acute allograft rejection. *Transplantation*. 1996;62(2):229-38.
45. Koyama I, Nadazdin O, Boskovic S, Ochiai T, Smith RN, Sykes M, et al. Depletion of CD8 memory T cells for induction of tolerance of a previously transplanted kidney allograft. *American journal of transplantation : official journal of the American Society of Transplantation and the American Society of Transplant Surgeons*. 2007;7(5):1055-61.

46. Barber DL, Wherry EJ, Ahmed R. Cutting edge: rapid in vivo killing by memory CD8 T cells. *Journal of immunology (Baltimore, Md : 1950)*. 2003;171(1):27-31.
47. Chalasani G, Dai Z, Konieczny BT, Baddoura FK, Lakkis FG. Recall and propagation of allospecific memory T cells independent of secondary lymphoid organs. *Proc Natl Acad Sci U S A*. 2002;99(9):6175-80.
48. Chen Y, Heeger PS, Valujskikh A. In vivo helper functions of alloreactive memory CD4+ T cells remain intact despite donor-specific transfusion and anti-CD40 ligand therapy. *Journal of immunology (Baltimore, Md : 1950)*. 2004;172(9):5456-66.
49. Brook MO, Wood KJ, Jones ND. The impact of memory T cells on rejection and the induction of tolerance. *Transplantation*. 2006;82(1):1-9.
50. Bain B, Vas MR, Lowenstein L. THE DEVELOPMENT OF LARGE IMMATURE MONONUCLEAR CELLS IN MIXED LEUKOCYTE CULTURES. *Blood*. 1964;23:108-16.
51. Lechler RI, Batchelor JR. Restoration of immunogenicity to passenger cell-depleted kidney allografts by the addition of donor strain dendritic cells. *J Exp Med*. 1982;155(1):31-41.
52. Larsen CP, Morris PJ, Austyn JM. MIGRATION OF DENDRITIC LEUKOCYTES FROM CARDIAC ALLOGRAFTS INTO HOST SPLEENS - A NOVEL PATHWAY FOR INITIATION OF REJECTION. *Journal of Experimental Medicine*. 1990;171(1):307-14.
53. Wang W, Man S, Gulden PH, Hunt DF, Engelhard VH. Class I-restricted alloreactive cytotoxic T lymphocytes recognize a complex array of specific MHC-associated peptides. *Journal of immunology (Baltimore, Md : 1950)*. 1998;160(3):1091-7.
54. Heath WR, Kane KP, Mescher MF, Sherman LA. Alloreactive T cells discriminate among a diverse set of endogenous peptides. *Proc Natl Acad Sci U S A*. 1991;88(12):5101-5.
55. Bevan MJ. High determinant density may explain the phenomenon of alloreactivity. *Immunology today*. 1984;5(5):128-30.
56. Lombardi G, Barber L, Sidhu S, Batchelor JR, Lechler RI. The specificity of alloreactive T cells is determined by MHC polymorphisms which contact the T cell receptor and which influence peptide binding. *International immunology*. 1991;3(8):769-75.
57. Liu Q, Rojas-Canales DM, Divito SJ, Shufesky WJ, Stolz DB, Erdos G, et al. Donor dendritic cell-derived exosomes promote allograft-targeting immune response. *The Journal of clinical investigation*. 2016;126(8):2805-20.

58. Marino J, Babiker-Mohamed MH, Crosby-Bertorini P, Paster JT, LeGuern C, Germana S, et al. Donor exosomes rather than passenger leukocytes initiate alloreactive T cell responses after transplantation. *Sci Immunol*. 2016;1(1).
59. Benichou G. Direct and indirect antigen recognition: the pathways to allograft immune rejection. *Frontiers in bioscience : a journal and virtual library*. 1999;4:D476-80.
60. Stegall MD, Tezuka K, Oluwole SF, Engelstad K, Jing MX, Andrew J, et al. Interstitial class II-positive cell depletion by donor pretreatment with gamma irradiation. Evidence of differential immunogenicity between vascularized cardiac allografts and islets. *Transplantation*. 1990;49(2):246-51.
61. Takata N, Yamaguchi Y, Mori K, Misumi M, Katsumori T, Goto M, et al. Prolonged survival of rat hepatic allografts after total-body irradiation of the donors. *Transplantation*. 1992;54(2):215-8.
62. Stone JP, Critchley WR, Major T, Rajan G, Risnes I, Scott H, et al. Altered Immunogenicity of Donor Lungs via Removal of Passenger Leukocytes Using Ex Vivo Lung Perfusion. *American journal of transplantation : official journal of the American Society of Transplantation and the American Society of Transplant Surgeons*. 2016;16(1):33-43.
63. Gagne K, Brouard S, Guillet M, Cuturi MC, Souillou JP. TGF-beta1 and donor dendritic cells are common key components in donor-specific blood transfusion and anti-class II heart graft enhancement, whereas tolerance induction also required inflammatory cytokines down-regulation. *Eur J Immunol*. 2001;31(10):3111-20.
64. Degauque N, Lair D, Dupont A, Moreau A, Roussey G, Moizant F, et al. Dominant tolerance to kidney allografts induced by anti-donor MHC class II antibodies: cooperation between T and non-T CD103+ cells. *Journal of immunology (Baltimore, Md : 1950)*. 2006;176(7):3915-22.
65. GOLDBERG LC, BRADLEY JA, CONNOLLY J, FRIEND PJ, OLIVEIRA DBG, PARROTT NR, et al. ANTI-CD45 MONOCLONAL ANTIBODY PERFUSION OF HUMAN RENAL ALLOGRAFTS PRIOR TO TRANSPLANTATION A SAFETY AND IMMUNOHISTOLOGICAL STUDY. *Transplantation*. 1995;59(9):1285-92.
66. Brown K, Nowocin AK, Meader L, Edwards LA, Smith RA, Wong W. Immunotoxin Against a Donor MHC Class II Molecule Induces Indefinite Survival of Murine Kidney Allografts. *American journal of transplantation : official journal of the American Society of Transplantation and the American Society of Transplant Surgeons*. 2016;16(4):1129-38.

67. Golding H, Singer A. Role of accessory cell processing and presentation of shed H-2 alloantigens in allospecific cytotoxic T lymphocyte responses. *Journal of immunology (Baltimore, Md : 1950)*. 1984;133(2):597-605.
68. Benichou G, Takizawa PA, Ho PT, Killion CC, Olson CA, McMillan M, et al. Immunogenicity and tolerogenicity of self-major histocompatibility complex peptides. *The Journal of experimental medicine*. 1990;172(5):1341-6.
69. Liu Z, Braunstein NS, Suci-Foca N. T cell recognition of allopeptides in context of syngeneic MHC. *Journal of immunology (Baltimore, Md : 1950)*. 1992;148(1):35-40.
70. Fangmann J, Dalchau R, Sawyer GJ, Priestley CA, Fabre JW. T cell recognition of donor major histocompatibility complex class I peptides during allograft rejection. *European journal of immunology*. 1992;22(6):1525-30.
71. Boisgerault F, Anosova NG, Tam RC, Illigens BM, Fedoseyeva EV, Benichou G. Induction of T-cell response to cryptic MHC determinants during allograft rejection. *Human immunology*. 2000;61(12):1352-62.
72. Noorchashm H, Reed AJ, Rostami SY, Mozaffari R, Zekavat G, Koeberlein B, et al. B cell-mediated antigen presentation is required for the pathogenesis of acute cardiac allograft rejection. *Journal of immunology (Baltimore, Md : 1950)*. 2006;177(11):7715-22.
73. Rulifson IC, Szot GL, Palmer E, Bluestone JA. Inability to induce tolerance through direct antigen presentation. *American journal of transplantation : official journal of the American Society of Transplantation and the American Society of Transplant Surgeons*. 2002;2(6):510-9.
74. Yamada A, Chandraker A, Laufer TM, Gerth AJ, Sayegh MH, Auchincloss H, Jr. Recipient MHC class II expression is required to achieve long-term survival of murine cardiac allografts after costimulatory blockade. *Journal of immunology (Baltimore, Md : 1950)*. 2001;167(10):5522-6.
75. Ochando JC, Krieger NR, Bromberg JS. Direct versus indirect allorecognition: Visualization of dendritic cell distribution and interactions during rejection and tolerization. *American journal of transplantation : official journal of the American Society of Transplantation and the American Society of Transplant Surgeons*. 2006;6(10):2488-96.
76. Brown K, Sacks SH, Wong W. Extensive and bidirectional transfer of major histocompatibility complex class II molecules between donor and recipient cells in vivo following solid organ transplantation. *FASEB journal : official publication of the Federation of American Societies for Experimental Biology*. 2008;22(11):3776-84.

77. Smyth LA, Lechler RI, Lombardi G. Continuous Acquisition of MHC:Peptide Complexes by Recipient Cells Contributes to the Generation of Anti-Graft CD8+ T Cell Immunity. *American journal of transplantation : official journal of the American Society of Transplantation and the American Society of Transplant Surgeons*. 2017;17(1):60-8.
78. Sachs DH, Kawai T, Sykes M. Induction of Tolerance through Mixed Chimerism. *Cold Spring Harbor Perspectives in Medicine*. 2014;4(1).
79. Wood KJ, Sakaguchi S. Regulatory T cells in transplantation tolerance. *Nature Reviews Immunology*. 2003;3(3):199-210.
80. Safinia N, Scotta C, Vaikunthanathan T, Lechler RI, Lombardi G. Regulatory T Cells: Serious Contenders in the Promise for Immunological Tolerance in Transplantation. *Frontiers in immunology*. 2015;6:438.
81. Hutchinson JA, Riquelme P, Sawitzki B, Tomiuk S, Miqueu P, Zuhayra M, et al. Cutting Edge: Immunological consequences and trafficking of human regulatory macrophages administered to renal transplant recipients. *Journal of immunology (Baltimore, Md : 1950)*. 2011;187(5):2072-8.
82. Harding FA, McArthur JG, Gross JA, Raulet DH, Allison JP. CD28-mediated signalling co-stimulates murine T cells and prevents induction of anergy in T-cell clones. *Nature*. 1992;356(6370):607-9.
83. Pearson TC, Alexander DZ, Winn KJ, Linsley PS, Lowry RP, Larsen CP. Transplantation tolerance induced by CTLA4-Ig. *Transplantation*. 1994;57(12):1701-6.
84. Larsen CP, Pearson TC, Adams AB, Tso P, Shirasugi N, Strobert E, et al. Rational development of LEA29Y (belatacept), a high-affinity variant of CTLA4-Ig with potent immunosuppressive properties. *American journal of transplantation : official journal of the American Society of Transplantation and the American Society of Transplant Surgeons*. 2005;5(3):443-53.
85. Henn V, Slupsky JR, Grafe M, Anagnostopoulos I, Forster R, Muller-Berghaus G, et al. CD40 ligand on activated platelets triggers an inflammatory reaction of endothelial cells. *Nature*. 1998;391(6667):591-4.
86. Wang L, Han R, Hancock WW. Programmed cell death 1 (PD-1) and its ligand PD-L1 are required for allograft tolerance. *Eur J Immunol*. 2007;37(10):2983-90.

87. Tumei PC, Harview CL, Yearley JH, Shintaku IP, Taylor EJM, Robert L, et al. PD-1 blockade induces responses by inhibiting adaptive immune resistance. *Nature*. 2014;515(7528):568-71.
88. Ochando JC, Homma C, Yang Y, Hidalgo A, Garin A, Tacke F, et al. Alloantigen-presenting plasmacytoid dendritic cells mediate tolerance to vascularized grafts. *Nat Immunol*. 2006;7(6):652-62.
89. Barker CF, Billingham RE. ROLE OF AFFERENT LYMPHATICS IN REJECTION OF SKIN HOMOGRAFTS. *Journal of Experimental Medicine*. 1968;128(1):197-&.
90. Lakkis FG, Arakelov A, Konieczny BT, Inoue Y. Immunologic 'ignorance' of vascularized organ transplants in the absence of secondary lymphoid tissue. *Nature Medicine*. 2000;6(6):686-8.
91. Chin R, Zhou P, Alegre ML, Fu YX. Confounding factors complicate conclusions in aly model. *Nature medicine*. 2001;7(11):1165-6.
92. Loukas M, Bellary SS, Kuklinski M, Ferraiola J, Yadav A, Shoja MM, et al. The lymphatic system: a historical perspective. *Clinical anatomy (New York, NY)*. 2011;24(7):807-16.
93. Hong YK, Harvey N, Noh YH, Schacht V, Hirakawa S, Detmar M, et al. Prox1 is a master control gene in the program specifying lymphatic endothelial cell fate. *Developmental dynamics : an official publication of the American Association of Anatomists*. 2002;225(3):351-7.
94. Wigle JT, Harvey N, Detmar M, Lagutina I, Grosveld G, Gunn MD, et al. An essential role for Prox1 in the induction of the lymphatic endothelial cell phenotype. *The EMBO journal*. 2002;21(7):1505-13.
95. Yaniv K, Isogai S, Castranova D, Dye L, Hitomi J, Weinstein BM. Live imaging of lymphatic development in the zebrafish. *Nature medicine*. 2006;12(6):711-6.
96. Karkkainen MJ, Haiko P, Sainio K, Partanen J, Taipale J, Petrova TV, et al. Vascular endothelial growth factor C is required for sprouting of the first lymphatic vessels from embryonic veins. *Nature immunology*. 2004;5(1):74-80.
97. Francois M, Short K, Secker GA, Combes A, Schwarz Q, Davidson TL, et al. Segmental territories along the cardinal veins generate lymph sacs via a ballooning mechanism during embryonic lymphangiogenesis in mice. *Developmental biology*. 2012;364(2):89-98.
98. Martinez-Corral I, Ulvmar MH, Stanczuk L, Tatin F, Kizhatil K, John SW, et al. Nonvenous origin of dermal lymphatic vasculature. *Circulation research*. 2015;116(10):1649-54.

99. Klotz L, Norman S, Vieira JM, Masters M, Rohling M, Dube KN, et al. Cardiac lymphatics are heterogeneous in origin and respond to injury. *Nature*. 2015;522(7554):62-7.
100. Srinivasan RS, Oliver G. Prox1 dosage controls the number of lymphatic endothelial cell progenitors and the formation of the lymphovenous valves. *Genes & development*. 2011;25(20):2187-97.
101. Lutter S, Xie S, Tatin F, Makinen T. Smooth muscle-endothelial cell communication activates Reelin signaling and regulates lymphatic vessel formation. *The Journal of cell biology*. 2012;197(6):837-49.
102. Makinen T, Adams RH, Bailey J, Lu Q, Ziemiecki A, Alitalo K, et al. PDZ interaction site in ephrinB2 is required for the remodeling of lymphatic vasculature. *Genes & development*. 2005;19(3):397-410.
103. Gordon EJ, Rao S, Pollard JW, Nutt SL, Lang RA, Harvey NL. Macrophages define dermal lymphatic vessel calibre during development by regulating lymphatic endothelial cell proliferation. *Development (Cambridge, England)*. 2010;137(22):3899-910.
104. Hall JE. *Guyton and Hall Textbook of Medical Physiology*. Saint Louis, UNITED STATES: Elsevier Health Sciences; 2015.
105. Irrthum A, Karkkainen MJ, Devriendt K, Alitalo K, Vikkula M. Congenital hereditary lymphedema caused by a mutation that inactivates VEGFR3 tyrosine kinase. *American journal of human genetics*. 2000;67(2):295-301.
106. Kholova I, Dragneva G, Cermakova P, Laidinen S, Kaskenpaa N, Hazes T, et al. Lymphatic vasculature is increased in heart valves, ischaemic and inflamed hearts and in cholesterol-rich and calcified atherosclerotic lesions. *European journal of clinical investigation*. 2011;41(5):487-97.
107. Harvey NL, Srinivasan RS, Dillard ME, Johnson NC, Witte MH, Boyd K, et al. Lymphatic vascular defects promoted by Prox1 haploinsufficiency cause adult-onset obesity. *Nature genetics*. 2005;37(10):1072-81.
108. Mehrara BJ, Greene AK. Lymphedema and obesity: is there a link? *Plastic and reconstructive surgery*. 2014;134(1):154e-60e.
109. Baluk P, Fuxe J, Hashizume H, Romano T, Lashnits E, Butz S, et al. Functionally specialized junctions between endothelial cells of lymphatic vessels. *J Exp Med*. 2007;204(10):2349-62.

110. Danussi C, Spessotto P, Petrucco A, Wassermann B, Sabatelli P, Montesi M, et al. Emilin1 deficiency causes structural and functional defects of lymphatic vasculature. *Molecular and cellular biology*. 2008;28(12):4026-39.
111. Petrova TV, Karpanen T, Norrmen C, Mellor R, Tamakoshi T, Finegold D, et al. Defective valves and abnormal mural cell recruitment underlie lymphatic vascular failure in lymphedema distichiasis. *Nature medicine*. 2004;10(9):974-81.
112. Bazigou E, Makinen T. Flow control in our vessels: vascular valves make sure there is no way back. *Cellular and molecular life sciences : CMLS*. 2013;70(6):1055-66.
113. Bazigou E. Integrin- α 9 is required for fibronectin matrix assembly. 2009;17(2):175-86.
114. Zhang G, Brady J, Liang W-C, Wu Y, Henkemeyer M, Yan M. EphB4 forward signalling regulates lymphatic valve development. 2015;6:6625.
115. Eklund L, Kangas J, Saharinen P. Angiopoietin-Tie signalling in the cardiovascular and lymphatic systems2016. 87-103 p.
116. Zhou F, Chang Z, Zhang L, Hong Y-K, Shen B, Wang B, et al. Akt/Protein Kinase B Is Required for Lymphatic Network Formation, Remodeling, and Valve Development. *The American Journal of Pathology*. 2010;177(4):2124-33.
117. Wang Y, Nakayama M, Pitulescu ME, Schmidt TS, Bochenek ML, Sakakibara A, et al. Ephrin-B2 controls VEGF-induced angiogenesis and lymphangiogenesis. *Nature*. 2010;465(7297):483-6.
118. Pasquale EB. Eph-ephrin bidirectional signaling in physiology and disease. *Cell*. 2008;133(1):38-52.
119. Braun J, Hoffmann SC, Feldner A, Ludwig T, Henning R, Hecker M, et al. Endothelial cell ephrinB2-dependent activation of monocytes in arteriosclerosis. *Arteriosclerosis, thrombosis, and vascular biology*. 2011;31(2):297-305.
120. Zamora DO, Babra B, Pan Y, Planck SR, Rosenbaum JT. Human leukocytes express ephrinB2 which activates microvascular endothelial cells. *Cellular immunology*. 2006;242(2):99-109.
121. Yu G, Luo H, Wu Y, Wu J. Ephrin B2 induces T cell costimulation. *Journal of immunology (Baltimore, Md : 1950)*. 2003;171(1):106-14.
122. Card CM, Yu SS, Swartz MA. Emerging roles of lymphatic endothelium in regulating adaptive immunity. *The Journal of clinical investigation*. 2014;124(3):943-52.

123. Thomas SN, Rutkowski JM, Pasquier M, Kuan EL, Alitalo K, Randolph GJ, et al. Impaired Humoral Immunity and Tolerance in K14-VEGFR-3-Ig Mice That Lack Dermal Lymphatic Drainage. *Journal of Immunology*. 2012;189(5):2181-90.
124. Lammermann T, Sixt M. Mechanical modes of 'amoeboid' cell migration. *Current opinion in cell biology*. 2009;21(5):636-44.
125. Lammermann T, Bader BL, Monkley SJ, Worbs T, Wedlich-Soldner R, Hirsch K, et al. Rapid leukocyte migration by integrin-independent flowing and squeezing. *Nature*. 2008;453(7191):51-5.
126. Tal O, Lim HY, Gurevich I, Milo I, Shipony Z, Ng LG, et al. DC mobilization from the skin requires docking to immobilized CCL21 on lymphatic endothelium and intralymphatic crawling. *The Journal of experimental medicine*. 2011;208(10):2141-53.
127. Pflücke H, Sixt M. Preformed portals facilitate dendritic cell entry into afferent lymphatic vessels. *The Journal of experimental medicine*. 2009;206(13):2925-35.
128. Overstreet MG, Gaylo A, Angermann BR, Hughson A, Hyun YM, Lambert K, et al. Inflammation-induced interstitial migration of effector CD4(+) T cells is dependent on integrin α V. *Nature immunology*. 2013;14(9):949-58.
129. Johnson LA, Clasper S, Holt AP, Lalor PF, Baban D, Jackson DG. An inflammation-induced mechanism for leukocyte transmigration across lymphatic vessel endothelium. *J Exp Med*. 2006;203(12):2763-77.
130. Johnson LA, Jackson DG. Inflammation-induced secretion of CCL21 in lymphatic endothelium is a key regulator of integrin-mediated dendritic cell transmigration. *International immunology*. 2010;22(10):839-49.
131. Weber M, Hauschild R, Schwarz J, Moussion C, de Vries I, Legler DF, et al. Interstitial dendritic cell guidance by haptotactic chemokine gradients. *Science (New York, NY)*. 2013;339(6117):328-32.
132. Platt AM, Rutkowski JM, Martel C, Kuan EL, Ivanov S, Swartz MA, et al. Normal dendritic cell mobilization to lymph nodes under conditions of severe lymphatic hypoplasia. *Journal of immunology (Baltimore, Md : 1950)*. 2013;190(9):4608-20.
133. Martinez de la Torre Y, Locati M, Buracchi C, Dupor J, Cook DN, Bonecchi R, et al. Increased inflammation in mice deficient for the chemokine decoy receptor D6. *European journal of immunology*. 2005;35(5):1342-6.

134. Banerji S, Ni J, Wang SX, Clasper S, Su J, Tammi R, et al. LYVE-1, a new homologue of the CD44 glycoprotein, is a lymph-specific receptor for hyaluronan. *The Journal of cell biology*. 1999;144(4):789-801.
135. Jackson DG. Immunological functions of hyaluronan and its receptors in the lymphatics. *Immunological reviews*. 2009;230(1):216-31.
136. Cui Y, Liu K, Monzon-Medina ME, Padera RF, Wang H, George G, et al. Therapeutic lymphangiogenesis ameliorates established acute lung allograft rejection. *The Journal of clinical investigation*. 2015;125(11):4255-68.
137. Mummert ME, Mummert D, Edelbaum D, Hui F, Matsue H, Takashima A. Synthesis and surface expression of hyaluronan by dendritic cells and its potential role in antigen presentation. *Journal of immunology (Baltimore, Md : 1950)*. 2002;169(8):4322-31.
138. Zhao H, Perez JS, Lu K, George AJ, Ma D. Role of Toll-like receptor-4 in renal graft ischemia-reperfusion injury. *American journal of physiology Renal physiology*. 2014;306(8):F801-11.
139. Kang S, Lee SP, Kim KE, Kim HZ, Memet S, Koh GY. Toll-like receptor 4 in lymphatic endothelial cells contributes to LPS-induced lymphangiogenesis by chemotactic recruitment of macrophages. *Blood*. 2009;113(11):2605-13.
140. Sawa Y, Ueki T, Hata M, Iwasawa K, Tsuruga E, Kojima H, et al. LPS-induced IL-6, IL-8, VCAM-1, and ICAM-1 Expression in Human Lymphatic Endothelium. *Journal of Histochemistry and Cytochemistry*. 2008;56(2):97-109.
141. Stacker SA, Williams SP, Karnezis T, Shayan R, Fox SB, Achen MG. Lymphangiogenesis and lymphatic vessel remodelling in cancer. *Nature reviews Cancer*. 2014;14(3):159-72.
142. Kim H. Inflammation-associated lymphangiogenesis: a double-edged sword? 2014;124(3):936-42.
143. Kerjaschki D. Lymphatic neoangiogenesis in renal transplants: a driving force of chronic rejection? *Journal of Nephrology*. 2006;19(4):403-6.
144. Tammela T, Alitalo K. Lymphangiogenesis: Molecular Mechanisms and Future Promise. *Cell*. 2010;140(4):460-76.
145. Xu Y, Yuan L, Mak J, Pardanaud L, Caunt M, Kasman I, et al. Neuropilin-2 mediates VEGF-C-induced lymphatic sprouting together with VEGFR3. *The Journal of cell biology*. 2010;188(1):115-30.

146. Makinen T, Veikkola T, Mustjoki S, Karpanen T, Catimel B, Nice EC, et al. Isolated lymphatic endothelial cells transduce growth, survival and migratory signals via the VEGF-C/D receptor VEGFR-3. *The EMBO journal*. 2001;20(17):4762-73.
147. Coso S, Zeng Y, Opeskin K, Williams ED. Vascular endothelial growth factor receptor-3 directly interacts with phosphatidylinositol 3-kinase to regulate lymphangiogenesis. *PloS one*. 2012;7(6):e39558.
148. Wirzenius M, Tammela T, Uutela M, He Y, Odorisio T, Zambruno G, et al. Distinct vascular endothelial growth factor signals for lymphatic vessel enlargement and sprouting. *The Journal of experimental medicine*. 2007;204(6):1431-40.
149. Dellinger MT, Meadows SM, Wynne K, Cleaver O, Brekken RA. Vascular endothelial growth factor receptor-2 promotes the development of the lymphatic vasculature. *PloS one*. 2013;8(9):e74686.
150. Zheng W, Tammela T, Yamamoto M, Anisimov A, Holopainen T, Kaijalainen S, et al. Notch restricts lymphatic vessel sprouting induced by vascular endothelial growth factor. *Blood*. 2011;118(4):1154-62.
151. Hogan BM, Bos FL, Bussmann J, Witte M, Chi NC, Duckers HJ, et al. Ccbe1 is required for embryonic lymphangiogenesis and venous sprouting. *Nature genetics*. 2009;41(4):396-8.
152. Alders M, Hogan BM, Gjini E, Salehi F, Al-Gazali L, Hennekam EA, et al. Mutations in CCBE1 cause generalized lymph vessel dysplasia in humans. *Nature genetics*. 2009;41(12):1272-4.
153. Bos FL, Caunt M, Peterson-Maduro J, Planas-Paz L, Kowalski J, Karpanen T, et al. CCBE1 is essential for mammalian lymphatic vascular development and enhances the lymphangiogenic effect of vascular endothelial growth factor-C in vivo. *Circulation research*. 2011;109(5):486-91.
154. Karpanen T, Heckman CA, Keskitalo S, Jeltsch M, Ollila H, Neufeld G, et al. Functional interaction of VEGF-C and VEGF-D with neuropilin receptors. *FASEB journal : official publication of the Federation of American Societies for Experimental Biology*. 2006;20(9):1462-72.
155. Yuan L, Moyon D, Pardanaud L, Breant C, Karkkainen MJ, Alitalo K, et al. Abnormal lymphatic vessel development in neuropilin 2 mutant mice. *Development (Cambridge, England)*. 2002;129(20):4797-806.

156. Jurisic G, Maby-El Hajjami H, Karaman S, Ochsenbein AM, Alitalo A, Siddiqui SS, et al. An unexpected role of semaphorin3a-neuropilin-1 signaling in lymphatic vessel maturation and valve formation. *Circulation research*. 2012;111(4):426-36.
157. Tammela T, Saaristo A, Lohela M, Morisada T, Tornberg J, Norrmen C, et al. Angiopoietin-1 promotes lymphatic sprouting and hyperplasia. *Blood*. 2005;105(12):4642-8.
158. Daly C, Pasnikowski E, Burova E, Wong V, Aldrich TH, Griffiths J, et al. Angiopoietin-2 functions as an autocrine protective factor in stressed endothelial cells. *Proc Natl Acad Sci U S A*. 2006;103(42):15491-6.
159. Dellinger M, Hunter R, Bernas M, Gale N, Yancopoulos G, Erickson R, et al. Defective remodeling and maturation of the lymphatic vasculature in Angiopoietin-2 deficient mice. *Developmental biology*. 2008;319(2):309-20.
160. Tabruyn SP, Colton K, Morisada T, Fuxe J, Wiegand SJ, Thurston G, et al. Angiopoietin-2-driven vascular remodeling in airway inflammation. *The American journal of pathology*. 2010;177(6):3233-43.
161. Yoon CM, Hong BS, Moon HG, Lim S, Suh PG, Kim YK, et al. Sphingosine-1-phosphate promotes lymphangiogenesis by stimulating S1P1/Gi/PLC/Ca²⁺ signaling pathways. *Blood*. 2008;112(4):1129-38.
162. Jang C, Koh YJ, Lim NK, Kang HJ, Kim DH, Park SK, et al. Angiopoietin-2 exocytosis is stimulated by sphingosine-1-phosphate in human blood and lymphatic endothelial cells. *Arteriosclerosis, thrombosis, and vascular biology*. 2009;29(3):401-7.
163. Pham TH, Baluk P, Xu Y, Grigorova I, Bankovich AJ, Pappu R, et al. Lymphatic endothelial cell sphingosine kinase activity is required for lymphocyte egress and lymphatic patterning. *J Exp Med*. 2010;207(1):17-27.
164. Abengozar MA, de Frutos S, Ferreiro S, Soriano J, Perez-Martinez M, Olmeda D, et al. Blocking ephrinB2 with highly specific antibodies inhibits angiogenesis, lymphangiogenesis, and tumor growth. *Blood*. 2012;119(19):4565-76.
165. Oka M, Iwata C, Suzuki HI, Kiyono K, Morishita Y, Watabe T, et al. Inhibition of endogenous TGF-beta signaling enhances lymphangiogenesis. *Blood*. 2008;111(9):4571-9.
166. Clavin NW, Avraham T, Fernandez J, Daluvoy SV, Soares MA, Chaudhry A, et al. TGF-beta1 is a negative regulator of lymphatic regeneration during wound repair. *American journal of physiology Heart and circulatory physiology*. 2008;295(5):H2113-27.

167. Kataru RP, Kim H, Jang C, Choi DK, Koh BI, Kim M, et al. T Lymphocytes Negatively Regulate Lymph Node Lymphatic Vessel Formation. *Immunity*. 2011;34(1):96-107.
168. Dohlman TH, Omoto M, Hua J, Stevenson W, Lee SM, Chauhan SK, et al. VEGF-trap aflibercept significantly improves long-term graft survival in high-risk corneal transplantation. *Transplantation*. 2015;99(4):678-86.
169. Baluk P, Yao LC, Feng J, Romano T, Jung SS, Schreiter JL, et al. TNF-alpha drives remodeling of blood vessels and lymphatics in sustained airway inflammation in mice. *The Journal of clinical investigation*. 2009;119(10):2954-64.
170. Kataru RP, Jung K, Jang C, Yang H, Schwendener RA, Baik JE, et al. Critical role of CD11b+ macrophages and VEGF in inflammatory lymphangiogenesis, antigen clearance, and inflammation resolution. *Blood*. 2009;113(22):5650-9.
171. Tammela T, Saaristo A, Holopainen T, Lyytikka J, Kotronen A, Pitkonen M, et al. Therapeutic differentiation and maturation of lymphatic vessels after lymph node dissection and transplantation. *Nature medicine*. 2007;13(12):1458-66.
172. Kerjaschki D, Regele HM, Moosberger I, Nagy-Bojarski K, Watschinger B, Soleiman A, et al. Lymphatic neoangiogenesis in human kidney transplants is associated with immunologically active lymphocytic infiltrates. *Journal of the American Society of Nephrology*. 2004;15(3):603-12.
173. Mobley JE, O'Dell RM. The role of lymphatics in renal transplantation. Renal lymphatic regeneration. *The Journal of surgical research*. 1967;7(5):231-3.
174. Kerjaschki D, Huttary N, Raab I, Regele H, Bojarski-Nagy K, Bartel G, et al. Lymphatic endothelial progenitor cells contribute to de novo lymphangiogenesis in human renal transplants. *Nature Medicine*. 2006;12(2):230-4.
175. Halin C, Tobler NE, Vigl B, Brown LF, Detmar M. VEGF-A produced by chronically inflamed tissue induces lymphangiogenesis in draining lymph nodes. *Blood*. 2007;110(9):3158-67.
176. Brown K, Badar A, Sunassee K, Fernandes MA, Shariff H, Jurcevic S, et al. SPECT/CT Lymphoscintigraphy of Heterotopic Cardiac Grafts Reveals Novel Sites of Lymphatic Drainage and T Cell Priming. *American Journal of Transplantation*. 2011;11(2):225-34.
177. Edwards LA, Nowocin AK, Jafari NV, Meader L, Brown K, Sarde A, et al. Chronic Rejection of Cardiac Allografts is Associated with Increased Lymphatic Flow and Cellular Trafficking. *Circulation*. 2017.

178. Yin N, Zhang N, Xu J, Shi Q, Ding Y, Bromberg JS. Targeting lymphangiogenesis after islet transplantation prolongs islet allograft survival. *Transplantation*. 2011;92(1):25-30.
179. Nykanen AI, Sandelin H, Krebs R, Keranen MA, Tuuminen R, Karpanen T, et al. Targeting lymphatic vessel activation and CCL21 production by vascular endothelial growth factor receptor-3 inhibition has novel immunomodulatory and antiarteriosclerotic effects in cardiac allografts. *Circulation*. 2010;121(12):1413-22.
180. Maruyama K, Li M, Cursiefen C, Jackson DG, Keino H, Tomita M, et al. Inflammation-induced lymphangiogenesis in the cornea arises from CD11b-positive macrophages. *The Journal of clinical investigation*. 2005;115(9):2363-72.
181. Flister MJ, Wilber A, Hall KL, Iwata C, Miyazono K, Nisato RE, et al. Inflammation induces lymphangiogenesis through up-regulation of VEGFR-3 mediated by NF-kappaB and Prox1. *Blood*. 2010;115(2):418-29.
182. Geissler HJ, Dashkevich A, Fischer UM, Fries JW, Kuhn-Regnier F, Addicks K, et al. First year changes of myocardial lymphatic endothelial markers in heart transplant recipients. *European journal of cardio-thoracic surgery : official journal of the European Association for Cardio-thoracic Surgery*. 2006;29(5):767-71.
183. Ruggiero R, Fietsam R, Jr., Thomas GA, Muz J, Farris RH, Kowal TA, et al. Detection of canine allograft lung rejection by pulmonary lymphoscintigraphy. *The Journal of thoracic and cardiovascular surgery*. 1994;108(2):253-8.
184. Soong TR, Pathak AP, Asano H. Lymphatic Injury and Regeneration in Cardiac Allografts (vol 89, pg 500, 2010). *Transplantation*. 2010;90(11):1244-.
185. Tabibiazar R, Cheung L, Han J, Swanson J, Beilhack A, An A, et al. Inflammatory manifestations of experimental lymphatic insufficiency. *Plos Medicine*. 2006;3(7):1114-39.
186. Brown K, Sacks SH, Wong W. Tertiary lymphoid organs in renal allografts can be associated with donor-specific tolerance rather than rejection. *European Journal of Immunology*. 2011;41(1):89-96.
187. Chang JE, Turley SJ. Stromal infrastructure of the lymph node and coordination of immunity. *Trends in Immunology*. 36(1):30-9.
188. Miyasaka M, Tanaka T. Lymphocyte trafficking across high endothelial venules: dogmas and enigmas. *Nat Rev Immunol*. 2004;4(5):360-70.
189. Liu K, Victora GD, Schwickert TA, Guermontprez P, Meredith MM, Yao K, et al. In vivo analysis of dendritic cell development and homeostasis. *Science*. 2009;324(5925):392-7.

190. Pham TH, Okada T, Matloubian M, Lo CG, Cyster JG. S1P1 receptor signaling overrides retention mediated by G alpha i-coupled receptors to promote T cell egress. *Immunity*. 2008;28(1):122-33.
191. van de Pavert SA, Mebius RE. New insights into the development of lymphoid tissues. *Nat Rev Immunol*. 2010;10(9):664-74.
192. Angeli V, Ginhoux F, Llodra J, Quemeneur L, Frenette PS, Skobe M, et al. B cell-driven lymphangiogenesis in inflamed lymph nodes enhances dendritic cell mobilization. *Immunity*. 2006;24(2):203-15.
193. Breiteneder-Geleff S, Soleiman A, Horvat R, Amann G, Kowalski H, Kerjaschki D. [Podoplanin--a specific marker for lymphatic endothelium expressed in angiosarcoma]. *Verhandlungen der Deutschen Gesellschaft fur Pathologie*. 1999;83:270-5.
194. Achen MG, Jeltsch M, Kukk E, Makinen T, Vitali A, Wilks AF, et al. Vascular endothelial growth factor D (VEGF-D) is a ligand for the tyrosine kinases VEGF receptor 2 (Flk1) and VEGF receptor 3 (Flt4). *Proc Natl Acad Sci U S A*. 1998;95(2):548-53.
195. Cohen JN, Guidi CJ, Tewalt EF, Qiao H, Rouhani SJ, Ruddell A, et al. Lymph node-resident lymphatic endothelial cells mediate peripheral tolerance via Aire-independent direct antigen presentation. *J Exp Med*. 2010;207(4):681-8.
196. Tewalt EF, Cohen JN, Rouhani SJ, Guidi CJ, Qiao H, Fahl SP, et al. Lymphatic endothelial cells induce tolerance via PD-L1 and lack of costimulation leading to high-level PD-1 expression on CD8 T cells. *Blood*. 2012;120(24):4772-82.
197. Fletcher AL, Lukacs-Kornek V, Reynoso ED, Pinner SE, Bellemare-Pelletier A, Curry MS, et al. Lymph node fibroblastic reticular cells directly present peripheral tissue antigen under steady-state and inflammatory conditions. *J Exp Med*. 2010;207(4):689-97.
198. Lund Amanda W, Duraes Fernanda V, Hirosue S, Raghavan Vidya R, Nembrini C, Thomas Susan N, et al. VEGF-C Promotes Immune Tolerance in B16 Melanomas and Cross-Presentation of Tumor Antigen by Lymph Node Lymphatics. *Cell Reports*. 2012;1(3):191-9.
199. Dubrot J, Duraes FV, Potin L, Capotosti F, Brighouse D, Suter T, et al. Lymph node stromal cells acquire peptide-MHCII complexes from dendritic cells and induce antigen-specific CD4+ T cell tolerance. *The Journal of experimental medicine*. 2014;211(6):1153-66.
200. Rouhani SJ, Eccles JD, Riccardi P, Peske JD, Tewalt EF, Cohen JN, et al. Roles of lymphatic endothelial cells expressing peripheral tissue antigens in CD4 T-cell tolerance induction. *Nat Commun*. 2015;6.

201. Noerder M, Gutierrez MG, Zicari S, Cervi E, Caruso A, Guzman CA. Lymph node-derived lymphatic endothelial cells express functional costimulatory molecules and impair dendritic cell-induced allogenic T-cell proliferation. *Faseb Journal*. 2012;26(7):2835-46.
202. Hassan J, Reen DJ. IL-7 promotes the survival and maturation but not differentiation of human post-thymic CD4+ T cells. *Eur J Immunol*. 1998;28(10):3057-65.
203. Soares MV, Borthwick NJ, Maini MK, Janossy G, Salmon M, Akbar AN. IL-7-dependent extrathymic expansion of CD45RA+ T cells enables preservation of a naive repertoire. *Journal of immunology (Baltimore, Md : 1950)*. 1998;161(11):5909-17.
204. Onder L, Narang P, Scandella E, Chai Q, Iolyeva M, Hoorweg K, et al. IL-7-producing stromal cells are critical for lymph node remodeling. *Blood*. 2012;120(24):4675-83.
205. Miller CN, Hartigan-O'Connor DJ, Lee MS, Laidlaw G, Cornelissen IP, Matloubian M, et al. IL-7 production in murine lymphatic endothelial cells and induction in the setting of peripheral lymphopenia. *International immunology*. 2013;25(8):471-83.
206. Kataru RP, Kim H, Jang C, Choi DK, Koh BI, Kim M, et al. T lymphocytes negatively regulate lymph node lymphatic vessel formation. *Immunity*. 2011;34(1):96-107.
207. Pappu R, Schwab SR, Cornelissen I, Pereira JP, Regard JB, Xu Y, et al. Promotion of lymphocyte egress into blood and lymph by distinct sources of sphingosine-1-phosphate. *Science*. 2007;316(5822):295-8.
208. Srinivas S, Watanabe T, Lin CS, William CM, Tanabe Y, Jessell TM, et al. Cre reporter strains produced by targeted insertion of EYFP and ECFP into the ROSA26 locus. *BMC developmental biology*. 2001;1:4.
209. Truett GE, Heeger P, Mynatt RL, Truett AA, Walker JA, Warman ML. Preparation of PCR-quality mouse genomic DNA with hot sodium hydroxide and tris (HotSHOT). *BioTechniques*. 2000;29(1):52, 4.
210. Billingham RE, Medawar PB. THE TECHNIQUE OF FREE SKIN GRAFTING IN MAMMALS. *Journal of Experimental Biology*. 1951;28(3):385-&.
211. Corry RJ, Winn HJ, Russell PS. PRIMARILY VASCULARIZED ALLOGRAFTS OF HEARTS IN MICE - ROLE OF H-2D, H-2K, AND NON-H-2 ANTIGENS IN REJECTION. *Transplantation*. 1973;16(4):343-50.
212. Superina RA, Peugh WN, Wood KJ, Morris PJ. ASSESSMENT OF PRIMARILY VASCULARIZED CARDIAC ALLOGRAFTS IN MICE. *Transplantation*. 1986;42(2):226-7.

213. Han WR, Murray-Segal LJ, Mottram PL. Modified technique for kidney transplantation in mice. *Microsurgery*. 1999;19(6):272-4.
214. Nagamine CM, Chan K, Hake LE, Lau YF. The two candidate testis-determining Y genes (Zfy-1 and Zfy-2) are differentially expressed in fetal and adult mouse tissues. *Genes & development*. 1990;4(1):63-74.
215. An N, Kang Y. Using quantitative real-time PCR to determine donor cell engraftment in a competitive murine bone marrow transplantation model. *Journal of visualized experiments : JoVE*. 2013(73):e50193.
216. Gregory TR. Animal genome size database 2017. Available from: <http://www.genomesize.com>.
217. Teteris SA, Hochheiser K, Kurts C. Isolation of functional dendritic cells from murine kidneys for immunological characterization. *Nephrology (Carlton, Vic)*. 2012;17(4):364-71.
218. Broggi MA, Schmalzer M, Lagarde N, Rossi SW. Isolation of murine lymph node stromal cells. *Journal of visualized experiments : JoVE*. 2014(90):e51803.
219. Iwami D, Brinkman CC, Bromberg JS. Vascular endothelial growth factor c/vascular endothelial growth factor receptor 3 signaling regulates chemokine gradients and lymphocyte migration from tissues to lymphatics. *Transplantation*. 2015;99(4):668-77.
220. Wang Q, Zhang M, Ding G, Liu Y, Sun Y, Wang J, et al. Anti-ICAM-1 antibody and CTLA-4Ig synergistically enhance immature dendritic cells to induce donor-specific immune tolerance in vivo. *Immunology letters*. 2003;90(1):33-42.
221. Grazia TJ, Gill RG, Gelhaus HC, Jr., Doan AN, Sleater ML, Pietra BA. Perturbation of leukocyte function-associated antigen-1/intercellular adhesion molecule-1 results in differential outcomes in cardiac vs islet allograft survival. *The Journal of heart and lung transplantation : the official publication of the International Society for Heart Transplantation*. 2005;24(9):1410-4.
222. Isobe M, Yagita H, Okumura K, Ihara A. Specific acceptance of cardiac allograft after treatment with antibodies to ICAM-1 and LFA-1. *Science (New York, NY)*. 1992;255(5048):1125-7.
223. Brandt M, Steinmann J, Steinhoff G, Haverich A. Treatment with monoclonal antibodies to ICAM-1 and LFA-1 in rat heart allograft rejection. *Transplant international : official journal of the European Society for Organ Transplantation*. 1997;10(2):141-4.

224. He Y, Mellon J, Apte R, Niederkorn JY. Effect of LFA-1 and ICAM-1 antibody treatment on murine corneal allograft survival. *Investigative ophthalmology & visual science*. 1994;35(8):3218-25.
225. Huang X, Moore DJ, Mohiuddin M, Lian MM, Kim JI, Sonawane S, et al. Inhibition of ICAM-1/LFA-1 Interactions Prevents B-Cell-Dependent Anti-CD45RB-Induced Transplantation Tolerance. *Transplantation*. 2008;85(5):675-80.
226. Arai K, Sunamura M, Wada Y, Takahashi M, Kobari M, Kato K, et al. Preventing effect of anti-ICAM-1 and anti-LFA-1 monoclonal antibodies on murine islet allograft rejection. *International Journal of Pancreatology*. 1999;26(1):23-31.
227. Laird CD. Chromatid structure: relationship between DNA content and nucleotide sequence diversity. *Chromosoma*. 1971;32(4):378-406.
228. Baaten BJJ, Li CR, Bradley LM. Multifaceted regulation of T cells by CD44. *Communicative & Integrative Biology*. 2010;3(6):508-12.
229. Tay SS, Lu B, Siervo F, Benseler V, McGuffog CM, Bishop GA, et al. Differential migration of passenger leukocytes and rapid deletion of naive alloreactive CD8 T cells after mouse liver transplantation. *Liver transplantation : official publication of the American Association for the Study of Liver Diseases and the International Liver Transplantation Society*. 2013;19(11):1224-35.
230. Tohda S, Nara N. [Molecular diagnostic tests in hematologic diseases]. *Rinsho byori The Japanese journal of clinical pathology*. 2001;49(3):205-9.
231. Watzinger F, Ebner K, Lion T. Detection and monitoring of virus infections by real-time PCR. *Molecular aspects of medicine*. 2006;27(2-3):254-98.
232. Brown K, Moxham V, Karegli J, Phillips R, Sacks SH, Wong W. Ultra-localization of Foxp3(+) T cells within renal Allografts shows infiltration of tubules mimicking rejection. *Am J Pathol*. 2007;171(6):1915-22.
233. Ziegler E, Gueler F, Rong S, Mengel M, Witzke O, Kribben A, et al. CCL19-IgG prevents allograft rejection by impairment of immune cell trafficking. *Journal of the American Society of Nephrology : JASN*. 2006;17(9):2521-32.
234. Chong AS, Alegre ML, Miller ML, Fairchild RL. Lessons and limits of mouse models. *Cold Spring Harbor Perspectives in Medicine*. 2013;3(12):a015495.
235. Roth SJ, Carr MW, Rose SS, Springer TA. Characterization of transendothelial chemotaxis of T lymphocytes. *Journal of immunological methods*. 1995;188(1):97-116.

236. Lebedeva T, Dustin ML, Sykulev Y. ICAM-1 co-stimulates target cells to facilitate antigen presentation. *Current opinion in immunology*. 2005;17(3):251-8.
237. Reichardt P, Patzak I, Jones K, Etemire E, Gunzer M, Hogg N. A role for LFA-1 in delaying T-lymphocyte egress from lymph nodes. *The EMBO journal*. 2013;32(6):829-43.
238. Kullander K, Klein R. Mechanisms and functions of Eph and ephrin signalling. *Nature reviews Molecular cell biology*. 2002;3(7):475-86.
239. Klein R. Eph/ephrin signalling during development. *Development (Cambridge, England)*. 2012;139(22):4105-9.
240. Janes PW, Adikari S, Lackmann M. Eph/ephrin signalling and function in oncogenesis: lessons from embryonic development. *Current cancer drug targets*. 2008;8(6):473-9.
241. Tewalt E, Cohen J, Rouhani S, Engelhard V. Lymphatic endothelial cells - key players in regulation of tolerance and immunity. *Frontiers in Immunology*. 2012;3(305).
242. Pfaff D, Heroult M, Riedel M, Reiss Y, Kirmse R, Ludwig T, et al. Involvement of endothelial ephrin-B2 in adhesion and transmigration of EphB-receptor-expressing monocytes. *Journal of cell science*. 2008;121(Pt 22):3842-50.
243. Johnson LA, Jackson DG. Control of dendritic cell trafficking in lymphatics by chemokines. *Angiogenesis*. 2014;17(2):335-45.
244. Vigl B, Aebischer D, Nitschke M, Iolyeva M, Rothlin T, Antsiferova O, et al. Tissue inflammation modulates gene expression of lymphatic endothelial cells and dendritic cell migration in a stimulus-dependent manner. *Blood*. 2011;118(1):205-15.
245. Potin L, Maillat L, Dubrot J, Duraes F, Hugues S, Swartz M. Antigen presentation via MHC class II by lymphatic endothelial cells dampens CD4⁺ T cell response (IRC7P.436). *The Journal of Immunology*. 2015;194(1 Supplement):128.17-.17.
246. Norder M, Gutierrez MG, Zicari S, Cervi E, Caruso A, Guzman CA. Lymph node-derived lymphatic endothelial cells express functional costimulatory molecules and impair dendritic cell-induced allogenic T-cell proliferation. *FASEB journal : official publication of the Federation of American Societies for Experimental Biology*. 2012;26(7):2835-46.
247. Tobler NE, Detmar M. Tumor and lymph node lymphangiogenesis--impact on cancer metastasis. *Journal of leukocyte biology*. 2006;80(4):691-6.
248. Halin C, Detmar M. An Unexpected Connection: Lymph Node Lymphangiogenesis and Dendritic Cell Migration. *Immunity*. 2006;24(2):129-31.

249. Wang C, Cordoba S, Hu M, Bertolino P, Bowen DG, Sharland AF, et al. Spontaneous acceptance of mouse kidney allografts is associated with increased Foxp3 expression and differences in the B and T cell compartments. *Transpl Immunol.* 2011;24(3):149-56.
250. DeNucci CC, Mitchell JS, Shimizu Y. INTEGRIN FUNCTION IN T CELL HOMING TO LYMPHOID AND NON-LYMPHOID SITES: GETTING THERE AND STAYING THERE. *Critical reviews in immunology.* 2009;29(2):87-109.
251. Haug CE, Colvin RB, Delmonico FL, Auchincloss H, Jr., Tolkoff-Rubin N, Preffer FI, et al. A phase I trial of immunosuppression with anti-ICAM-1 (CD54) mAb in renal allograft recipients. *Transplantation.* 1993;55(4):766-72; discussion 72-3.
252. Vincenti F, Mendez R, Pescovitz M, Rajagopalan PR, Wilkinson AH, Butt K, et al. A phase I/II randomized open-label multicenter trial of efalizumab, a humanized anti-CD11a, anti-LFA-1 in renal transplantation. *American journal of transplantation : official journal of the American Society of Transplantation and the American Society of Transplant Surgeons.* 2007;7(7):1770-7.
253. Vuorte J, Lindsberg PJ, Kaste M, Meri S, Jansson SE, Rothlein R, et al. Anti-ICAM-1 monoclonal antibody R6.5 (Enlimomab) promotes activation of neutrophils in whole blood. *Journal of immunology (Baltimore, Md : 1950).* 1999;162(4):2353-7.
254. Gale NW, Prevo R, Espinosa J, Ferguson DJ, Dominguez MG, Yancopoulos GD, et al. Normal Lymphatic Development and Function in Mice Deficient for the Lymphatic Hyaluronan Receptor LYVE-1. *Molecular and Cellular Biology.* 2007;27(2):595-604.
255. Lawrence W, Banerji S, Day AJ, Bhattacharjee S, Jackson DG. Binding of Hyaluronan to the Native Lymphatic Vessel Endothelial Receptor LYVE-1 Is Critically Dependent on Receptor Clustering and Hyaluronan Organization. *The Journal of Biological Chemistry.* 2016;291(15):8014-30.
256. Lynskey NN, Banerji S, Johnson LA, Holder KA, Reglinski M, Wing PAC, et al. Rapid Lymphatic Dissemination of Encapsulated Group A Streptococci via Lymphatic Vessel Endothelial Receptor-1 Interaction. *PLoS Pathogens.* 2015;11(9).
257. Boyd AW, Bartlett PF, Lackmann M. Therapeutic targeting of EPH receptors and their ligands. *Nature reviews Drug discovery.* 2014;13(1):39-62.
258. Sugaya M, Watanabe T, Yang A, Starost MF, Kobayashi H, Atkins AM, et al. Lymphatic dysfunction in transgenic mice expressing KSHV k-cyclin under the control of the VEGFR-3 promoter. *Blood.* 2005;105(6):2356-63.

259. Gardenier JC, Hespe GE, Kataru RP, Savetsky IL, Torrisi JS, Nores GDG, et al. Diphtheria toxin–mediated ablation of lymphatic endothelial cells results in progressive lymphedema. *JCI Insight*.1(15).
260. Clatworthy MR, Harford SK, Mathews RJ, Smith KGC. FcγRIIb inhibits immune complex-induced VEGF-A production and intranodal lymphangiogenesis. *Proceedings of the National Academy of Sciences*. 2014;111(50):17971-6.